ARISTOTLE UNIVERSITY OF THESSALONIKI
Interinstitutional Program of Postgraduate Studies in
PALAEONTOLOGY – GEOBIOLOGY

ELPINIKI MARIA PARPAROUSI
Biologist

# THE VILLAFRANCHIAN MAMMAL FAUNA OF AGHIA KYRIAKI, AETOLOAKARNANIA, GREECE: TAXONOMY AND TAPHONOMY.

MASTER THESIS

*DIRECTION: Macropalaeontology*
*Directed by: Aristotle University of Thessaloniki*

PATRAS
2022

# Interinstitutional Program of Postgraduate Studies in PALAEONTOLOGY – GEOBIOLOGY

supported by:

Τμήμα Γεωλογίας ΑΠΘ
School of Geology AUTh

Τμήμα Βιολογίας ΑΠΘ
School of Biology AUTh

National and Kapodistrian University of Athens
Faculty of Geology and Geoenvironment

Τμήμα Γεωλογίας & Γεωπεριβάλλοντος ΕΚΠΑ
Faculty of Geology & Geoenvironment NKUA

Department of GEOLOGY

Τμήμα Γεωλογίας Παν/μίου Πατρών
Department of Geology, Patras Univ.

UNIVERSITY OF THE AEGEAN

Τμήμα Γεωγραφίας Παν/μίου Αιγαίου
Department of Geography, Aegean Univ.

ELPINIKI MARIA PARPAROUSI
ΕΛΠΙΝΙΚΗ ΜΑΡΙΑ ΠΑΡΠΑΡΟΥΣΗ
Πτυχιούχος Βιολόγος

# THE VILLAFRANCHIAN MAMMAL FAUNA OF AGHIA KYRIAKI, AETOLOAKARNANIA, GREECE: TAXONOMY AND TAPHONOMY.

## Η ΒΙΛΛΑΦΡΑΓΚΙΑ ΠΑΝΙΔΑ ΘΗΛΑΣΤΙΚΩΝ ΤΗΣ ΑΓΙΑΣ ΚΥΡΙΑΚΗΣ, ΑΙΤΩΛΟΑΚΑΡΝΑΝΙΑ, ΕΛΛΑΔΑ: ΤΑΞΙΝΟΜΗΣΗ ΚΑΙ ΤΑΦΟΝΟΜΙΑ.

Υποβλήθηκε στο ΔΠΜΣ Παλαιοντολογία–Γεωβιολογία

Ημερομηνία Προφορικής Εξέτασης: 28/01/2022
Oral Examination Date: 28/01/2022

**Three–member Examining Board**

Associate Professor Iliopoulos Georgios, Supervisor
Professor Kostopoulos Dimitrios, Member
Assistant Porfessor Roussiakis Sokratis, Member

**Τριμελής Εξεταστική Επιτροπή**

Αναπληρωτής Καθηγητής Ηλιόπουλος Γεώργιος, Επιβλέπων
Καθηγητής Κωστόπουλος Δημήτριος, Μέλος Τριμελούς Εξεταστικής Επιτροπής
Επίκουρος Καθηγητής Ρουσιάκης Σωκράτης, Μέλος Τριμελούς Εξεταστικής Επιτροπής

THE VILLAFRANCHIAN MAMMAL FAUNA OF AGHIA KYRIAKI, AETOLOAKARNANIA, GREECE: TAXONOMY AND TAPHONOMY. – *Master Thesis*


Η ΒΙΛΛΑΦΡΑΓΚΙΑ ΠΑΝΙΔΑ ΘΗΛΑΣΤΙΚΩΝ ΤΗΣ ΑΓΙΑΣ ΚΥΡΙΑΚΗΣ, ΑΙΤΩΛΟΑΚΑΡΝΑΝΙΑ, ΕΛΛΑΔΑ: ΤΑΞΙΝΟΜΗΣΗ ΚΑΙ ΤΑΦΟΝΟΜΙΑ. – *Μεταπτυχιακή Διπλωματική Εργασία*

Citation:
Parparousi, E.M., 2022. – The Villafranchian mammal fauna of Aghia Kyriaki, Aetoloakarnania, Greece: Taxonomy and Taphonomy. Master Thesis, Interinstitutional Program of Postgraduate Studies in Palaeontology–Geobiology. School of Geology, Aristotle University of Thessaloniki, 139 pp.



*Cover Figure: Leonardo Sorbelli, 2022.*

**ACKNOWLEDGEMENTS**

I would like to thank Associate Professor Georgios Iliopoulos (Department of Geology, University of Patras), for assigning me the present MSc thesis and trusting me with the studied material. Moreover, I would like to thank him for his guidance in the preparation and preservation of the specimens, as well as his advices throughout the past years of my studies. Moreover, I would like to express my deep gratitude to Professor Dimitrios Kostopoulos (Aristotle University of Thessaloniki) for his valuable guidance, offer of bibliography, his advices and immediate help in any problem and question I had during my Master's studies, as well as all the knowledge he has passed on to me during the past 2 years and I hope I will have the chance tpo work with him again. I would also like to thank all the members of the examining board, Associate Professor Georgios Iliopoulos (University of Patras), Professor Dimitrios Kostopoulos (Aristotle University of Thessaloniki) and Assistant Professor Socrates Roussiakis (National Technical University of Athens) for their suggestions on this text. I also thank PhD student Panagiotis Dimitrios Sianis (University of Patras) for his willing and generous help and support during my thesis practice, as well as his kind provision of his PhD thesis data and bibliography, which have been of great importance. I am also grateful to Emeritus Prof. George Koufos for his guidance, suggestions and offer of bibliography, as well as Pavlos Piskoulis (Aristotle University of Thessaloniki), for his immediate help and contribution in the identification of the Chiroptera specimens of the thesis.

To Professor Joan Madurell–Malapeira I express my deepest appreciation and gratitude for his guidance and generous help during and after my Erasmus traineeship in the ICP, as well as his offer of scientific knowledge, bibliography, advice and support and I hope I will have the chance to work with him again, soon. A huge thank you to PhD student of the ICP, Leonardo Sorbelli for his trust, valuable help and constant encouragement the past few months, his offer of bibliography and suggestions on my thesis, as well as his tours of Barcelona and Italian lessons and recipes. Moreover, I would like to thank him for the artistic edit of this thesis. His guidance and constant support were crucial in shaping my scientific way of thinking as well as my potential academic future. I would also like to thank Maria Prat Vericat, PhD student of the ICP, for consulting me about Ursidae specimens. I need to express my deep gratitude to Marco Cherin, for his friendly help, guidance, and teaching, offer of bibliography as well as hospitality in the Universita degli Studi di Perugia, as well as Saverio Bartolini–Lucenti (Università degli Studi di Firenze) for his help, offer of bibliography and contribution in taxonomy regarding Canidae specimens. A great thank you to my great flat mates and friends, Guillem and Florian that made my stay in Barcelona more than pleasant, as well as Alessandro, Andrea, Silvia and all the members of the ICP, with whom I shared my Erasmus days with, in and out of the office, for their friendly approach and for teaching me precious and useful expressions in Italian, Catalan and French. It turns out, I can speak a fluent mix of all of them.

Also, I would like to thank my friends in Greece for their encouragement and support all these years. Finally, and most of all, I feel the deep need to thank my beloved family: Athanasios, Stavroula and Vasiliki, as well as my grandmother Elpiniki for always being by my side, supporting, helping and encouraging me to make my dreams come true, more than anyone. This thesis is dedicated to them.

To my family,
Athanasios, Stavroula and Vasiliki

To my grandmother,
Elpiniki

**Content**

## 1. INTRODUCTION

Before referring to the Pliocene and Pleistocene biochronology and faunal synthesis of the locality of Aghia Kyriaki, it is crucial to specify that the limit between the two epochs has changed in June 2006 and is regarded to be at 2,588 Ma (International Union of Geological Sciences (IUGS); thus, the beginning of the Quaternary age and respectively of the Pleistocene epoch is in correspondence to the Gelasian base (Gibbard et al, 2010).

Biochronology is a relative dating method of continental sequences that does not use the geological concept of stratum but is based solely on fossil content. We can define the biochronology as the study of the stratigraphic continental successions based on the correlation between fossil content and time (Lindsay, 1990). On the contrary, biostratigraphy is not considered as a measure of time, but a characterization of rock strata based on their fossil content (Lindsay, 1990). Lindsay (1990) summarizes biochronology as: “The study of biochrons”. Prior to 1970, the use of the term "biochronology" (and, with it, "biochron") is rather rare in scientific literature. A first definition of "biochron" can be found in Williams (1901): "a time unit whose measure is the endurance of organic characters".

However, only after the spread of radiometric dating techniques and the consequent need of distinction between radiochronology and biochronology as two different aspects of geochronology it is possible to find more exhaustive definitions of biochronology (Lindsay, 1990). Berggren & Van Couvering (1974) suggest the application of the term "biochron" for geological time units based on palaeontological information without references to lithostratigraphy. In light of this definition, which is still valid, it is subsequently possible to define two different sequences that contain the same fossil taxa as contemporary.

Over the last decades, numerous types of biochrons have been described, based on different groups of land mammals and in different geographical contexts, both in Europe and in other parts of the world. Mein (1975) proposes a system of division of the European biochronological units called MN system ("Mammal Neogene"), based on small mammals. Guerin (2007) with his MNQ system, defines each biozone based on (i) first appearance of new taxa, (ii) evolutionary stage reached by certain well–defined mammal lineages and (iii) characteristic associations of taxa.

Using similar principles to MN and MNQ systems and focusing mainly on large mammals, Azzaroli (1977) describes the first biochronological scale of the Italian Peninsula, based on the concept of the Faunal Unit (FU). Following the general definition of biochron, according to Azzaroli (1977) the Faunal Unit is nothing more than a certain period of time characterized by the occurrence in a certain geographical area, of a certain mammal fauna. If a succession of FU is relatively homogeneous from the faunal point of view, it defines a Mammal Age. Then, when a new local faunal assemblage (as, for example, that of Pantalla or Pietrafitta in central Italy) is found and described in the Italian territory, it is, on the basis of the faunal content, attributed to a specific FU and to a given time interval. Obviously, magnetostratigraphic data, absolute dating, isotopic stages and other methods can be used supplementary to give a better time constrain to the various Faunal Units. After the pioneering work of Azzaroli, the most comprehensive publications on the Plio–Pleistocene Italian and European biochronology are those of Gliozzi et al. (1997) and Rook & Martínez–Navarro (2010), respectively. Since Faunal Units are based substantially on the fossil content of certain palaeontological locations, their chronological definition is necessarily variable in time, depending on the advancement in palaeontological discoveries and the identification of new sites. In other words, the chronological limits of Faunal Units may be subject to more or less substantial changes following the advancement of knowledge on first appearances (first occurrence, FO) or local extinctions (last occurrence, LO) for certain taxa. The Faunal Unit, based on the content of certain palaeontological localities, cannot be valid – by their own nature – for large geographical areas (e.g., Europe), but are commonly used on a regional scale

(e.g., Italy). However, scholars have often found similarities and tried to make correlations between Faunal Units also on extra–national scale, such as in the Mediterranean Basin. Due to the fact that this correlation is possible, in the present study we refer to the works in which the interval between the middle–upper Pliocene and Pleistocene is divided into three Mammal Ages, namely Villafranchian, Galerian and Aurelian, each characterized by its own succession of FUs. In particular, the most interesting age for our work is the so–called Villafranchian.

### 1.1 Villafranchian (app. 3.5– 1.0 Ma)

The biochronological unit "Villafranchian" was suggested by Pareto (1865) as a continental stage of fluvial and lacustrine fossil– bearing sediments in the locality of Villafranca d'Asti in Piedmont, Italy (Gibbard and Head, 2020). Pareto also suggested that the mammalian faunas from Upper and Lower Valdarno basins in Tuscany also belong to the Villafranchian unit (Rook and Martínez–Navarro, 2010). Moreover, according to Rook and Martinez–Navarro (2010) the Villafranchian unit was originally considered to be the earliest part of the continental Pliocene, however it is currently considered to refer to the time period between 3.5 Ma to 1.1–1.0 Ma (Rook and Martínez–Navarro, 2010). The attempt to subdivide the Villafranchian mammal assemblages had already begun in the 1960s by Howell (1959), Bout (1960, 1967), Bourdier (1961) and Azzaroli (1962) and after extensive discussions was finally divided into three different faunal units: early, middle and late Villafranchian (Rook and Martínez–Navarro, 2010).

#### 1.1.1 Early Villafranchian (~3.5 to ~2.6 Ma)– Late Pliocene

The early Villafranchian faunas of Eurasia are found in Italy (Piedmont– Villafranca d'Asti, Tuscany– Santa Barbara), Spain (Villaroya, Huescar–3, Las Higuerelas), France (Vialette, Les Etouaires), Romania (Tulucesti, Covrigi, Groserea, Cernatesti), Georgia (Kvabebi), Mongolia (Shamar) and Transbaikalia (Udunga) (Agusti et al., 2009; Mazo, 1989; Vislobokova et al., 1995, 2001; Oms et al., 1999; Radulescu and Samson, 2001; Lister and van Essen, 2003; Mazo et al., 2003; Lister et al., 2005) and Greece (Milia– Grevena Basin (van Logchem et al., 2010; Guerin and Tsoukala, 2013).

The Triversa FU (3.5–2.6 Ma) is one of the most important Faunal Units of the early Villafranchian (Rook and Martinez Navarro, 2010). It includes several taxa that still retain the affinities of subtropical faunal elements of the previous Mammal Age (Ruscinian), such as *Tapirus arvernensis, Mammut borsoni, Anancus arvernensis, Sus minor* and *Mesopithecus monspessulanus*, and are associated with new mammals that are more related to wooded environments, such as *Leptobos stenometopon, Stephanorhinus elatus, Pseudodama lyra, Pliocrocuta perrieri* and *Homotherium crenatidens* (Rook and Martínez–Navarro, 2010).

#### 1.1.2 Middle Villafranchian (~2.6 to 2.0 Ma)– Early part of the Early Pleistocene

The middle Villafranchian of Europe includes the Montopoli (Italy), St. Vallier (France) and Costa San Giacomo (Italy) FUs (Rook and Martínez–Navarro, 2010). According to Rook and Martinez– Navarro (2010), the Montopoli FU corresponds to the MN16b European MN system, and the lower limit of this unit corresponds to the Gauss/

Matuyama boundary (2.5–2.6 Ma) (Lindsay et al., 1980), thus correlating well with the redefined Pliocene– Pleistocene boundary.

Figure 1: Reconstruction of a middle Villafranchian landscape, based on the data from the site of Huélago (Spain). From left to right: *Equus stenonis, Gazellospira torticornis, "Leptobos elatus", Mammuthus meridionalis, Croizetoceros ramosus.* Illustration by Agusti and Anton (2005).

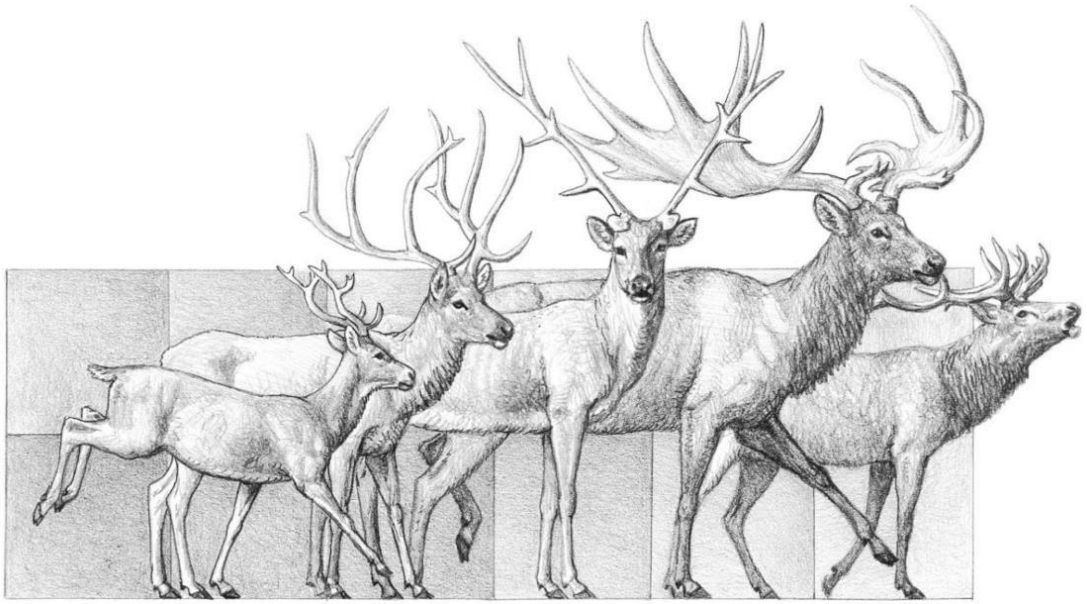

Figure 2: Comparison among five deer species from the European Pliocene and Pleistocene. From left to right: *Croizetoceros ramosus*, *Eucladoceros senezensis*, *Megaloceros savini*, M*egaloceros giganteus* and *Cervus elaphus*. Illustration by Agusti and Anton (2005).

During the early– middle Villafranchian, a faunal turnover took place, close to the Piacentian/ Gelasian boundary, known as the "elephant– *Equus* event" (Azzaroli, 1977; Lindsay et al., 1980) that describes the dispersal of two important large mammal genera in Europe: *Mammuthus* and *Equus* (Fig. 1). This turnover was characterized by the extinction of some subtropical species (Pradella and Rook, 2007) in favor of

prairie species caused by the "Glacial Plio/Pleistocene" climatic cooling, such as *Mammuthus gromovi, Equus liverzovensis, Stephanorhinus etruscus, Eucladoceros falconeri, Croizetocerus ramosus* (Fig. 2)*, Gazella borbonica, Lynx issiodorensis, Megantereon cultridens* and *Pliocrocuta perrieri* (Petronio et al., 2011). In general, the middle Villafranchian units are characterized by the first appearances (FAD) of taxa like: *Stephanorhinus etruscus, Equus stenonis, Sus* cf. *strozzii*, the rupicaprine *Gallogoral meneghinii*, *Gazellospira torticornis* and *Canis cf. etruscus* (Rook and Torre, 1996; Rook and Martínez–Navarro, 2010; Cherin et al., 2020). According to Rook and Martinez– Navarro (2010), the term "elephant– *Equus* event" should not be vastly used, as the genus *Mammuthus* and the modern single– toed equids have already been reported in the early Villafranchian European sites of El Rincon–1, (Spain), Roca–Neyra (France) the Dacic Basin (Radulescu and Samson, 2001; Lister et al., 2005) and Vialette (Lacombat et al., 2008).

The most important middle Villafranchian sites in Europe are: Montpoli (Lower Valdarno basin, Tuscany) and Costa San Giacomo (Anagni Basin, Latium) in Italy, Saint Vallier in France, Varshets in Bulgaria, and Sesklo, Vatera, Dafnero and Volakas in Greece (Spassov, 1997, 2000; Koufos, 2001, 2016; Kostopoulos and Athanassiou, 2005).

### 1.1.3 Late Villafranchian (~2.0 to ~1.0 Ma)– Rest of the Early Pleistocene (Olduvai to Jaramillo)

Figure 3: A riverine woodland at the site of Atapuerca (Spain) from the early Pleistocene. From left to right: *Sus scrofa*, *Eucladoceros giulii* and *Bison voigtstedtensis*. Illustration by Agusti and Anton (2005).

According to Rook and Martinez– Navarro (2010), the faunal turnover that took place during the Olduvai subchron affected both herbivore and carnivore assemblages. Most species from the earliest part of the Early Pleistocene disappeared, especially herbivores, whereas new carnivores and herbivores gradually appeared (Sala et al., 1992; Torre et al., 1992).
The faunal Units of the late Villafranchian are: Olivola FU, Tasso FU, Farneta FU and Pirro FU.

Olivola FU, the first stage of the late Villafranchian is characterized by two new important events: the so–called "*Pachycrocuta breviostris* event" (Martinez–Navarro, 2010) and the "wolf event" (Azzaroli, 1983) due to the impact of these two important carnivore taxa on the Early Pleistocene faunal assemblages in Eurasia. Rook and Martinez– Navarro (2010) suggest that the term "wolf event" should not be considered, as the presence of *Canis etruscus* has been confirmed in the previous stages of the Villafranchian in Eurasia, like in Costa San Giacomo and Vialette faunas. Other first occurrences are the ones of the following species: *Eucladoceros dicranios– ctenoides*, *Pseudodama nestii*, *Procamptoceras brivatense* and *Panthera gombazoegensis* (Rook and Martínez–Navarro, 2010).

The faunal assemblage of the Tasso FU is characterized by the appearance of the new taxa: the canids *Canis arnensis* and *Lycaon falconeri* (Rook, 1994; Martinez–Navarro and Rook, 2003), the ovibovinae *Praeovibos* sp. (De Giuli and Masini, 1983, 1987), *Leptobos vallisarni* and *Equus stehlini* (Rook and Martinez–Navarro, 2010), and *Pseudodama eurygonos–farnetensis* (Azzaroli, 1992). Moreover, the Tasso FU is characterized by the disappearance of the species *Megantereon cultridens* (Martinez–Navarro and Palmqvist, 1995; Palmqvist et al., 2007) and *Lycaon falconeri* (Martinez–Navvaro and Rook, 2003). Shortly after the Tasso FU, a new important first occurrence is recorded in the Mediterranean Europe: the genus *Homo* makes its first appearance (Rook and Martínez–Navarro, 2010); the Caucasian site of Dmanisi in Georgia marks the earliest Hominini out of the African continent (Gabunia et al., 2000; Lordkipanidze et al., 2007), as well as the first appearance of some herbivores coming from Asia, such as *Soergelia minor*, the antelope *Pontoceros ambiguous* and the primitive bison *Bison georgicus* (Fig. 3) (Bukhsianidze, 2005; Lordkipanidze et al., 2007; Palmqvist et al., 2007).

Farneta is the third late Villafranchian FU, whose faunal composition includes the first appearance of the megalocerine group, with the large deer *Praemegaceros obscurus* (Abbazzi, 2004) and the rhinocerotid *Stephanorhinus* cf. *hundsheimensis* (Alberdi et al., 1998).

Pirro FU is the last late Villafranchian Unit (De Giuli et al., 1987; Gliozzi et al., 1997), that is characterized by the occurrence of *Equus altidens*, *Praemegaceros verticornis*, *Lycaon lycaonoides* (Martinez– Navarro and Rook, 2003) and the first occurrence of *Theropithecus* sp. coming from the African continent (Rook et al., 2004; Rook and Martínez–Navarro, 2013).

The most important late Villafranchian sites are: Upper Valdarno (Florence and Arezzo provinces, Italy), Tasso, Farnetta, Olivola (Tuscany, Italy), Cava Pirro (Puglia, Italy) Fonelas P–1 (Guadix– Baza Basin, Spain (Arribas, 2008), Seneze (France) (Roger et al., 2000), Valea Graunceanului (Romania), Slivnitsa (Bulgaria), Gerakarou, Vassiloudi, Krimni, Kalamoto and Tsiotra Vryssi (Mygdonia Basin, Greece), Livakos (Western Macedonia, Greece), Alykes (Thessaly), Dmanisi (Georgia) and Untermassfeld (Germany) (Bolomey, 1965; Koufos, 1987, 2001, 2006; Koufos et al., 1992; Koufos and Kostopoulos, 1997; Malez et al., 1999; Roger et al., 2000; Arribas, 2008; Rook and Martinez– Navarro, 2010; Konidaris et al., 2016).

### 1.2 Palaeoenvironmental background

During the earliest part of the Villafranchian (approx. 3.5 Ma) the warm and humid environmental conditions of the Ruscinian (approx. 5.3–3.6 Ma) remained almost constant but at 3.2 Ma, a glacial phase began in the Northern Hemisphere. The first development of an ice cover in Greenland and the first aridity pulse in the Sahara was associated to this glacial phase (Madurell–Malapeira et al., 2014). At the same time, the series of climatic shifts started to characterize the Mediterranean area and led to the establishment of the modern Mediterranean climate, with warm and dry summers,

temperate winters and humid springs and autumns (Agustí & Antón, 2002). After this first short glacial pulse, an increase in temperature occurred, with average temperatures in the Mediterranean area being about 5 ºC higher than today (Lisiecki & Raymo, 2005; Bertini, 2010).

The Pliocene–Pleistocene (i.e., Early– late Villafranchian) boundary (about 2.6 Ma) marks the beginning of new climatic conditions completely different from the Pliocene ones. New bipolar dynamics of extensive glaciations, with glacial periods alternated with interglacial periods, modulated by the obliguity cycles of 41,000 years and which characterized the northern hemisphere (Clark et al., 2006). Although these first glacial pulses were less intense than the hard pulses of the Late Pleistocene, they caused significant changes in the ecosystems of middle and high latitudes, resulting to the first replacement of dense wooded areas by open landscapes similar to the tundra in Central and Northern Europe (Bertini, 2010).

Several strong glacial pulses have been documented during the Gelasian–Calabrian boundary (approx. 1.8 Ma) representing the beginning of another cold phase (Lisiecki & Raymo, 2005). In the Mediterranean area alternations between wooded environments and open landscapes were probably caused by this pulse (Bertini, 2010). At the end of the late Villafranchian (around 1.2 Ma) the tropical ecosystems were definitively replaced by deciduous forests habitats (Combourieu–Nebout, 1993, 1995).

### 1.3 Geological background

The site of Aghia Kyriaki is located in the South–Western part of Central Greece (Fig. 4) and near the settlement of Aghia Kyriaki (altitude approximately 1300 m.), municipality of Nafpaktia, district of Aetoloakarnania, Greece. The area belongs to the mountain range of Pindos.

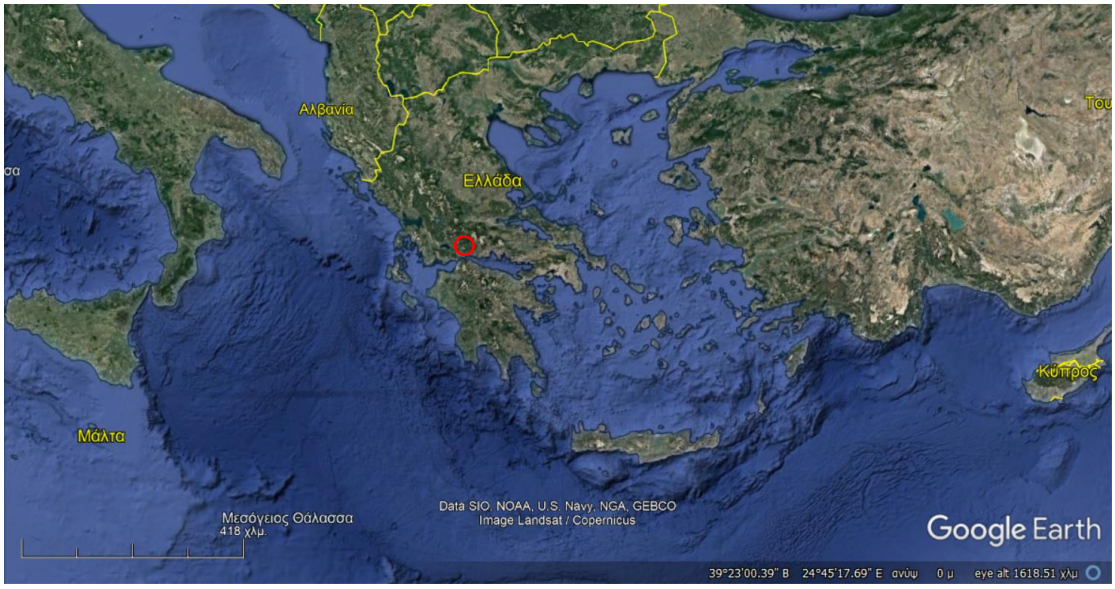


Figure 4: Map of Greece. The locality of Aghia Kyriaki is dispayed within a red circle. Map source: Google Earth Pro, accessed 05/01/2022.

The fossiliferous site, known as “Trypa” (i.e.: “Hole”) was a karstic cavity, filled with coarse material, reddish–brown clay, as well as fragments of limestones and cherts (Fig. 5). The palaeontological site is a fissure filling, thus, it has not been possible to

perform a stratigraphical study on it. The cavity is located at the transition from the "Radiolarites" Formation to the "Platy limestones" Formation, i.e. in the passage from the Lower to the Upper Cretaceous (Aptian–Cenomanian). Bouma sequences were identified in some horizons of Platy limestones, meaning that those sediments were deposited by turbidity flows. The cave entrance was recently damaged during the construction works associated with the cutting of a new dirt road.

Figure 5: Fossiliferous locality of Aghia Kyriaki. Photo during the excavations in 2019, personal archive.

### 1.4 Taphonomy

Taphonomy (from Greek words τάφος and νόμος, meaning burial and law, accordingly) is the study of the way organic remains pass from the biosphere to the lithosphere, as was originally proposed by Efremov (1940), and Taphonomy includes all the physical, chemical and biological processes that cause changes to an organism from the moment of its death through the decomposition, burial and preservation as a fossil (Behrensmeyer, 2021). The scientific meaning of the term taphonomy has been debated during the last century, as the approach has been used in different disciplines like palaeontology, archaeozoology and archaeology. The main difference between palaeontologists/ palaeobiologists and archaeologists is that the former use taphonomy for the study of organic/ living materials, whereas the latter for the study of both organic/ living and non–living materials (Lyman, 2010). According to Lyman (2010), taphonomy is divided in two different stages: the first one includes biostratinomy and refers to the time span between the organism's death and its final burial, whereas the second one, known as diagenesis, refers to the time span from the final burial (even in case of multiple burial events) till the recovery from the palaeontologists. During the latter stage the fossilization process occurs. That distinction is made as during the first taphonomical stage the main processes affecting the organisms' remains are biological, whereas during the second stage they are mostly geological and chemical (Lawrence, 1979a, 1979b, 1979c). Moreover, the

study of Taphonomy has now multiple applications, as it combines information on the conditions of death, burial and preservation of organisms as well as quality control mechanisms of the fossil record, especially when it is used to draw indirect conclusions, such as palaeoenvironmental and palaeoecological ones (Behrensmeyer and Kidwell, 1985; Behrensmeyer et al., 2000; Kostopoulos and Koufos, 2015). As a matter of fact, Behrensmeyer and Kidwell (1985) indicated that gnawing marks on bones suggesting predator activity and identity were also part of the taphonomical information.

According to Kostopoulos and Koufos (2015), after the death of an organism, starts the procedure of its decomposition caused by mechanical and climatic factors that take place on the surface of the earth. The main factor needed for the preservation and the fossilization of an organism is its quick burial in a certain place, usually sediment and in rare occasions ice, raisin etc. (Kostopoulos and Koufos, 2015 and refs therein). The quality and the completeness of the fossil record depend mostly on the time span between its death and burial, the distance and dynamics of transport from the death to the burial site, the intensity of the decomposition process (necrolysis), the composition, structure, form and durability of each part of the organism as well as the nature and size of the granules of the sediment of the final burying site (Wlison, 1988; Martin, 1999).

The resistance/durability against decomposition of the skeletal parts of the vertebrate organisms varies depending on the body type, the age of the individual, the type of tissues of the organism subjected to decomposition as well as their natural relationship within the organism (Kostopoulos and Koufos, 2015 and refs therein). The conditions of decomposition of the organic matter, depend on the environment in which they take place and in the case of surface decomposition on climatic and soil factors (humidity, soil temperature, type and abundance of the decomposing organisms etc.); thus, necrolysis is a complex process, that is hard to estimate accurately, especially as far as terrestrial vertebrates are concerned (Kostopoulos and Koufos, 2015). Moreover, in the ground surface there might be transportation of the body parts of the organisms by water flow or gravity, happening at the same time as necrolysis, as well as further actions caused by carnivorous and scavenging organisms, that result in higher levels of decomposition (Wilson, 1988, Martin, 1999). As far as transportation of the body parts is concerned, the main means of transportation in sea envionments are the sea currents, whereas in the land, the water currents (Babin, 1991; Martin, 1999). The effect of transportation of terrestrial vertebrates depends on five main factors: the dynamics of the mean of transportation, the depth of the means, the transport potential of the musculoskeletal parts themselves, their resistance to transport, rolling and abrasion and finally the dynamics of the transported materials moving through, like sand and cobbles (Kostopoulos and Koufos, 2015). Destructive events such as floods, result in mammal carcasses floating and then being deposited in river bands, where flow velocities are reduced (Kostopoulos and Koufos, 2015). In assemblages like these, all bone categories occur with similar frequencies, there is no particular orientation of the long bones and often complete skeletons and/or limbs are observed in a natural articulated position (Shipman, 1993; Kostopoulos and Koufos, 2015). However, in the case of non destructive events, known also as cumulative events where each bone moves independently, it is experimentally proved that the general shape, density and size of each one determine both its transport capacity and the way it moves (Voorhies, 1969).

Experimental research conducted both by Voorhies (1969) and by other later has shown that the long bones tend to be placed parallel to the flow direction, unless the water is very shallow, so they are placed transversely; the bones of the second group tend to be placed closer to the point of origin, while those of the first group tend to be placed further from the point of origin (Kostopoulos and Koufos, 2015 and refs therein).

The modification of the body parts of the organisms mainly concerns the hard skeletal parts and can be caused both during the transition from the death community to the burial community (ancestral modifications) and later during the diagenesis, but also after the formation of fossils (diagenetic modifications) (Shipman, 1993; Martin, 1999). Temporal modifications are mainly scratches and fractures, which can be due either to mechanical causes, from the rolling and collision of bones with each other and after coarse sedimentary components (gravel, cobbles), or to bio–disorders such as carnivory, scavenging, or etc. (Kostopoulos and Koufos, 2015 and refs therein). Several post–burial modifications during diagenesis and fossilization are due to the pressure of the overlying sediments towards the fossil horizon, in combination with the parallel chemical alteration to which the bones are subjected (Kostopoulos and Koufos, 2015). These modifications can be plastic, as in many cases of skulls, but also microcracks or collapses (Kostopoulos and Koufos, 2015 and refs therein). Finally, rupture fractures can occur after the completion of fossilization due to newer geological processes, such as tectonism (Shipman,1993; Koufos, 2004)

## 2. RESEARCH METHOD

The fossil specimens studied in this work include the whole fossil record from the locality of Aghia Kyriaki recovered so far. The excavations were carried out in four different phases: the first one during the year 2017 (141 fossils recovered), the next two in November 4$^{th}$ and 10$^{th}$ of the year 2018 (512 fossils recovered) and the fourth one in October 2019 (113 fossils recovered). Thus, the excavations ended up with 766 mammalian fossil specimens. The fossil collection of this site is hosted in the Laboratory of Palaeontology and Stratigraphy, Department of Geology, University of Patras.

In the present Thesis the basic stages of a palaeontological study were carried out: excavation and recovery of fossil material, preparation and conservation of the fossil material, their reconstruction, coding, identification in the level of osteology and basic taxonomy, biometric analysis and anatomical description. More specifically, the specimens were prepared, using chisels, geological hammers, GMT air compressor as well as brushes. Moreover, the plaster mold method was used in remarkably fragile and of significant value specimens, such as the *Ursus* cranium. Finally, a 10% acetone solution of acrylic resin Paraloid B72 was applied to the clean surface of the specimens in order to enhance the strength and the cohesion of the bone tissues. The excavation was done in parts, in blocks, then the excavated bones and fragments of these were separated and subsequently coded based on the exact location in which were initially identified. Then, with careful observation of the bone fragments, sections belonging to the same bone were bonded, using acrylic resin of UHU type. Each specimen was given a code beginning with the “AT” and then with a serial number. In total, 766 bones and fragments of those were coded.

As far as the micromammals are concerned, sediment from the locality of Aghia Kyriaki was collected during the three last excavation campagnes. The sediment was kept in bags and was later transferred in the Laboratory of Palaeontology and Stratigraphy, School of Geology, University of Patras. In the context of the present Master thesis, part of the sediment material was studied in the following way: the sediment samples were firstly sieved with the use of running water. Thus, the removal of particles of finer or larger size than the one of micromammals was achieved. As noticed, the finer particles usually were dispersed clays, whereas the larger particles were mostly rocks and stones. Three different sizes of shieves were used during this process. Later, the microfossils were dried in an electric oven, under relatively low and steady temperature. Then, followed the selection of the microfossils, amongst similar sized,

non fossil particles: the samples were divided in smaller quantities, observed with the use of a stereoscope under different magnification, and isolated with the use of precision tweezers and/or a small sized sable–hair brush. Finally, the specimens were carefully transferred to different microscope slides, supported onto plasteline–type adhesives and observed again under different magnification stereoscopes.
The specimens osteologically and classified, thus, each bone was identified by its type (e.g. ulna, tibia, vertebra), its relative position/ orientation in the body (left, right, frontal, distal) and finally the taxon of the animal to which it was considered to belong to.

**2.1 Anatomical description.**
The anatomical description of each specimen was carried out. Concerning the Artiodactyla, the anatomical description of teeth and mandibles followed Bärmann and Rössner (2011) (Fig. 6) and Suraprasit et al. (2016) (Fig. 7-8), whereas the anatomical description of the postcranial elements followed Brown and Gustafson (2000). As far as the Ursidae specimens are concerned, the anatomical description of the teeth followed Prat–Vericat et al. (2020) (Fig. 9), whereas the anatomical description of the postcranial elements followed Mazza and Rustioni (1992); astragali and calcanei were described according to Fournier et al (2020) (Fig. 10–11).

**2.1.a Ruminantia anatomical terminology**

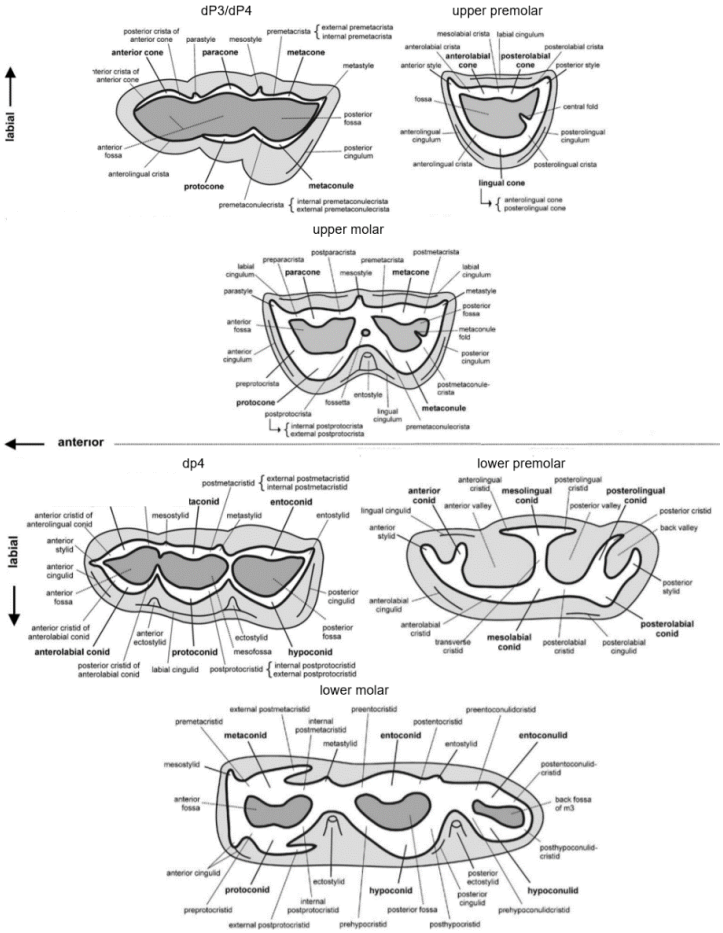


Figure 6: Terminology of Ruminantia teeth. From left to right: anatomical terminology of upper deciduous P3 and P4, upper premolar, upper molar and lower deciduous p4, lower premolar and lower molar. Figure by Bärmann and Rössner (2011), modified.

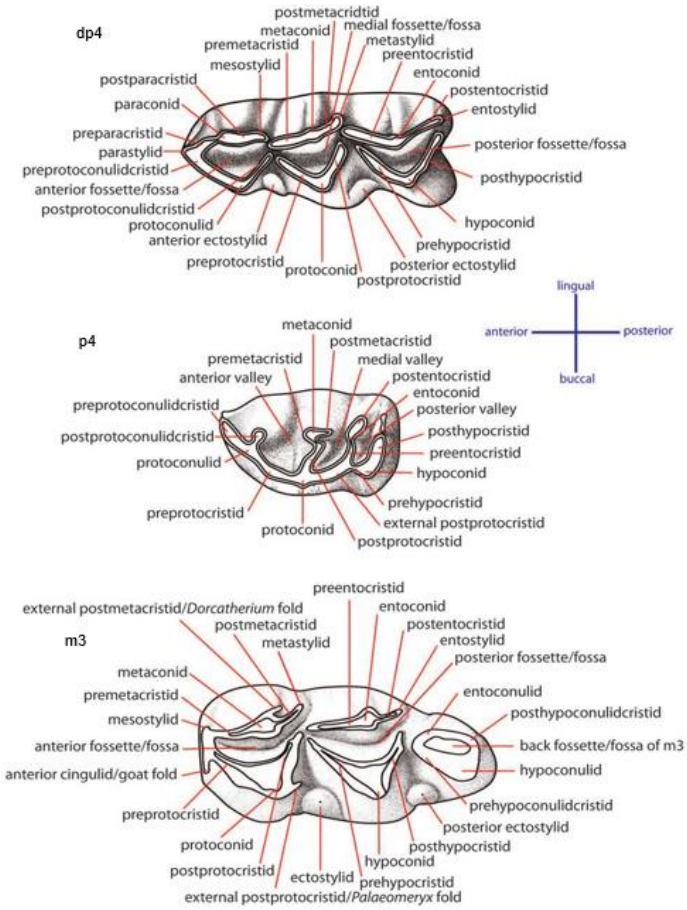


Figure 7: Anatomical terminology of Ruminantia lower teeth. From top to bottom: deciduous p4, p4, m3. Figure by Suraprasit et al. (2016), based on Heintz (1970), Gentry et al. (1999) and Bärmann and Rössner (2011), modified

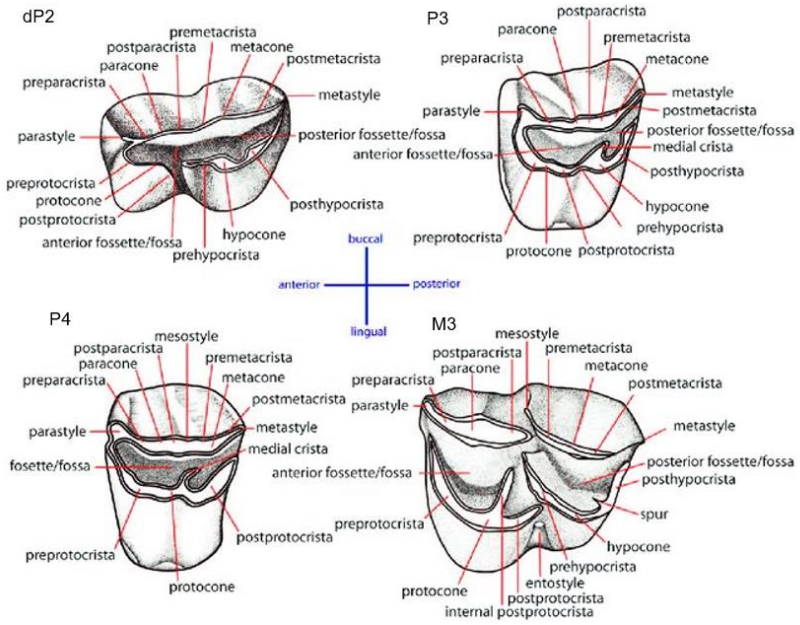


Figure 8: Anatomical terminology of Ruminantia upper teeth. From left to right: deciduous P2, upper P3, upper P4 and upper M3. Figure by Suraprasit et al. (2016), based on Heintz (1970), Gentry et al. (1999) and Bärmann and Rössner (2011), modified.

**2.1.b Ursidae anatomical terminology**:

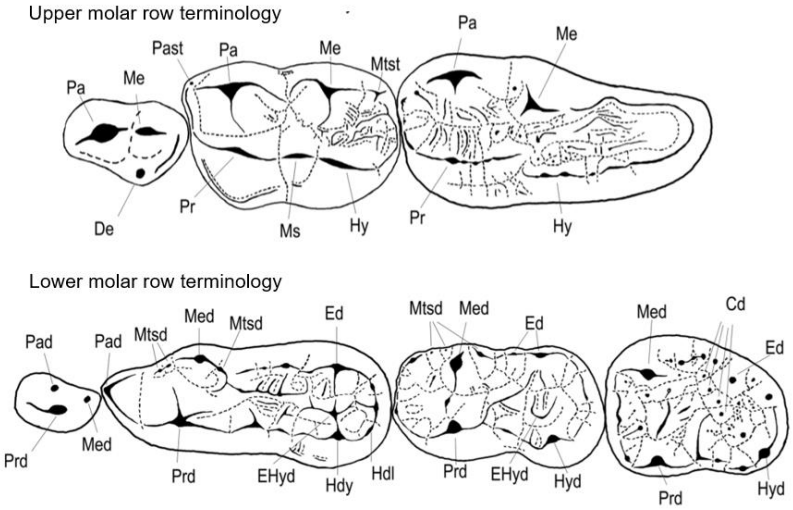


Figure 7: Anatomical terminology of Upper and lower molars. Upper molars abbreviations: Pa: Paracone, Me: Metacone, Mtst: Metastyle, De: Deuterocone, Pr: Protocone, Ms: Mesocone, Hy: Hypocone, T: Talonfield. Lower molars abbreviations: Pad: Paraconid, Prd: Protoconid, Med: Metaconid, Mtsd: Metastylid, Ed: Entoconid, Hyd: Hypoconulid, Ehyd: Enthypoconid, Cd: Centrolophid. Figure by Prat– Vericat (2020), based on Rabeder (1999), modified.

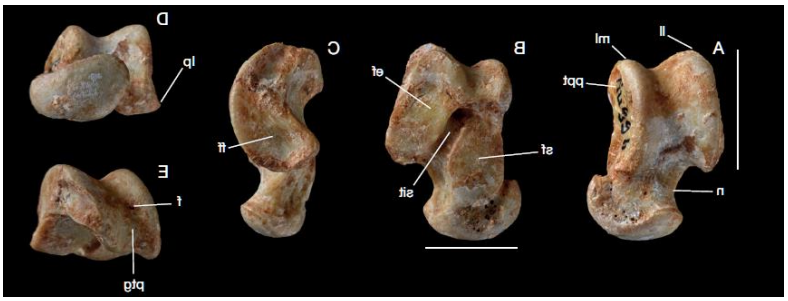


Figure 8: Anatomical terminology of left astragalus, in A: dorsal view, B: ventral view, C: lateral view, D: distal view, E: proximal view. Abbreviations: ll: lateral lip, lp: lateral process, ml: medial lip, ppt: proximal plantar tuberosity, n: neck, sf: sustentacular facet, sit: sinus of the tarsus, ef: ectal facet, ff: fibular facet, f: foramen, ptg: plantar tendon groove. Figure by: Fournier et al. (2020), modified.

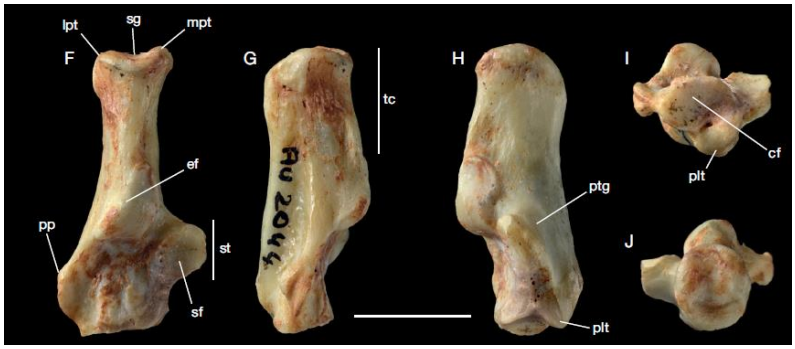


Figure 9: Anatomical terminology of right calcaneus in F: dorsal view, G: lateral view, H: medial view, I: distal view, J: proximal view. Abbreviations: cf: cuboid facet, ff: fibular facet. h: head, lpt: lateral process of tuber, mpt: medial process of tuber, plt: plantar tubercle, pp: peroneal process, sg: sagittal groove, st: sustentaculum tali, tc: tuber calcanei, tr: trochlea. Figure by: Fournier et al. (2020), modified.

## 2.2 Measurements

### 2.2.a Ursidae

Cranium

The measurements of the *Ursus* skull were taken according to Van den Driesch (1976) and Mazza and Rustioni (1992), as can be seen in Figure 12.

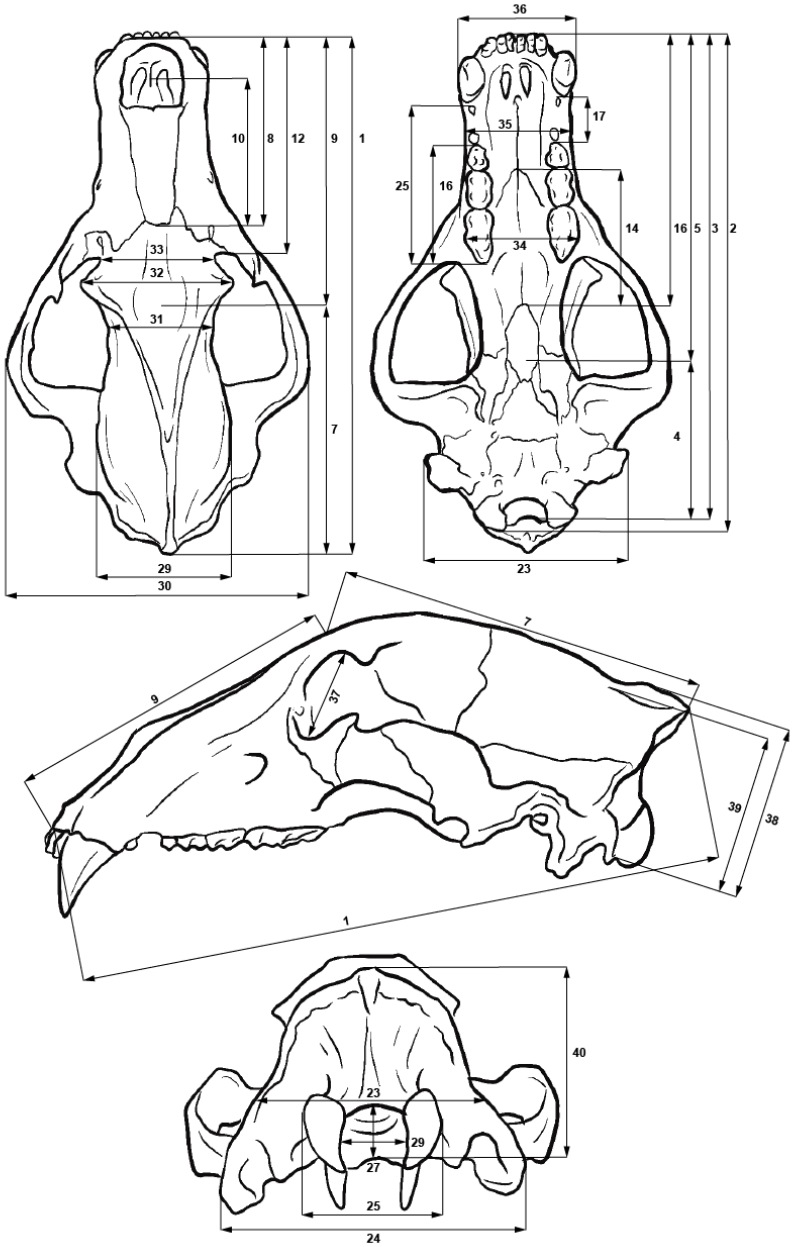


Figure 10: Measurements of *Ursus* cranium, following Van den Driesch (1976). Artwork by Leonardo Sorbelli (2021).

For the measurement of the cheek teeth of the Ursidae specimens, two basic dimensions were measured: Length and Width of the occlusal surface.

### 2.2.b Ruminantia

For the teeth measurements of Bovidae specimens, the method of Cregut–Bonnoure (1995a) was followed (Fig. 13).

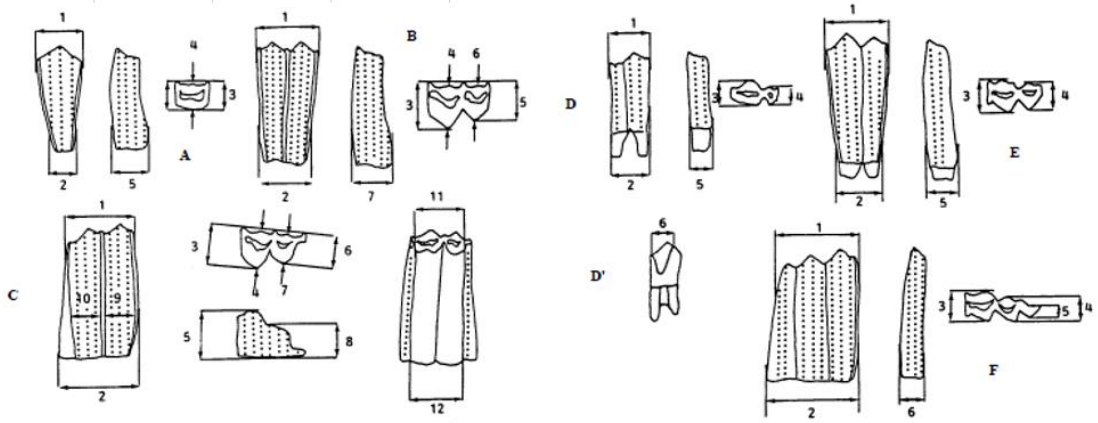

Figure 11: A: upper premolar, B: first upper molar, C: third upper molar, D: lower premolar, D': lower third premolar, E: second lower molar, F: lower molar. Figure by Rivals (2002) based on Cregut– Bonnoure (1995a), modified.

For the measurement of postcranial elements of specimens attributed to the order of Artiodactyla, the method of Sorbelli et al. (2021) was followed, as shown in Fig. 14.

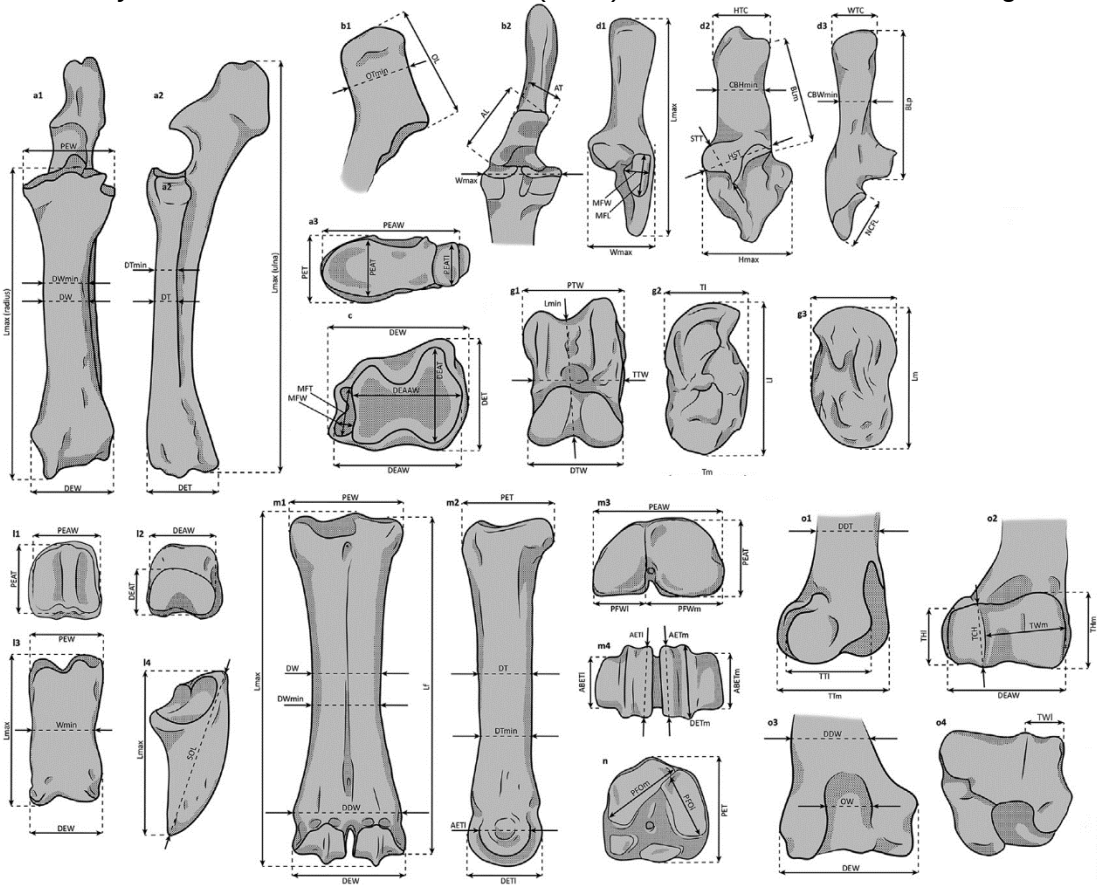

Figure 12: a. Radio–ulna in (1) anterior, (2) proximal and (3) distal view., b. ulna in (1) lateral and (2) anterior view; c. tibia in distal view; d, calcaneum in (1) anterior, (2) medial and (3) posterior view, g. astragalus in (1) anterior, (2) lateral and (3) medial view, h. cuneiform in (1) distal and (2) medial view, l. phalanx in (1) proximal, (2) distal and (3) anterior view, l. distal phalanx in (4) anterior view, m. metacarpal in (1) anterior, (2) posterior, (3) proximal and (4)

distal view, n. metatarsal in proximal view, o. humerus in(1) lateral, (2) posterior, (3) anterior and (4) distal view, p. thoracic vertebra in (1) anterior and (2) lateral view. Measurement abbreviations in Sorbelli et al. (2021). Figure by Sorbelli et al. (2021), modified.

### 2.3 Taphonomy

In the present thesis, the taphonomy was approached using the bone weathering characterization according to Behrensmeyer (1978), the abrasion stage according to Fernandez– Jalvo (2016), biting and gnawing traces according to Mikulas et al (2006), discoloration and staining characterization according to Fernandez– Jalvo (2016).

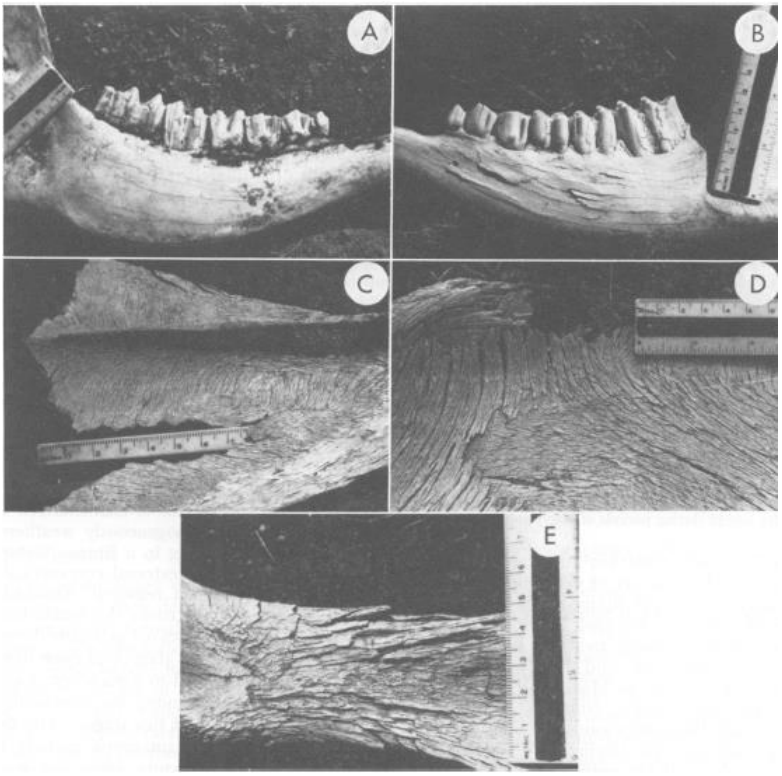


Figure 13: Weathering stages of bones according to Behrensmeyer (1978): A: weathering stage 1, B: weathering stage 2, C: weathering stage 3, D: weathering stage 4, 3: weathering stage 5. Figure from Behrensmeyer (1978).

As far as the bone weathering characterization is concerned, Behrensmeyer (1978) describes six successive stages:

Stage 0: no cracking or flaking signs due to weathering (Behrensmeyer, 1978).

Stage 1: Cracking, mainly parallel to the fiber structure, the articular surfaces might present mosaic cracking (Fig. 15–A) (Behrensmeyer, 1978).

Stage 2: the outer layers of the bone are flaking and might have crackings in the edges. In the initial part, long, thin flakes are still attached to the bone. In the final part of the second stage, the flaking is deeper and more extensive, so that most of the outer part of the bone is gone (Fig. 15–B) (Behrensmeyer, 1978).

Stage 3: The surface of the bone is rough, homogeneously weathered, resulting in a fibrous texture; the depth of the weathering is no deeper than 1.0–1.5 mm. in this stage (Fig.15–C) (Behrensmeyer, 1978).

Stage 4: The surface of the bone is fibrous and rough, with fragile splinters and open cracks (Fig. 15– D) (Behrensmeyer, 1978).

Stage 5: The bone is fragile, easily broken and falling apart in situ, thus making the determination of the original bone shapes difficult (Fig. 15–E) (Behrensmeyer, 1978).

Behrensmeyer (1978), suggested that each weathering stage as determined from the Amboseli region could be correlated to a possible time range since the death of each carcass she studied: thus, weathering stage 0 can be correlated with deaths occurring 0–1 years ago, weathering stage 1 can be correlated to deaths occurring 0–3 years ago, weathering stage 2 can be correlated to deaths occurring 2–6 years ago, weathering stage 3 can be correlated to deaths occurring 4 till more than 15 years ago, weathering stage 4 can be correlated to deaths occurring 6 to more than 15 years ago and weathering stage 5 can be correlated to deaths occurring 6 to more than 15 years ago.

Behrensmeyer (1978) also proposed that the application of this system to fossils could be simplified, by using three main categories: fresh weathering (stage 0), slight weathering (stage 1–2) and weathered (stage 3–5). Moreover, the weathering stage of a bone could also be affected by the habitat of the animal, and thus it could be indicative of it. As a matter of fact, swamp and dense woodlands, where moisture and shade tend to moderate the seasonal range of temperature and humidity, lead to slower weathering and thus to a lower weathering stage, than in other habitats (Behrensmeyer, 1978). Moreover, Behrensmeyer (1978) suggested that animals with a small body mass tend to exhibit faster weathering signs than animals with a body mass larger than 100kg. Moreover, an assemblage with all bones in the same weathering stage could indicate a catastrophic event or local conditions (rapid burial etc.) that inhibited weathering of gradually accumulating skeletal remains (Behrensmeyer, 1978).

As far as the abrasion degree of the bones is concerned, the system proposed by Fernandez–Jalvo (2016) was followedwhich proposes four degrees of abrasion: slight, moderate, heavy and extreme. In our study, we included no abrasion into the first category, thus transforming it into no to slight abrasion degree. According to Fernandez–Jalvo (2016), the degree of abrasion of the bones of mammals is affected by four main factors: type of bone (a. fresh, b. dry, c. weathered, d. fossilized) the sediment type of deposit, the duration and the strength of the factor causing the abrasion. In an experiment set by Fernandez–Jalvo (2016) in all types of bones, for a monitored period of 31 days, bones deposited in fine sand sediments had lightly rounded broken ends, bones deposited in coarse sand sediments noted a slight abrasion degree, whereas bones deposited in gravel sediments had an extensive abrasion degree, with loss of bone tissue and extreme broken ends.

According to Mikulas et al. (2006), there are six categories of biting and gnawing traces: a) traces of solitary bites, with outlines of individual teeth or a series of teeth,

b) gnawing traces, with parallel to subparallel dense grooves

c) scratching traces, not densely spaced traces, that could be parallel or crossing

d) nibbling traces, that appear as pits or short striae of random orientations

e) tooth imprints, represented by solitary or grouped pits, with mainly flat bottoms

f) traces of bone breaking, with fractures straight to acute, created by breaking the cortical into the cancellous bone.

Tooth imprints could be attributed to hunting, consumption of soft tissue or crushing bones whereas neebling traces can be attributed to consumption of bone tissue (Mikulas et al., 2006). However, gnawing marks are more complex to be attributed to a specific factor (Mikulas et al., 2006).

Other modifications of the surface of bones are discoloration and staining. Discoloration and staining of bones, belong to inorganic and organic modifications. More specifically, black staining in all the surface of a specimen or even in a patchy outline, is an indicator of manganese dioxide presence in the sediments where the fossils are deposited (Fernandez–Jalvo, 2016). The extent of the black staining could indicate the degree and the velocity of immersion of the bone to water or wet surfaces (Fernandez–Jalvo, 2016). Other characteristic causes of manganese dioxide is the formation of dentritic like patterns in the surface of the bones (Fernandez–Jalvo, 2016). In some bones, other discolorations may appear, like brown and black variable staining. Mainly, brown staining or lightening of the color of the surface of fossilized bones, might be an indicator of activity of organisms in the soil (bacterial attack), corrosion, fire, or root marks (Fernandez–Jalvo, 2016). Finally, reddish brown color staining could be an indicator of iron rich as well as oxygenated and biologically active soils (Fernandez–Jalvo, 2016).

## 3. TAPHONOMY

### 3.1 Completeness of material

As far as the completeness of the Aghia Kyriaki material is concerned, from the 767 collected elements, only the 54 (7.04%) are complete anatomical elements, 319 (41.59%) are parts of bones and 394 (51.37%) are fragments (Fig. 16).
Consequently, only a small part of the fossil material could be safely recognized, measured and attributed to a specific taxon.

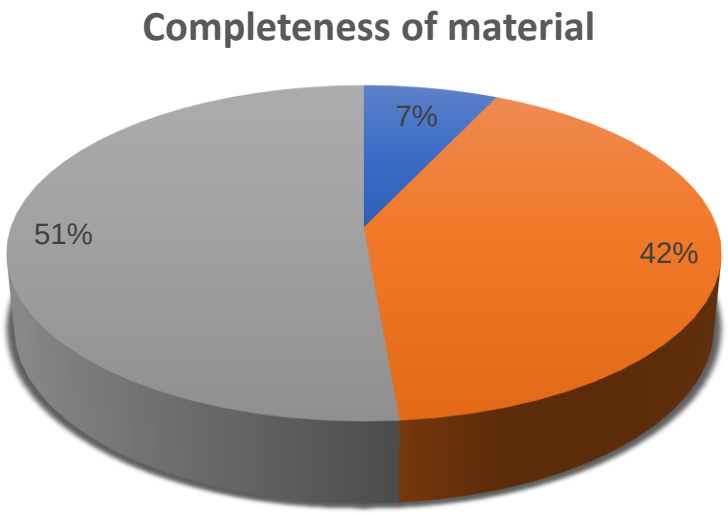


Figure 14: Pie chart of percentages of different types of material., based in their completeness. Blue: complete anatomical elements, Orange: broken anatomical elements and Grey: Fragments.

### 3.2 Abrasion

All the studied material showed no to slight abrasion signs. No rounding of bones was noted. The fact that bones in coarse sand have less abrasion signs than the ones in fine sand or gravel (Fernandez Jalvo, 2016), leads us to the assumption that the specimens of Aghia Kyriaki could have been deposited in coarse sand sediments, without excluding the possibility that the sediments were not of other type. Knowing that rounding of bones is a general indication of a long– term movement of water and sediment on beaches and in rivers (Fernandez–Jalvo, 2016), we can safely exclude the possibility of strong stream waters in the locality, as well as high energy underground waters. Since the bones were deposited in a karstic context as an infill we can assume that either the carcasses of the animals were placed in the cave or their bones were transported from a short distance by water and gravity and finally dropped in the cavity from an opening at the roof of the cave.

### 3.3 Bone weathering

All the fossiliferous material (besides the dental elements) was characterized based on its weathering stage, according to Behrensmeyer (1978). Thus, each element was characterized by a code from 0 to 5, based on how strong its weathering stage was (Fig. 17).

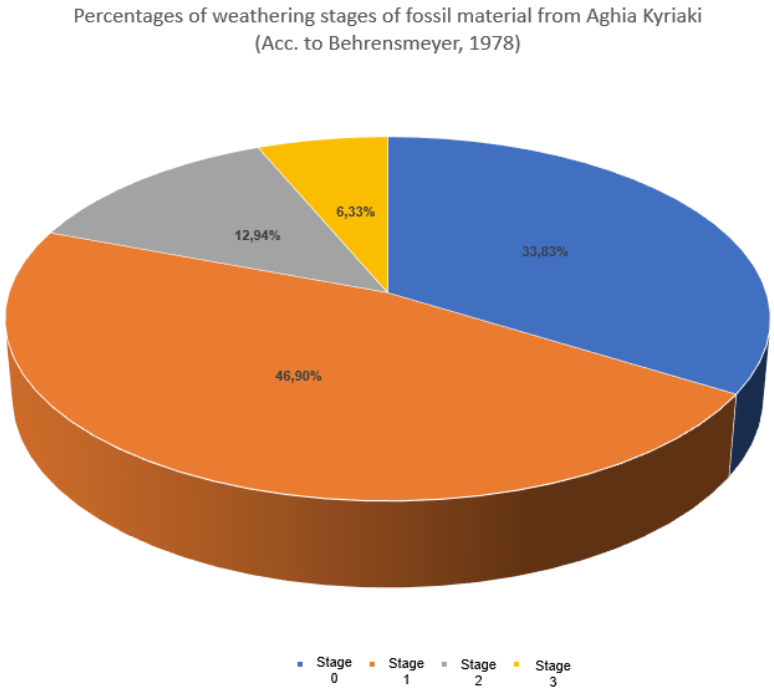


Figure 15: Pie chart of weathering stages of the non– dental material from Aghia Kyriaki. In Blue: weathering stage 0, Orange: weathering stage 1, Grey: weathering stage 2, Yleoow: weathering stage 3. Weathering stages acc. to Behrensmeyer (1978).

The study of the material showed that from the 742 non dental elements, 251 belong to weathering stage 0, 348 to weathering stage 1, 96 to weathering stage 2 and 47 to weathering stage 3, thus corresponding to percentages of 33.83%, 46.90%, 12.94% and 6.33%, respectively (Fig. 17).

The fact that not all the material has the same weathering stage, shows that the animals did not die due to a catastrophic event (Behrensmeyer, 1978), and that several of the bones were exposed on the surface for a certain time period before they were transported through the opening at the roof in the cave. Thus, we could assume that the fossiliferous material was gradually accumulated in the locality of Aghia Kyriaki and obtained different weathering stages based on the time the bones were exposed to the environment, the time of burial as well as the climatic conditions of the region. The zero to low weathering stages of the majority of the material could be an indication that most of the animals were buried relatively quickly after their deposit to the site, thus were not severely damaged by extrinsic environmental factors like rain, extreme temperature range etc., without that being a scenario completely excluded.

### 3.4 Biting and gnawing traces

None of the studied material had biting and gnawing traces, thus gives us no straight ichnological information about possible hunting behavior in the site.

### 3.5 Discoloration and Staining

Most of the studied material is characterized by slight brown and black variable staining, dots of black discoloration, whereas some material is characterized by black patches of discoloration. According to Fernandez–Jalvo (2016), the brown staining could be an indicator of bacterial attack to the bones, whereas the black staining is indicative of the presence of manganese dioxide. The fact that most black stained specimens are not stained all over the surface but mainly in one surface, could be indicative that they were resting in a damp surface and periodically immersed in wet sediment, thus this is an additional information that argues that the bones were buried gradually and not immediately after the deposition of the corpses of the animals.

## 4. SYSTEMATIC PALAEONTOLOGY

**4.1 Mammalia indet.** Linnaeus, 1758

Cranial and dental elements: fragments of cranium (AT91, AT101), fragments of teeth (AT643, AT644)

Postcranial elements: fragments of ribs (AT197/AT207, AT320/AT321, AT423, AT492, AT493, AT579/AT581/AT582), fragment of rib with head of rib (AT213), glenoid fossa (AT253, AT308), fragments of long bones (AT108, AT118, AT721, AT738, AT740, AT741, AT749, AT750, AT751, AT752, AT753), diaphysis of radius (AT121), diaphysis of right humerus (AT123), diaphysis of femur? (AT146), fragments of pelvis (AT20, AT22, AT97, AT101, AT717), fragment of long bone (AT195, AT264, AT266, AT285, AT360, AT361, AT362, AT363, AT366, AT381, AT384/AT385, AT395/AT397, AT396, AT398, AT399, AT431, AT584, AT585, AT628, AT711, AT737, AT745), fragments (AT07, AT08, AT14, AT18, AT24, AT25, AT26, AT29, AT30, AT33, AT34, AT35, AT36, AT38, AT39, AT44, AT47, AT48, AT49/AT52/AT55/AT57, AT50/AT51, AT52, AT55, AT56, AT57, AT62, AT67, AT69, AT71, AT75, AT82/AT86/AT87/AT90, AT83a, AT83b, AT84, AT85, AT86, AT87, AT89, AT90, AT92, AT100/AT102, AT103, AT104, AT105, AT107, AT109, AT110, AT112, AT114, AT125, AT126, AT127, AT128, AT129, AT130, AT132, AT134, AT140, AT141, AT142, AT143, AT144, AT145, AT147, AT150/AT152, AT151, AT155b, AT156, AT157, AT161, AT162, AT163, AT164, AT165, AT166, AT167, AT169, AT170, AT171, AT172, AT173, AT174, AT175, AT176, AT177, AT180, AT181, AT184, AT158, AT179, AT191, AT194/AT211, AT195, AT215, AT219, AT220, AT221, AT229, AT231, AT233, AT234, AT235, AT236, AT237, AT238, AT240, AT242, AT245, AT246, AT247, AT249, AT250, AT322, AT324, AT358, AT368, AT369, AT370, AT373, AT375, AT380, AT381, AT382, AT383, AT386, AT394, AT419, AT424, AT425, AT434, AT435, AT436, AT437, AT440, AT442, AT448, AT478, AT479, AT480, AT481, AT482, AT483, AT486, AT487, AT488, AT489, AT490, AT491, AT503, AT578/AT583, AT584, AT585, AT586, AT592, AT604, AT605, AT607, AT609, AT625, AT626, AT642, AT203, AT204, AT206, AT209, AT223, AT224, AT226, AT255, AT258, AT259, AT267, AT268, AT269, AT273, AT274, AT275, AT276, AT277, AT278, AT279, AT280, AT281, AT283, AT287, AT291, AT317, AT334, AT337, AT338, AT339, AT340, AT343, AT344, AT345, AT347, AT348, AT349, AT350, AT351, AT372, AT377, AT378, AT379, AT387, AT388, AT389, AT390, AT391, AT400, AT401, AT402, AT404, AT405, AT406, AT407, AT408, AT409, AT410, AT411, AT413, AT414, AT415, AT416, AT420, AT421, AT422, AT439, AT446, AT451, AT452, AT453, AT502, AT506, AT507, AT508, AT509, AT510, AT511, AT512, AT513, AT514, AT515, AT516, AT517, AT518, AT519, AT520, AT521, AT522, AT523, AT524, AT525, AT526, AT527, AT528, AT529, AT530, AT531, AT532, AT533, AT534, AT535, AT536, AT537, AT538, AT539, AT540, AT541, AT542, AT543, AT544, AT545, AT546, AT547, AT548, AT549, AT550, AT551, AT552, AT553, AT554, AT555, AT556, AT557, AT558, AT559, AT560, AT561, AT562, AT564, AT566, AT568, AT569, AT570, AT571, AT572, AT573, AT574, AT575, AT576, AT580, AT587, AT588, AT589, AT590, AT591, AT593, AT594, AT596, AT597, AT598, AT599, AT600, AT601, AT603, AT606, AT608, AT610, AT611, AT612, AT613, AT614, AT615, AT617, AT618, AT619, AT620, AT621, AT622, AT623, AT624, AT629, AT633, AT634, AT635, AT641, AT648, AT649, AT650, AT715, AT716, AT746, AT747, AT655, AT660, AT720, AT728, AT729, AT730, AT737, AT739, AT742, AT744)

AT108
Diaphysis of long bone. Highly fragmented, not identifiable.

AT121
Diaphysis of radius. No measurements can be taken.

AT123
Diaphysis of long bone, probably mid–distal part of diaphysis of right humerus. No measurements can be taken.

AT118
Long bone, not recognizable, highly fragmented.

AT146
Incomplete part of diaphysis, probably of femur. Highly fragmented. No measurements can be taken.

AT737
Highly fragmented bone, not identifiable.

All of the material attributed to Mammalia indet. is composed by highly fragmented elements that do not retain anatomical identifiable features. The really scanty preservation of these elements didn't allow us to ascribe them to a specific taxon.

Order **Carnivora** Bowdich, 1821
Suborder Fissipedia Simpson, 1945
Family Ursidae Gray, 1825
Genus *Ursus* Linnaeus, 1758
*Ursus etruscus*, **Cuvier 1823**

**4.2 *Ursus etruscus*** Cuvier, 1758

**Material**

Cranium: ATcranium1

Dentition: P4 (AT260), one fragmented left maxilla with M2, M1 and P4 (AT656), three incisors (AT261, AT393, AT428), lower m3 (AT430), right lower m1 (AT652), two fragmented hemimandibles with empty tooth cases (AT567, AT713), three fragmented right hemimandibles without teeth (AT707, AT708, AT709), one fragmented left hemimandible without teeth (AT706), one mandible without teeth (AT712), upper canine (AT647) and one lower canine (AT595) (Table 1).

Table 1: Table of dental/ mandibular material from the site of Aghia Kyriaki, attributed to the species *Ursus etruscus*

| ID code | Site | Excavation Date | Orientation | Anatomical element |
|---|---|---|---|---|
| AT260 | Aghia Kyriaki | Nov. 2018 | | Lower p3 |
| AT261 | Aghia Kyriaki | Nov. 2018 | | Incisor |
| AT393 | Aghia Kyriaki | Nov. 2018 | | Tooth |
| AT428 | Aghia Kyriaki | Nov. 2018 | | Incisor |
| AT430 | Aghia Kyriaki | Nov. 2018 | Right | Lower m3 |
| AT567 | Aghia Kyriaki | Nov. 2018 | | Mandible |
| AT595 | Aghia Kyriaki | Nov. 2018 | | Lower canine |
| AT647 | Aghia Kyriaki | Nov. 2018 | | Upper canine |
| AT652 | Aghia Kyriaki | Nov. 2018 | Right | Mandible fragment (complete m1) |
| AT656 | Aghia Kyriaki | Nov. 2019 | Left | Maxilla (M2, M1, P4) |
| AT659 | Aghia Kyriaki | Nov. 2019 | | Tooth |
| AT706 | Aghia Kyriaki | Nov. 2019 | Left | Mandible |
| AT707 | Aghia Kyriaki | Nov. 2019 | Right | Mandible |
| AT708 | Aghia Kyriaki | Nov. 2019 | Right | Mandible |
| AT709 | Aghia Kyriaki | Nov. 2019 | Right | Mandible |
| AT710 | Aghia Kyriaki | Nov. 2019 | Right | Canine |
| AT712 | Aghia Kyriaki | Nov. 2019 | | Mandible |
| AT713 | Aghia Kyriaki | Nov. 2019 | | Mandible |

Postcranial skeleton: right humerus (AT19), left/right radius (AT21), fragmented tibia (AT670), three calcanei (right/leftAT433, AT754, AT755), left astragalus (AT718), right astragalus (AT719), 5 metacarpals (AT443– Mc1, AT355– Mc2, AT41– Mc2?, AT494– Mc3?, AT65– Mc4?), 15 unidentifiable metapodials (AT670, AT202, AT498, AT265, AT79, AT671, AT43, AT66, AT615, AT636, AT403/AT417, AT627, AT263, AT639,

AT499), 6 metatarsals (AT230– Mt1, AT217–Mt1, AT726–Mt1, AT663– Mt1, AT727–Mt2, AT364– Mt3).

**Description**

AT Cranium1

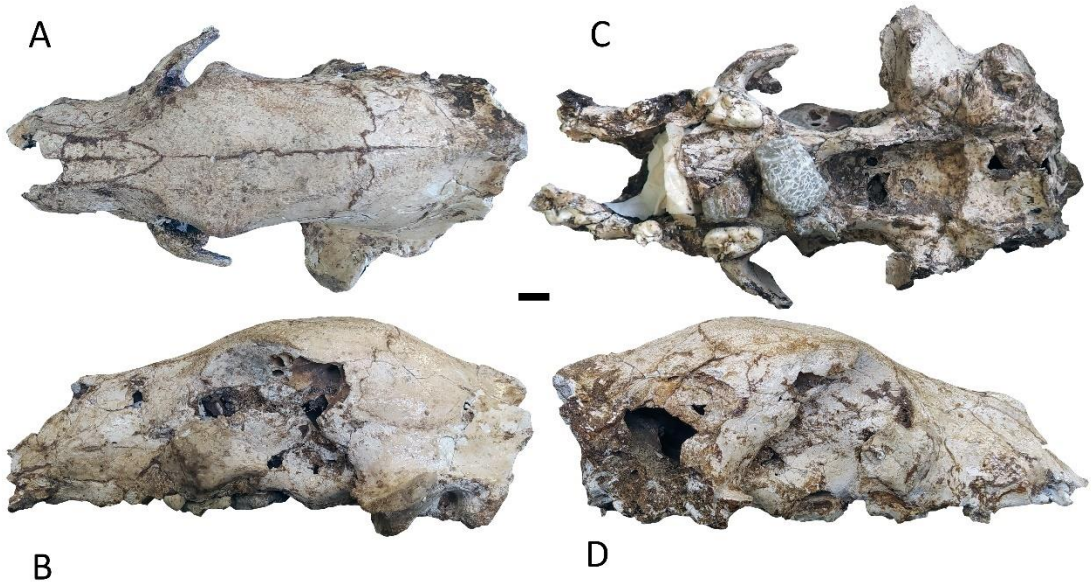


Figure 16: ATcranium1 in A: dorsal view, B: left side, C: ventral view and D: right side. Cranium from the locality of Aghia Kyriaki attributed to the species *Ursus etruscus*. Scale bar: 20mm.

The specimen is in a relatively well– preserved state, with a few broken parts. The zygomatic arch is not fully preserved in neither side. The squamosal is preserved only in the left side of the cranium. Part of the premaxilla is missing, as the cranium is broken at the anterior part of the nasal bone. On the frontal surface of the cranium, a number of cracks can be seen. The interparietal is destroyed on the right side (Fig. 18D), whereas intact on the left side (Fig. 18B). The parietal bone is well preserved, especially in the left side, and although several cracks appear it is not deformed. The mandibular fossa is well preserved, mostly in the left part of the cranium; it is cracked in the right part. Only in the left part, the paraoccipital process and the occipital condyle are preserved, whereas in the right part they are not complete. In posterior view, the interparietal seems slightly damaged. The occipital condyles as well as the lateral edges of the foramen magnum and the postorbital process are slightly broken. The lateral part of the frontal bone is also slightly damaged. In right–lateral view, the cranium is not as well preserved. Right anteriorly of the occipital bone, the squamosal is destroyed, resulting in a hole of the bone. The postorbital process is complete and in good preservation status, as well as the frontal and parietal bones. In ventral view, part of the maxilla is missing (Fig. 18C), whereas the borders and the morphology of the palatine and the vomer bones are not well visible, due to the adhesion of cemented sediment on the bone surface. In the right hemimaxilla, the M2 is almost complete, with a deep breakage in the anteriobuccal surface. The left M2 is cracked but preserved in its largest part. The right P4 is also preserved, but its occlusal surface is missing.

The neurocranium is elongated (Fig. 18A) and the forehead is straight (Fig. 18B, D). Between the akrokranion and the orbits, the cranium has a notable lateral constriction. The ectorbital processes are protruding, and the frontal appears rather flat to slightly convex. The temporal ridges are smooth and converging towards the posterior part of the cranium, located right proximally of the akrokranion. The suture between the frontal and the parietal bone is irregular. In left–lateral view, the sagittal crest is short and slightly protruding (Fig. 18B). The outline of the occipital condyles seems to be drop shaped, with an inclination towards the ventral side of the cranium. In ventral view (Fig. 18C), the jugal bone seems to develop laterally of the M2, right proximally of the talon. The right M2 is elongated with a relatively long talon and is characterized by the absence of a premetacone (small cusps in the lingual slope of the protoconid). The palatine appears to be thin and straight (Fig. 18C). The basioccipial is thin.

Figure 17: Selected dental material attributed to *Ursus etruscus*. Top: fragmented left maxilla with M2, M1 and broken P4, AT656in occlusal view, Bottom: Lower m3, AT430 in occlusal view. Scale bar: 20 mm.

Maxilla

The specimen AT656 is a fragmented left maxilla with M2, M1 and broken P4. The M2 is mediodistally longer and has an elongated talon (Fig. 19). The metacone and paracone of the M2 are both preserved and well- developed, with the paracone being stronger than the metacone. The anterior part of the M2 is higher than the talon. There is no premetacone (small cusps in the lingual slope of the protoconid) noted. In occlusal view, the M1 has a rectangular outline and bears a relatively weak parastyle and metastyle, with the former being more developed than the latter. The protocone and the hypocone are even less developed. The P4 is broken.

Upper canine

The upper canine (AT647) is almost complete and broken slightly above the base and appears to be slender.

Incisors

Two complete incisors that appear to be non–specialized and of simple morphology. (specimens AT261 and AT393)

AT640

Carnivoran tooth. The dental element is highly fragmented, with only four visible cusps. Its oreservation status does not allow the conduction of morphometrical analysis.

Hemimandibles

In posterior view, the outline of the mandibular condyle is oval shaped, with a mediolateral direction. The distal edge of the mandibular condyle is straight, whereas the proximal edge is slightly curved. The bone curves right distally of the mandibular condyle until the angular process. The angular process bends towards the medial side and it is laterally concave for the ligament of the mandibular muscles. The cavity between the mandibular condyle and the angular process is concave and smooth. In lateral view, an obvious ridge is formed and proceeds from the angular process towards the mandibular corpus, with a posterodistal to proximoanterior direction; the messeteric fossa is concave. The mental foramen of the mandible is drop– shaped. In medial view, the mandibular foramen is deep and proceeds towards the anterior side. In distal view, a stepped ridge is formed, with a slightly curved medioposterior to lateroproximal orientation. The most posterior part of this ridge is slightly pointed. The bone curves right distally of the mandibular condyle until the angular process. The medial surface of the ramus ascedens is curved, whereas the lateral one seems to be straight.

The specimen AT708 (right hemimandible, without teeth), has a crashed mandibular condyle in the posterior view. The specimen AT713 (tight hemimandible without teeth) has a partly broken mandibular condyle, as well as a broken angular process and coronoid process. The specimens AT706 (left hemimandible with empty alveolar cavities) and AT567 (left hemimandible with transversally cracked m3 and m2 in the base of the teeth and empty m1 alveolar cavity), are broken anteriorly of the mandibular condyle and the angular process. The specimen AT709, is vertically broken posteriorly of the p3 tooth, and all of the teeth are broken in the base; However, the specimen AT710 (lower carnassial, fragmented on the base), seems to belong to this specimen.

Lower canines

The lower canines (AT595, AT710) are slender and relatively short. The specimen AT595 is broken on the root surface and in the upper part of the tooth as well, whereas the specimen AT710 is broken under the base and seems to belong to the same individual as the specimen AT709.

Lower m1

The specimen AT652 is a right mandibular fragment with partly preserved m2 tooth, an almost complete m1 and a damaged p4 tooth. The m1 is buccolongually

compressed, whereas anteroposteriorly elongated. The talonid has a rather subrectangular outline on occlusal view, whereas the trigonid ends anteriorly in a rather curved paraconid.

Lower m3

The right lower m3 AT430 is broken right below the occlusal surface. In occlusal view (Fig. 19), the tooth appears oval to subrectangular, with the anterior part being slightly more oval shaped than the posterior one. There are no developed cingula in this tooth. The anteroposterior dimension is broader than the buccolingual one.

Postcranial elements

Several postcranial elements from Aghia Kyriaki were attributed to *Ursus etruscus*; some selected elements can be seen in the Fig. 20.

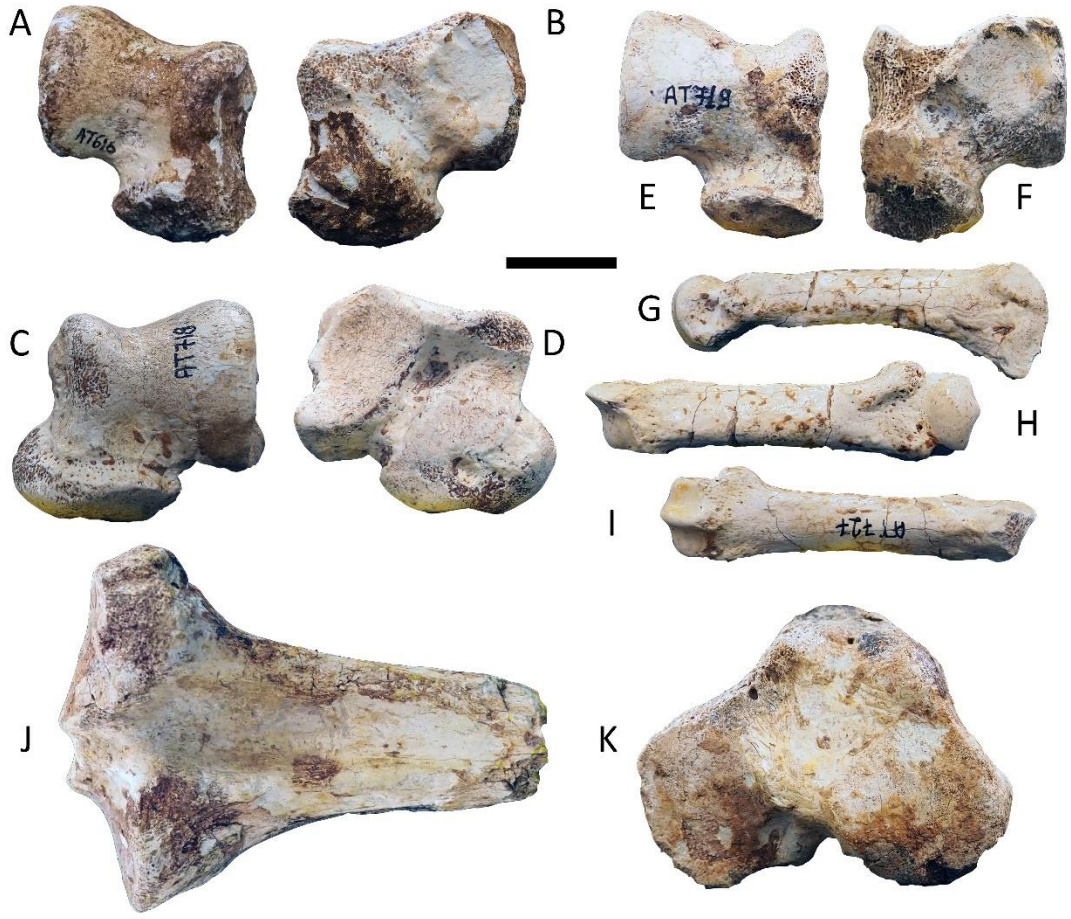


Figure 18: Postcranial elements of *Ursus etruscus* from Aghia Kyriaki, Greece Right astragalus AT616 in A: dorsal and B: ventral view, right astragalus AT718 in C: dorsal and D: ventral view, left astragalus AT719 in E: dorsal and F: ventral view, left metacarpal IV AT727 in G: medial, H: anterior and I: posterior views, tibia AT670 in J: posterior and K: proximal views.

Tibia

The specimen AT670 is a complete proximal extremity of a right tibia. In proximal view, the proximal epiphysis is characterized by a medial and a lateral condyle, that are relatively flattened (Fig. 20K). In posterior view, the tibia is characterized by a deep

valley (Fig. 20J), whereas in anterior view, the tibial crest is broken right distally of the proximal epiphysis.

Astragali

In proximal view, the plantar tendon groove is relatively shallow and has a slightly proximodorsal to ventromedial direction. The lateral, medial and ventral borders of the proximal end seem to be well developed, in proximal view. In dorsal view (Fig. 20 A, C, E), the medial margin is slightly convergent to the lateral margin of the trochlea towards the distal end. The lateral rim is complete and parallel to the anteroposterior axis. Thus, the medial and the lateral rim are not parallel to each other. The neck of the astragalus is short and wide and the wide head, has a curved, almost semilunar–shaped outline. In ventral view (Fig. 20 B, D, F), the ectal facet is slightly elongated with a proximomedial to distolateral direction. The lateral border towards the distal part of the ectal facet is slightly broken, thus not allowing the exact description of the shape of the facet. The sustentacular facet (facies articularis talaris distalis*)* is oval–shaped, and its elongated axis is parallel to that of the ectal facet. Its medial and distal borders are well marked. The distolateral part of the sustentacular facet extends until the head of the astragalus (caput tali). Between the sustentacular facet and the head of the astragalus, a shallow round–oval shaped facet is visible. It is slightly convex except on its proximomedial extension, where it becomes concave. The sinus of the tarsus is dividing the ectal and the sustentacular facet and is oval shaped. A relatively shallow valley divides the ectal and sustentacular facets, with a direction parallel to both, and ends right proximally of the tarsal sinus. In lateral view, a slight depression is formed in the region of the fibular facet (Facis articularies calcaneae). The outline of the lateral view of the specimen is almost semilunar, with a wider distal base. In medial view, the proximal border of the astragalus seems wider than the head. In the distal view of the specimen, the head is dorsoventrally compressed, thinner on the medial side and wider towards the lateral side. The axis of the elongation of the head is parallel to the mediolateral axis of the bone. The distal view of the lateral lip of the trochlea is concave and ends in a pointed tip towards the ventral view.

The specimen AT718 is a complete right astragalus, exceptionally well preserved, with only slight weathering marks. The specimen AT719 is an almost complete left astragalus, with a broken ventral view and an outer medial surface of the specimen. These two specimens are of similar size. The specimen AT616 is an almost complete, left astragalus, that shares the same morphological characteristics as the specimens AT718, AT719. However, in proximal view, the ventral border of the proximal end is missing, so as the medial surface of the specimen. At a first look the specimen, seems smaller than the previous ones; however, considering the relatively high percentage of cracks in the aforementioned surfaces, we could attribute the specimen AT616 to the same taxon.

Calcanei

In proximal view, the proximal end has an oval shaped outline, with the anteroposterior diameter being larger than the mediolateral one. In dorsal view the sustentacular facet seems to have an oval shaped outline. The sustentacular facet (facies articularis talaris distalis) is elongated in a laterodistal– proximomedial direction and extends strongly towards the medial side. The distal articular surface seems to be slightly concave. The peroneal process seems to be broad. The ectal facet is well developed. It is

proximomedially– distolaterally elongated and convex. The medial edge of the facet is well marked. The outline of the medial surface of the sustentacular facet in anterior view seems to be oval– shaped. The peroneal process is wide. In lateral view, the dorsal and ventral edges of the tuber are slightly curved, and the tuber is dorsoventrally wide, with a slight proximodorsal to distoventral direction. In medial view, the groove for the plantar tendon (sulcus tendinis musculus flexor digiti lateralis) is pronounced. In distal view, the cuboid facet is slightly concave and oval shaped, with the mediolateral width longer than the proximodistal one. The plantar tubercle is smaller than the plantar tendon groove and it forms a distally oriented curved tip.
The specimen AT46 is an incomplete, left calcaneus, with a relatively high percentage of shallow cracks. The proximal end is broken. Thus, in dorsal view, the tuber calcanei and sagittal groove are not preserved. In dorsal view, the ectal facet (facies articularis talaris proximalis) is cracked. The medial surface of the sustentacular facet, as well as the dorsal and ventral edges of the tuber in lateral view, are broken. In distal view, the cuboid facet and the plantar tubercle cannot be distinguished. The specimen AT133 is a distal end of a right calcaneus. The specimen is incomplete and characterized by a great percentage of weathering marks. The proximal end is broken. In dorsal view, the sustentacular facet (facies articularis talaris distalis) is broken medially, thus the level of elongation is not visible. Moreover, the lateral outline of the dorsal view is cracked. The level of weathering and cracking does not allow a proper morphological attribution to a certain taxon, however, the specimen is quite similar to AT46. Also, the size difference (AT133 seems to be smaller than AT46), could also be attributed to the high level of weathering and cracking of AT46, or sexual dimorphism. The specimen AT575 is a proximal end of a possibly right calcaneus, that could belong to the same specimen as AT133. The specimen AT433 is a complete left calcaneus. The specimen is really well–preserved, with slight superficial cracks. In dorsal view, the sustentaculum tali is cracked proximomedially. The peroneal process is also slightly cracked laterally but seems to be broad. The lateral edge of the facet is destroyed. The distal edge of the facet is slightly broken but seems to be difficult to delimit it with the body of the calcaneum. The specimen appears to be similar to the previous ones. The specimen AT755 is a complete distl end of left calcaneus. The sustentaculum tali is complete and has a curved– circular outline in dorsal view.

Metapodials, proximal and intermediate phalanges

The metapodials and proximal and intermediate phalanges in anterior and posterior views appear to be straight and slender (eg. Fig. 20H, I). In medial view, the metapodials (Fig. 20G) and proximate and intermediate phalanges appear to be slightly convex in their posterior surface.

**Measurements**

The measurements of the specimens from Aghia Kyriaki attributed to *Ursus etruscus* are given in the Tables 2–4.

Table 2: table of the two basic measurements Greatest **L**ength (abbreviation: GL) and Greatest Width (abbreviation: GW) for the teeth M2 and M1 of the specimen AT656 from Aghia Kyriaki. Measurements in mm.

| ID code | Locality | GL (M2) | GW (M2) | GL (M1) | GW (M2) |
|---|---|---|---|---|---|
| AT656 | Aghia Kyriaki | 31.93 | 18.46 | 22.2 | 16 |

Table 3: Table of the measurements of the dental elements AT430, AT652 and AT260 from Aghia Kyriaki.Greatest length (Abbreviation: GL), Greatest Width (Abbreviation: GW), Anterior Breadth (Abbreviation: AB) and Posterior breadth (PB), of the specimens AT430, AT652 and AT260 from Aghia Kyriaki. Measurements in mm.

| ID code | Locality | GL | GW | AB | PB |
|---|---|---|---|---|---|
| AT430 (m3) | Aghia Kyriaki | 21.09 | 15.67 | 15.64 | 13.53 |
| AT652 (m1) | Aghia Kyriaki | 26.05 | 11.24 | 11.24 | 9.69 |
| AT260 (P4) | Aghia Kyriaki | 16.5 | 13.85 | | |

Table 4: Table of measurements of the specimen ATcranium**1** from Aghia Kyriaki. Measurements in mm, according to Figure 12

| Van den Dreisch (1976) | Mazza & Rustioni, 1992 | | AT CRANIUM (Aghia Kyriaki) |
|---|---|---|---|
| 1 | LAP | Length prosthion–akrokranion | >310 |
| 2 | LCP | Length prosthion– occipital condyle | |
| 3 | LBP | Length basion– prosthion | >280.14 |
| 6 | LBN | Length basion– nasion | |
| 7 | LAF | Length akrokranion– frontal midpoint | 168.2 |
| 8 | LNP | nasion– prosthion length | >113 |
| 9 | LFP | frontal midpoint–prosthion length | >145.7 |
| 10 | LNR | Length nasion– rhinion | 91.5 |
| 12 | LOrP | orbital cavity–prosthion length | >114.5 |
| 13 | LStP | staphylion– prosthion length | 163 |
| 14 | LStPO | staphylion–palatinoorale length | 72.91 |
| 23 | BOtOt | otion–otion breadth | >124.46 |
| | BTcTc | least breadth between temporal crests | |
| 25 | BoC | greatest breadth of the occipital condyles | |
| 26 | Bpop | greatest breadth of the paraoccipital processes | |
| | Bsoc | greatest breadth of the supraoccipital crest | |
| 27 | Bfm | greatest breadth of the Foramen magnum | |
| 29 | BEuEu | greatest breadth between the eurions | 91.78 |
| 30 | BZyZy | greatest zygomatic breadth | |
| | BpOr | least postorbital breadth | |
| 32 | BEcEc | greatest frontal breadth | 93 |
| 33 | BEnEn | least breadth between the orbits | 67.65 |
| 34 | Bpal | greatest palatal breadth | 92.9 |
| | BpCa | least breadth behind the canine alveoli | 72.9 |
| 36 | BCaCa | greatest breadth of the canine alveoli | 75 |
| | Hor | greatest height of the orbital cavities | 46.13 |

**Comparison**

The cranium ATcranium1, bears the basic characteristics of Ursidae crania: large sized, with reduced sagittal crest, heavy zygomata and the occipital crest being the most posterior part of the skull; The orbits are open at the back and the nasal bones are short to medium in length. The molars vary in size and shape but are flat and large.

The morphology of the skull, with the slender appearance and weakly prominent temporal lines that converge in the posterior part of the neurocranium leads us to the assumption that the skull belongs to a female individual.

The main Plio–Pleistocenic representatives of the Ursidae family in the European area are *Ursus minumus* (early Pliocene– early Villafranchian), *Ursus etruscus, Ursus spelaeus, Ursus deningeri, Ursus thibetanus, Ursus ingressus*, *Ursus arctos* (Pappa and Tsoukala, 2022) and *Ursus dolinensis* (Garcia and Arsuaga, 2001). The morphology of the cranium of *Ursus spelaeus* is characteristic and distintinctive amongst the other species, as *U. spelaeus* is a big sized bear with a remarkably stepped forehead (Pappa and Tsoukala, 2022). *Ursus deningeri* is supposed to have a great variability in morphology but cannot reach the level of stepped forehead the former species notes (Pappa and Tsouukala, 2022). Moreover, *Ursus etruscus* may bear primitive characteristics (straight forehead, thin and straight palatine, arched anterodorsal profile of the brain cavity etc.) that distinguish it from the spelaeoid group of bears, i.e. *U. deningeri* and *U. spelaeus*. According to Koufos et al. (2017), *Ursus dolinensis* from Gran Dolina differentiates from *U. etruscus* by its thick palate. On the other hand, *U. etruscus* is difficult to differentiate from *U. arctos*, because the latter retains the primitive characteristics of the former.

In general, the morphology of the cranium ATcranium1 from Aghia Kyriaki shares primitive characteristics (straight forehead, thin and straight palate, thin basioccipital, teeth morphology). Thus, the specimen belongs to the primitive state group of bears and not in the spelaeoid– cave bears *U. spelaeus*, *U. deningeri*. Also, the specimen ATcranium1 is characterized by a thin palate, thus differs from the species *U. dolinensis*.

The preservation status of the specimen ATcranium1 from Aghia Kyriaki, does not allow taking measurements helpful for the conduction of diagrams that could distinguish or group our specimen with other Ursid representatives. Thus, we suggest that the craniodental morphology as well as the dental measurements could be more helpful in the attribution of the specimen to the lineage of *Ursus etruscus*.

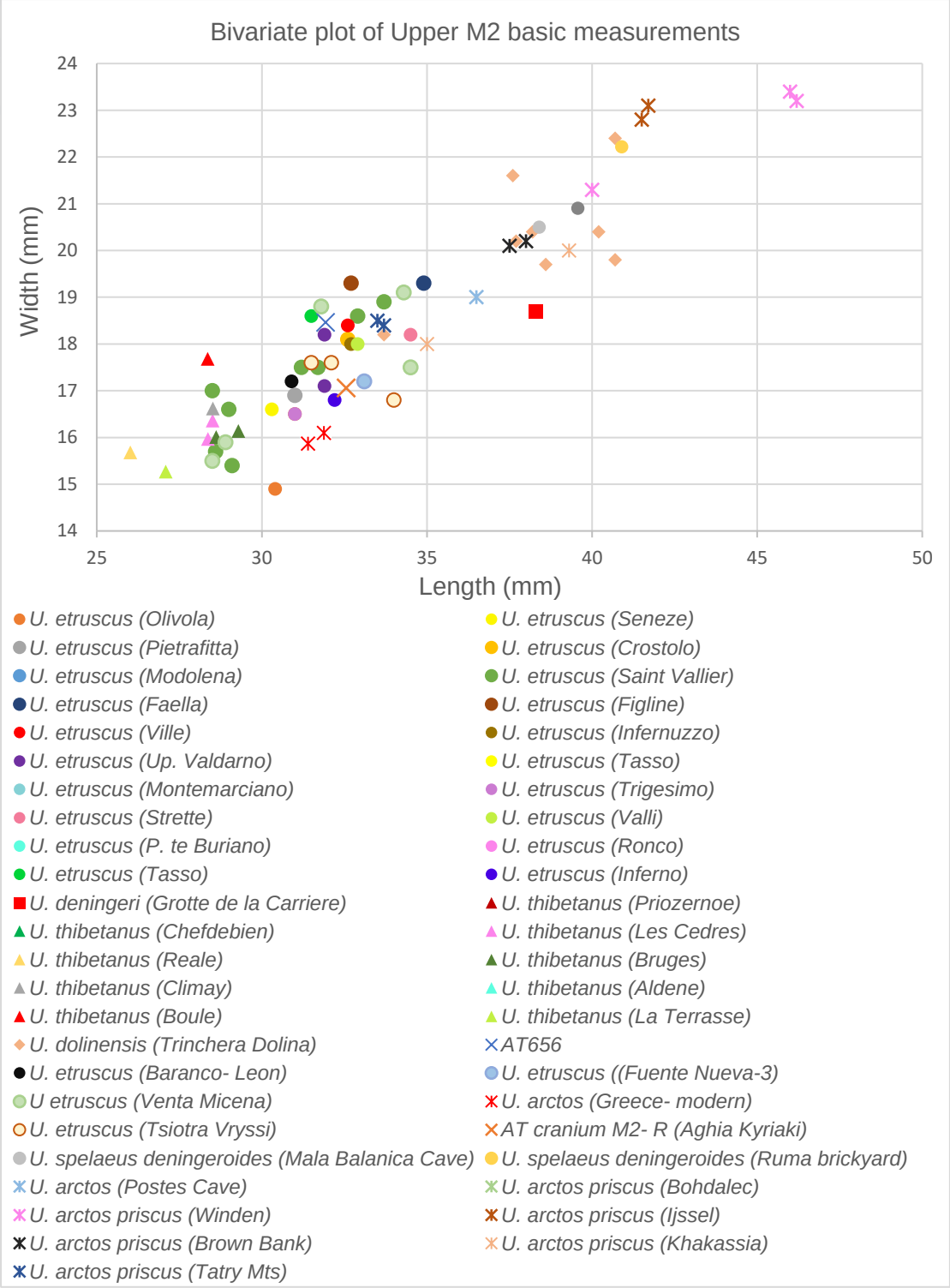


Figure 19: Bivariate plot of the total length and total width of the M2 tooth of the specimen AT656, the right M2 of the specimen AT–cranium as well as other specimens of *Ursus etruscus* from the localities of Olivola, Pietrafitta, Modolena, Faella, Ville, Up. Valdarno, Montemarciano, Strette, P. te Buriano, Tasso, Baranco– Leon, Venta Micena, Tsiotra Vryssi, Seneze, Crostolo, Saint Vallier, Figline, Infernuzzo, Trigesimo, Valli, Ronco, Inferno and Fuente Nueva–3. *Ursus deningeri* from the locality of Grotte de la Carriere, *Ursus thibetanus* from the localities of Chefdebien, Reale, Climay, Boule, Priozernoe, Les Cedres, Bruges, Aldene and La Terrasse, *Ursus dolinensis* from the locality of Trichnera Dolina, a modern specimen of *Ursus arctos* from Greece, Ursus arctos from the localities Postes Cave, Winden, Brown Bank, Tatry Mts, Bohdalec, Ijssel and Khakassia, as well as *Ursus spelaeus* from the localities of Mala Balcanica Cave and Ruma brickyard. Data from: Mazza and Rustioni (1992), Medin et al. (2017), Prat–

Vericat et al. (2020), Koufos et al. (2017), Cvetkovic and Dimitrijevic (2013), Cregut– Bonnoure (1995), Marciszak et al. (2019), Villalba de Alvarsado et al. (2021) and Garcia and Arsuaga (2001).

The proportions of M2 (Fig. 25) indicate that *U. thibetanus* has smaller dimensions than any of the other examined species. *Ursus etruscus* has quite expanded metrical ranges, especially as far as the total length is concerned: as a matter of fact, the range of the total length of M2 teeth of *U. etruscus* is 28.5–34.9 mm, whereas the range of total width of the M2 teeth of *U. etruscus* is 14.9–19.3 mm. We also notice an overlap of *Ursus arctos* and *Ursus etruscus* M2 measurements. Finally, it is clear that the total length of the M2 teeth of *U. spelaeus, U. deningeri* and *U. dolinensis* is greater than the one of *U. etruscus*.

Based on the M2 proportions, the specimen AT656 (M2) (31.93, 18.46) is metrically closer to the *Ursus etruscus* specimens VM12569 from Venta Micena, NMB–VA–353 from Tasso and VA1199 from Upper Valdarno. Accordingly, the M2 ATcranium(M2–R) is metrically closer to the *Ursus etruscus* specimens MPM– n. 5 from Up. Valdarno, NBM– VA 1827 from Inferno and FN 3 95,T8d, AB hfrom Fuente Nueva–3.

As far as morphology is concerned, both the specimens AT656(M2) and ATcranium(M2–R) are characterized by more developed buccal than lingual cusps, and an anterior part that is higher than the talon, characteristics also present in the *Ursus etruscus* M2 (Medin et al., 2017). Another characteristic, shared in the M2 teeth of Aghia Kyriaki and *U. etruscus* specimens, is the absence of a premetacone, characteristic present in some *U. deningeri* specimens (Jiangzuo et al., 2019).

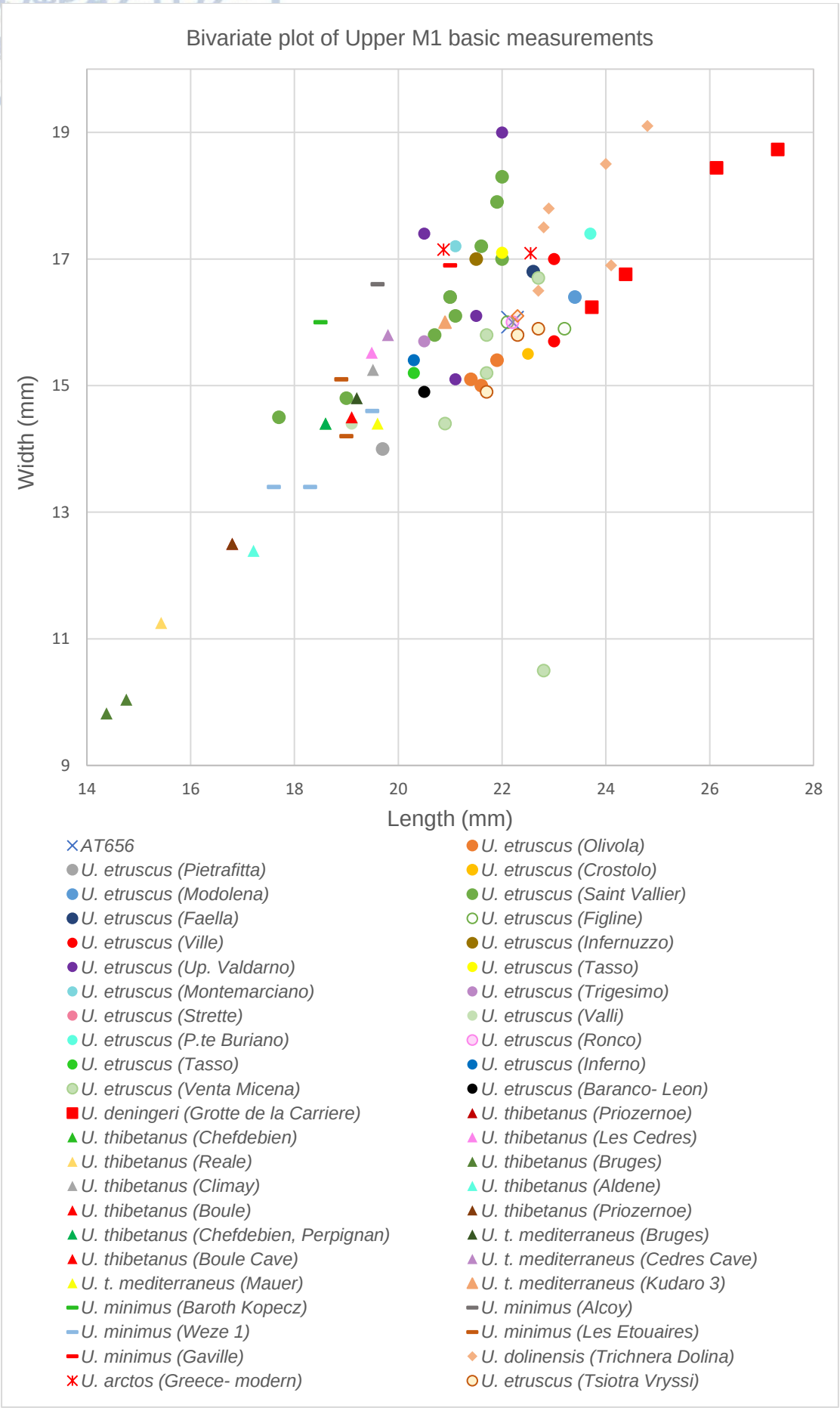

Figure 20: Bivariate plot of the total length and total width of the M1 tooth of the specimen AT656 as well as other specimens of *Ursus etruscus* from the localities Pietrafitta, Modolena, Faella, Ville, Up. Valdarno, Montemarciano, Strette, P. te Burriano, Tasso, Venta Micena, Olivola, Crostolo, Saint Vallier, Figline, Infernuzzo, Trigesimo, Valli, Ronco, Inferno, Barranco–Leon and Tsiotra Vryssi, *Ursus deningeri* from the locality Grotte de la Carriere, *Ursus thibetanus* from the localities Chefdebien, Reale, Climay, Boule, Mauer, Priozernoe, Les Cedres, Bruges, Aldene and Kudaro 3, *Ursus minimus* from the localities Baroth Kopecz, Weze 1, Gaville, Alcoy and Les Etouaires, *Ursus dolinensis* from the locality Trichnera Dolina and a modern specimen of *Ursus arctos* from Greece. Data from: Mazza and Rustioni (1992), Medin et al. (2017), Prat– Vericat et al. (2020), Koufos et al. (2017), Cvetkovic and Dimitrijevic (2013), Cregut– Bonnoure (1995), Marciszak et al. (2019), Villalba de Alvarsado et al. (2021) and Garcia and Arsuaga (2001).

In the Fig. 22 we notice that the M1 teeth of *U. thibetanus* and *U. minimus* are of shorter length than the ones of *U. etruscus*, *U. deningeri*, *U. dolinensis* and *U. arctos*.
The M1 of the specimen AT656 approaches by its proportions the ones of various specimens of *Ursus etruscus*. More specifically, the specimen AT656 (M1) is metrically identical to the specimens NMB– VA 1063 from Ronco, IGF 11600 from Figline, TSR–E21–50 (sin) from Tsiotra Vryssi, all attributed to *U. etruscus* and similar to Re–177 from Trichnera Dolina, attributed to *U. dolinensis*.
As far as the morphology is concerned, the M1 of *U. dolinensis* is characterized by a quadrangular–rectangular shape, lack of central constriction, with visible (but not very developed) styles vertically oriented (Garcia and Arsuaga, 2001). The main morphological characteristic of the upper first molars of *U. etruscus* is the rectangular shape, the weak parastyle and metastyle, the generally larger parastyle than metastyle as well as a robust accessory cone between the protocone and hypocone (Mazza and Rustioni, 1992); Also, often the two upper molars bear a weak cingulum on their lingual side, whereas an outer cingulum is rarely noted (Mazza and Rustioni, 1992). However, the main morphological difference between the upper M1 of *U. dolinensis* and *U. etruscus* is the extremely reduced styles of the former (Garcia and Arsuaga, 2001). The specimen AT656 (M1) is characterized by a central constriction in the occlusal surface, thus its attribution to *U. dolinensis* seems unlikely.
Consequently, taking into consideration both the metrical and morphological similarities of the specimen AT656(M1) to *Ursus etruscus* we can safely attribute it to *Ursus etruscus*.

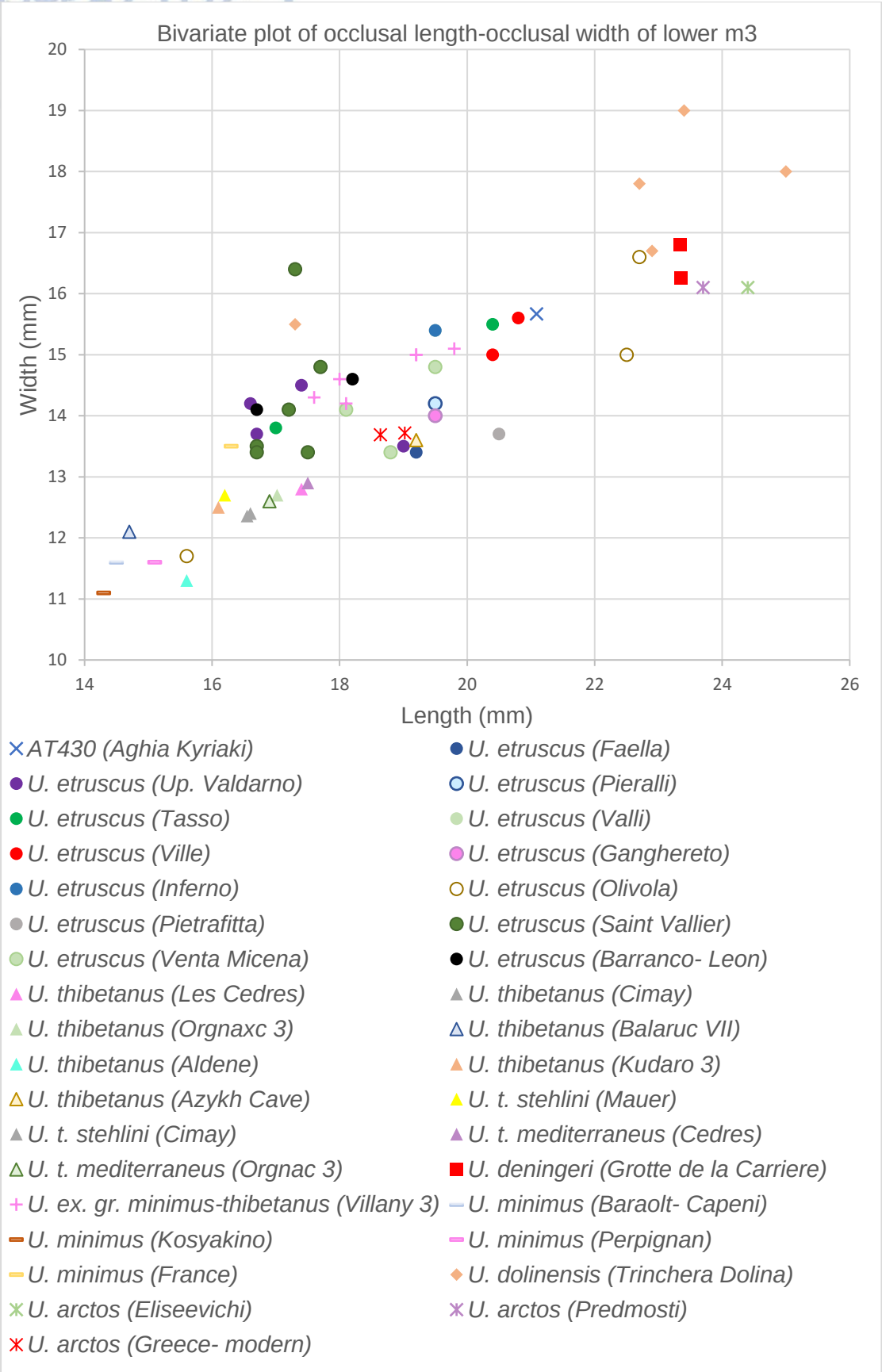


Figure 21: Bivariate plot of total length and total width of m3 AT430 from Aghia Kyriaki, as well as other m3 specimens belonging to the taxa *U. etruscus* from the localities Up. Valdarno, Tasso, Ville, Inferno, Pietrafitta, Venrta Micena, Faella, Pieralli, Valli, Ganghereto, Olivola, Saint

Vallier and Barranco**–** Leon, *Ursus thibetanus* from the localities Les Cedres, Orgnax 3, Aldene, Azykh Cave, Cimay, Balruc Vii,Kudaro 3, Mauer and Cedres, Ursus deningeri from Grotte de la Carriere, *Ursus minimus* from the localities Kosyakino, France, Baraolt**–** Capeni and Perpignan, *Ursus* ex. gr. *minimus***–***thibetanus* from the locality Villany 3, *Ursus dolinensis* from the locality Trichnera Dolina, Ursus arctos from the locality Predmosti as well as a modern specimen from Greece. Data from: Mazza and Rustioni (1992), Medin et al. (2017), Cregut–Bonnoure (1995), Baryshnikov (2010), Prat–Vericat et al. (2020), Bayshnikov and Lavrov (2013), Garcia and Arsuaga (2001) and personal measurements.

In the Fig. 23, we observe that the m3 AT430 from Aghia Kyriaki is metrically close to the specimens IGF 4002v from Ville and VA 1799 from Tasso, both attributed to *U. etruscus*. As far as morphology is concerned, the outline of the occlusal surface of the specimen AT430 is slightly pentagonal with several ridges, morphological characteristics of all the specimens from Barranco– Leon, attributed to the species *Ursus etruscus* (Medin et al., 2017). Thus, it is safe to attribute the specimen AT430 to the species *U. etruscus.*

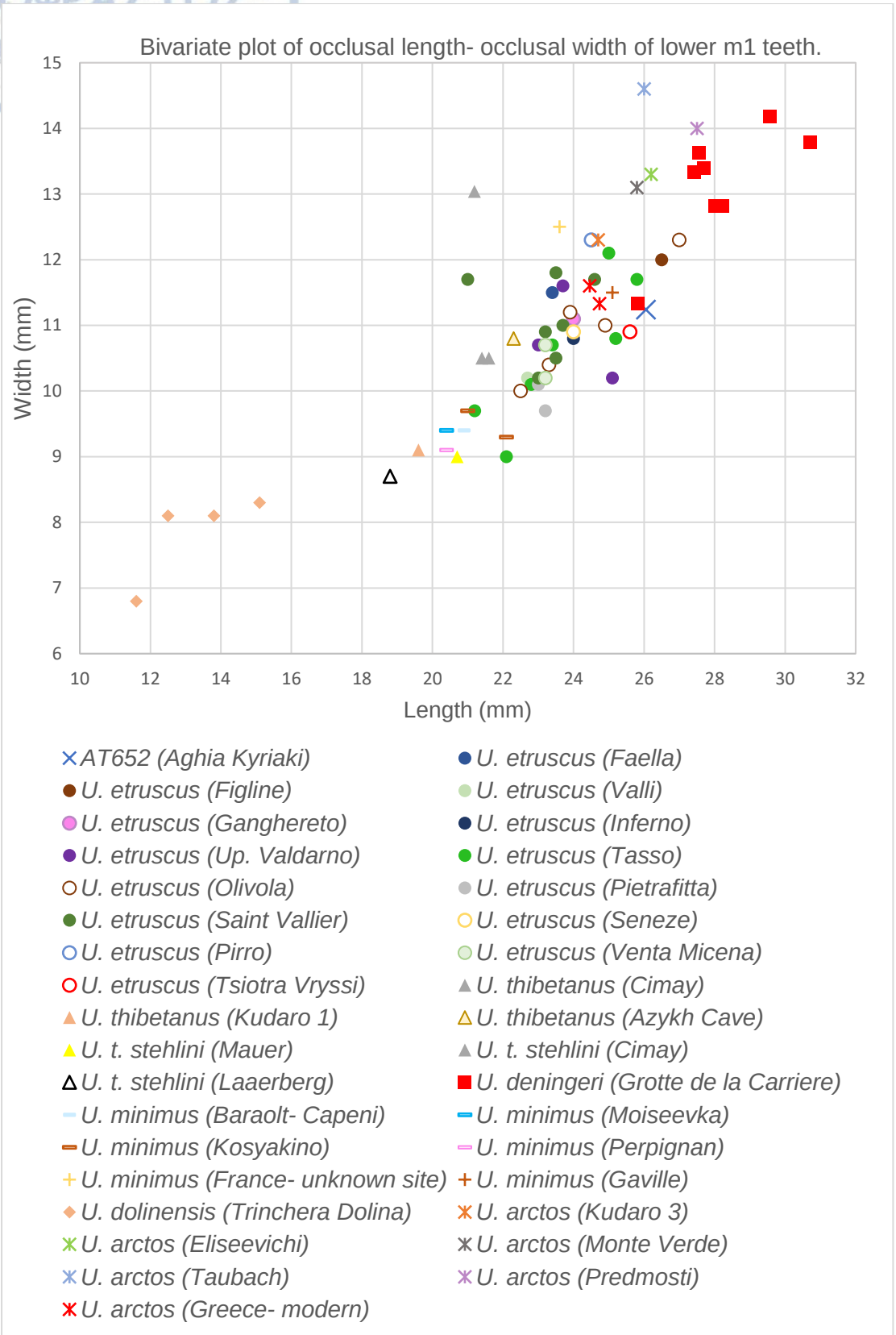


Figure 22: Bivariate plot of total length and total width of the m1 AT652 from Aghia Kyriaki, as well as other m1 specimens belonging to the taxa *Ursus etruscus* from the localities Figline, Ganghereto, Up. Valdarno, Olivola, Saint Vallier, Pirro, Tsiotra Vryssi, Faella, Valli, Inferno, Tasso, Pietrafitta, Seneze and Venta Micena, *Ursus thibetanus* from the localities Kudaro 1, Mauer, Laaeberg, Cima and Azykh Cave, *Ursus deningeri* from Grotte de la Carriere, *Ursus*

*minimus* from the localities Kosyakino, France, Moiseevka and Perpignan, *Ursus dolinensis* from the locality Trichnera Dolina, *Ursus arctos* from the localities Eliseevichi, Taubach, Kudaro 3, Monte Verde, Predmosti as well as a modern specimen from Greece. Data from: Mazza and Rustioni (1992), Medin et al. (2017), Cregut–Bonnoure (1995), Baryshnikov (2010), Prat–Vericat et al. (2020), Bayshnikov and Lavrov (2013), Garcia and Arsuaga (2001) and personal measurements.

The m1 AT652 from Aghia Kyriaki is metrically close to both *U. etruscus* specimens and the smallest specimen of *U. deningeri* from Grotte de la Carriere. Prat–Vericat et al. (2020) note that the lower m1 of *Ursus deningeri* tends to be buccolingually extended, as an adaptation to the feeding preferences of the species; on the other hand, the m1 teeth of *Ursus etruscus* remain buccolingually narrower than the cave bear species *U. spelaeus* and *U. deningeri*, fact also supported by the Table 24. However, its morphological characteristics (mainly buccolingually narrow and anteroposteriorly elongated tooth) suggest a closer attribution of the specimen to *U. etruscus;* The main difference of the m1 teeth of *Ursus deningeri* is the buccolingually extended talonid, as aforementioned.

Hence, taking into account all available morphological and metrical craniodental evidence we ascribe the Aghia Kyriaki ursid to *Ursus etruscus*. –

**Discussion**

The genus *Ursus* of the Ursinae subfamily, is represented in Greece by the extant taxon *U. arctos* and the extinct taxa *U. deningeri, U. etruscus, U. ingressus, U. spelaeus* and *U. thibetanus* (Pappa and Tsoukala, 2022).

The group of the Etruscan bears, as proposed by Mazza and Rustioni (1994), includes the extinct species *Ursus etruscus* (Cuvier, 1823). According to Mazza and Rustioni (1994) *Ursus etruscus* is characterized by an elongated muzzle, P1–P3 of smaller size, less wide m1 and M1, and M2 of greater length related to *Ursus* aff. *etruscus*. However, these bears are characterized by low polymorphy (Mazza and Rustioni, 1994). Moreover, the Etruscan bear is regarded to have a small body size that was gradually increasing (McIellan and Reiner, 1994). *Ursus etruscus* evolved from and replaced *Ursus minimus* (McIellan and Reiner, 1994) and was spread over Eurasia during the Early Pleistocene (2.0–1.8 Ma) (Rustioni and Mazza, 1993; Wagner, 2010; Wagner et al., 2011). McIellan and Reiner (1994) considered that *Ursus etruscus* gave rise to the cave bears, and the Asian brown bears, whereas Mazza and Rustioni (1994) believe that the brown bears derived from local populations of the species *U. minimus* and *U. thibetianus*. According to Torres (1992), the species' First Appearance Datum is in the early Villafranchian (Villaroya), and it disappeared during the late Villafranchian.

Geographic distribution: Specimens attributed to the species *U. etruscus* and *U.* cf. *etruscus* have been found in Western Europe: Saint Vallier, France (Viret, 1954) (middle Villafranchian), Kuruksay, Tadjikistan (Sotnikova, 1989) (middle Villafranchian), Tegelen, Netherlands Erdbrink, 1953) (Villafranchian), Crostolo–Modolena, Italy (Ambrosetti and Cremaschi, 1975) Western and Southeast Europe, including Spain (El Rincón, La Puebla de Valverde, and Venta Micena), France (Saint–Vallier, Chilhac, Senèze, and Ceyssaguet), the Netherlands (Tegelen), Italy (Olivola, Valdarno, Crostolo–Modolena, Pietrafitta, Colle Curti, Monte Argentario, and Pirro Nord), Germany (Erpfingen and Schernfeld), Romania (Graunceanului), Bulgaria (Varshets), and also Ukraine (Gorishnaya Vygnanka, Basin 1). The remains of *U. etruscus* found in Asia originate from Israel (Ubeidiya), Georgia (Dmanisi), Azerbaijan

(Palan–Tyukan), Tajikistan (Kuruksai, Obi–Garm, and Tutak), and China (Nihewan, Zhoukoudian 18, Jinyuan cave) (Jiangzuo et al., 2017). The single find in North Africa was made in Morocco (Ahl al Oughlam) (Baryshnikov, 2007).

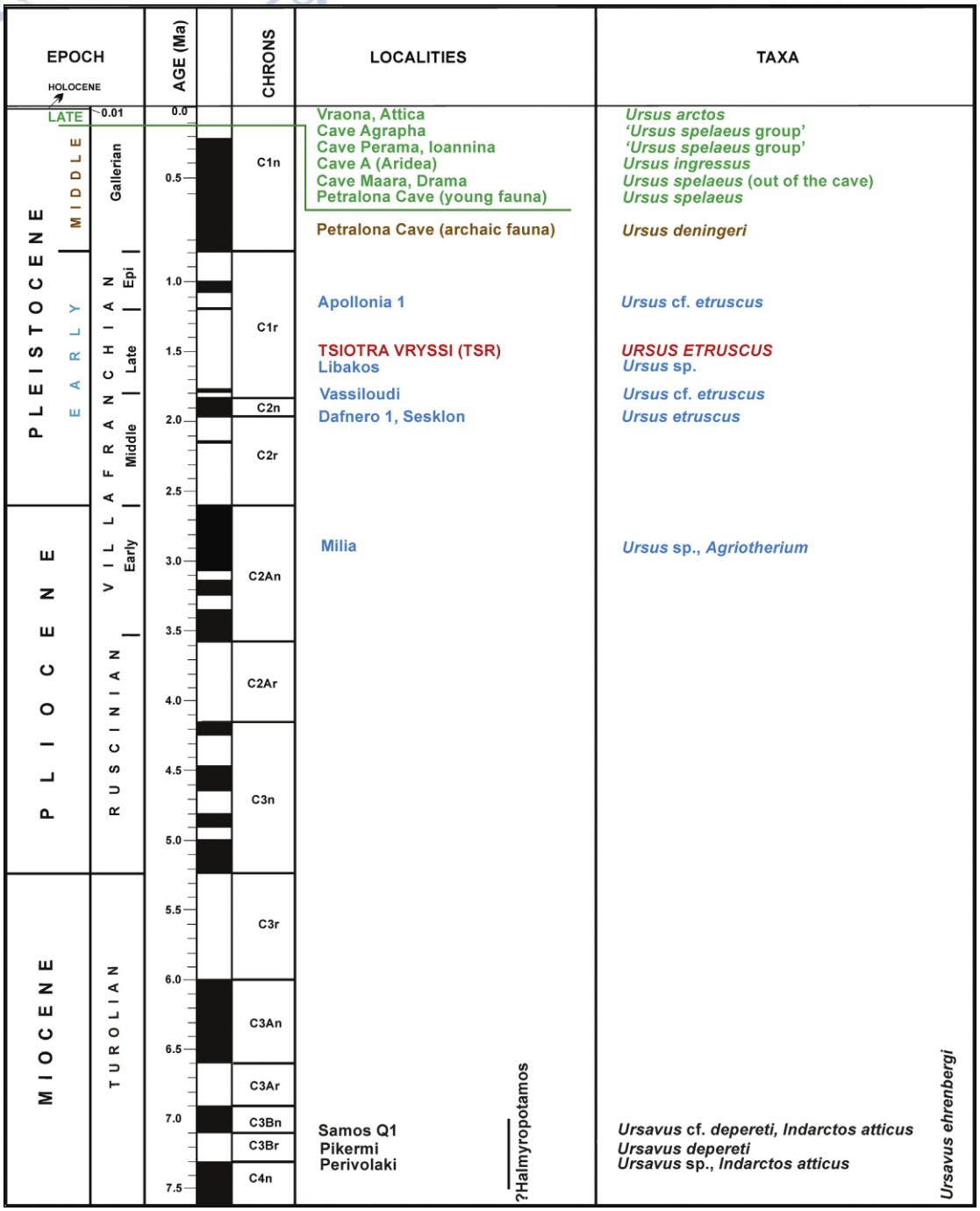


Figure 23: Biostratigraphic table with the chronological distribution of ursid taxa in the Neogene/Quaternary of Greece (Koufos et al., 2017).

According to Koufos (2014) and Pappa and Tsoukala (2022), the only representative of the family Ursidae in the Villafranchian of Greece is *Ursus etruscus*, as can also been seen in the Fig. 25 The species has been reported in the Early VillafranchIan fauna of Milia (Western Macedonia), the middle Villafranchian mammal assemblages of Dafnero and Sesklo, as well as in the late-latest Villafranchian faunas of Vassiloudi, Tsiotra Vryssi, Ptolemaida, Makinia, Kastritsi, Livakos and Apollonia 1, (Symeonidis et al., 1985/1986; Kostopoulos and Vasileiadou, 2006, Koufos, 2014; Pappa and

Tsoukala, 2022). According to Fig. 25, the southernmost occurrence of *Ursus etruscus* up to date is noted in Sesklo. However, our study shows that the southernmost site in Greece, in which remains of the species have been found is Aghia Kyriaki.

**4.3 Canidae indet.** Fischer von Waldheim, 1817

**Material**

Postcranial: diaphysis and distal epiphysis of metapodial (AT331), diaphysis of metapodial (AT333), third metatarsal (AT329), fourth metatarsal (AT328), three phalanges (proximal or intermediate) (AT330, AT327, AT322), left calcaneus AT336.

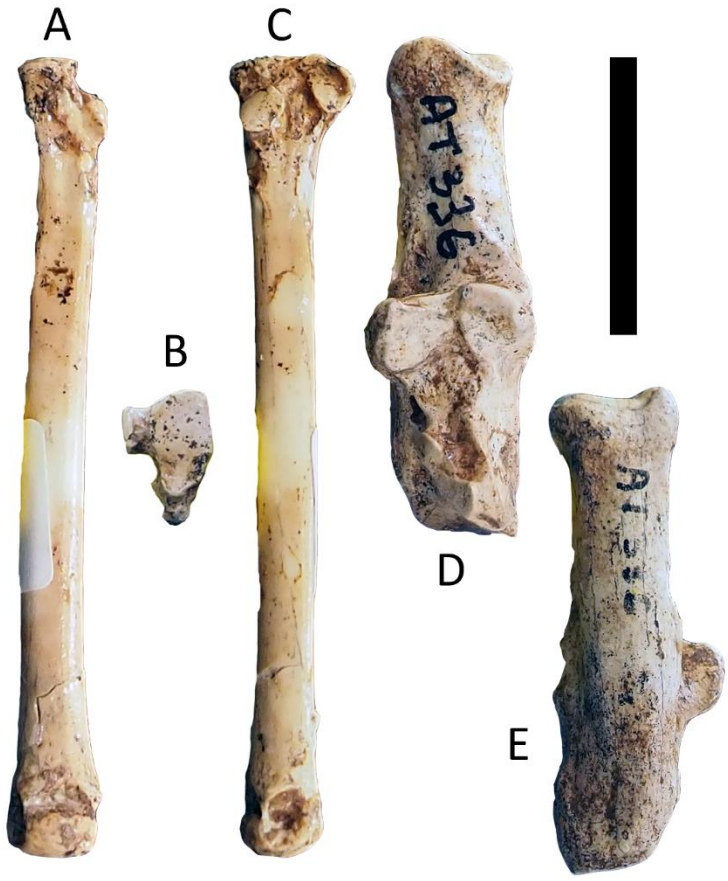


Figure 24: Canidae indet. specimens from Aghia Kyriaki. Left metatarsal III AT329 in A: anterior, B: proximal and C: medial view, left calcaneus, AT336 in D: dorsal and E: ventral views.

**Description**:

All the metapodials have a straight, slender elongated diaphysis (Fig. 26A–C). The phalanges are long and slender, with a gradual and smooth tendency of widening from the distal towards the proximal epiphysis.

A complete left calcaneus, AT336 is preserved. In dorsal view (Fig. 26D), the medial process of the tuber calcanei is more pointed and slightly more elongated towards the

proximal part of the bone than the lateral process of the tuber calcanei. The sagittal groove is slightly marked but could be characterized as relatively plain. The ectal facet (facies articularis talaris proximalis) is dorsolaterally broken. Its medial edge is steep and rather angular (Fig. 26D–E). The sustentacular facet (facies articularis talaris distalis) is of triangular outline. The peroneal process is not marked. The cuboid facet (facies articularis cuboides; Fig. 26D) forms a gradual valley, ascending towards the proximal part. In lateral view, the ventral edge of the calcaneus is straight, whereas the dorsal edge is slightly more curved. A well– marked ridge is formed at the continuity of the peroneal process and joins more distally the tuber calcanei. In medial view, the outline of the distal epiphysis is quite triangular. The plantar tubercle is widened towards the distal border. In distal view, the cuboid facet is concave, forming the aforementioned “valley” (Fig 26). In proximal view, the outline of the proximal epiphysis is relatively triangular, with curved borders. It is mediolaterally elongated.

**Measurements**

The measurements of the specimens from Aghia Kyriaki attributed to Canidae, are given in the Tables 5 and 6.

Table 5: Measurements of metapodials and phalanges of Canidae indet. From the locality of Aghia Kyriaki. Abbreviations: GL: Greatest Length, DT prox: transverse diameter of proximal epiphysis, DAP prox: anteroposterior diameter of the proximal epiphysis, DAP/DT diaph: DAP/DT of diaphysis, DAP/DT dist: DAP/DT distal epiphysis. Measurements in mm. Numbers in italics are approximate measurements.

| Taxon | Locality | ID code | Anat/cal element | GL | Proximal epiphysis | | Diaphysis | | Distal epiphysis | |
|---|---|---|---|---|---|---|---|---|---|---|
| | | | | | DAP | DT | DAP | DT | DAP | DT |
| Canidae indet. | Aghia Kyriaki | AT331 | Mtp | | | | *4.06* | *3.98* | 5.34 | 6 |
| Canidae indet. | Aghia Kyriaki | AT329 | Mt3 | 56.19 | 9.17 | 5.91 | 4.1 | 4.49 | 5.81 | 6.52 |
| Canidae indet. | Aghia Kyriaki | AT328 | Mt4 | 58.66 | 9.44 | 5.29 | 4.33 | 4.66 | 5.81 | 6.68 |
| Canidae indet. | Aghia Kyriaki | AT330 | Phnx | 27.7 | 5.47 | 6,89 | 4,02 | 3,76 | 4,45 | 4,92 |
| Canidae indet. | Aghia Kyriaki | AT327 | Phnx | 27.75 | 5.46 | 7 | 4,17 | 3,89 | 4,01 | 4,85 |
| Canidae indet. | Aghia Kyriaki | AT322 | Phnx | 22.39 | 5,2 | 5,94 | 3,65 | 3,55 | 3,69 | 4,6 |

Table 6: Measurements of the calcaneus AT336 from Aghia Kyriaki, attributed to Canidae indet. Abbreviations: same as Table 8, DT med: SBT: lowest breadth. Measurements in mm.

| Taxon | Locality | ID code | L | DT prox | DAP prox | DT med | DAP med |
|---|---|---|---|---|---|---|---|
| Canidae indet. | Aghia Kyriaki | AT336 | 34.5 | 9.14 | 7.66 | 6.22 | 7.88 |
| | | | **DT dist** | **DAP dist** | **DT max (GB)** | **SBT** | |

| | | | | | | |
|---|---|---|---|---|---|---|
| | | | 7.67 | 10.86 | 13.3 | 6.22 |

**Comparison**

The size of the specimens AT331, AT329, AT328, AT330, AT327, AT322 and AT336 is smaller than the one of the representatives of *Canis* sp. Also, by considering the morphology of the specimens (straight and slender metapodials, elongated talus), we can metrically and morphologically compare it to middle size canids, like the genera *Nyctereutes* and *Vulpes*, that were widespread during the Villafranchian in the European area.

Table 7**:** Table of measurements for the calcaneum AT336 as well as calcanei of the small canid species: *N. megamastoides* and *V. alopecoides* from Saint Vallier and Pirro Nord, accordingly. Measurements of the proximal and distal epiphysis, as well as the med. part of the diaphysis of *N. megamastoides* from Saint Vallier and *V. alopecoides* from Pirro Nord are not available. Measurements from: Argant (2004) and Petrucci et al. (2013). Measurements in mm.

| **Taxon** | **Locality** | **ID code** | **Length** | **DT max (GB)** | **SBT** |
|---|---|---|---|---|---|
| | Aghia Kyriaki | AT336 | 34.5 | 13.3 | 6.22 |
| *N. megamastoides* | Saint Vallier | SV.96.323 | 32.1 | | |
| *N. megamastoides* | Saint Vallier | SV.97.429–1 | 37.6 | 17.4 | |
| *N. megamastoides* | Saint Vallier | 161.643.QSV.1106 | 36.9 | 15.7 | |
| *N. megamastoides* | Saint Vallier | 161.652.QSV.1290 | 33.7 | 12.7 | |
| *N. megamastoides* | Saint Vallier | 161.639.QSV.1103 a | | 15.3 | |
| *V. alopecoides* | Pirro Nord | PU 104189 | 27.2 | 12 | 4.58 |

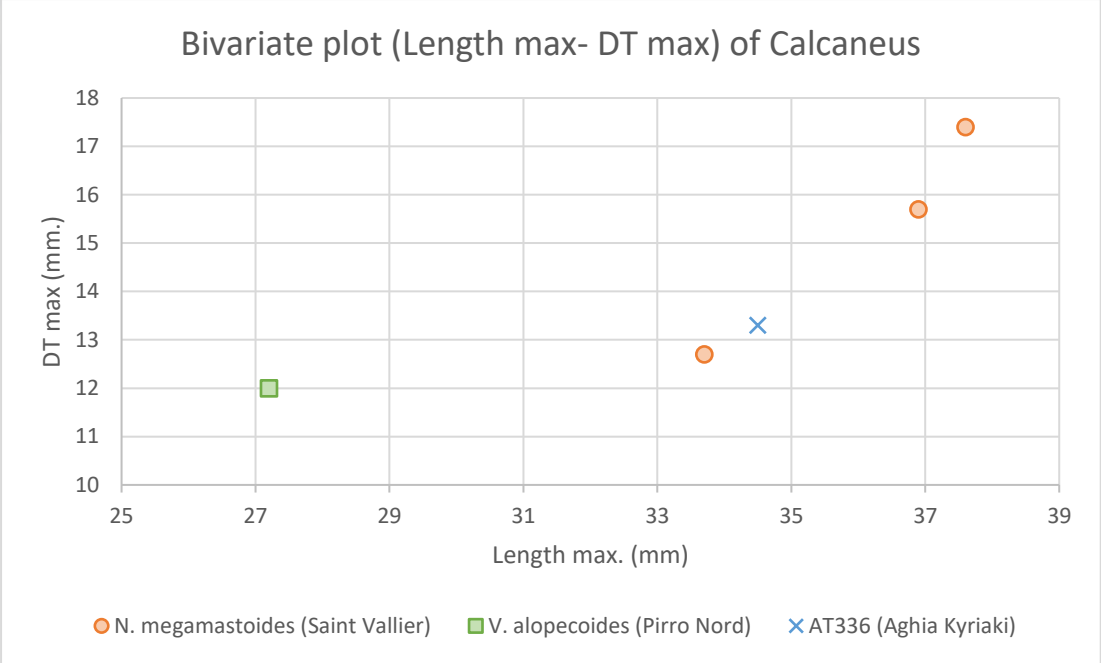


Figure 25: Bivariate plot of maximum length–DT max for the calcaneus AT336 from Aghia Kyriaki, as well as calcanei of the species *Vulpes alopecoides* from Pirro Nord and *Nyctereutes megamastoides* from Saint Vallier. Data from: Argant (2004) and Petrucci et al. (2013).

By its size, the calcaneus from Aghia Kyriaki, appears closer to calcanei of *N. megamastoides* than to *V. alopecoides* but the available data are not enough in order to attribute the specimen AT336 to either genus. However, we observe (Table 7, Fig. 27) that the maximum length of the specimen is closer to the maximum length of the specimen 161.652.QSV.1290, of *N. megamastoides* from Saint Vallier. The lack of comparative data does not allow for the moment a more specific attribution; Hence, is the Aghia Kyriaki canid is referred to as a middle– sized Canidae indet.

**Discussion**

The family Canidae is the oldest carnivoran family of the fossil record, with the first specimens attributed to the taxon being of late Eocene age (Koufos, 2022). The family is divided into three subfamilies: † Hesperocyoninae, † Borophaginae and Caninae (Fahey and Myers, 2000). The typical characteristics of the family are –amongst others– the elongated and narrow facial region (length ≥ orbital breadth), usually small auditory bullae, large and slender canines and large carnassials (Orlov, 1968; Koufos, 2022). The family Canidae entered the Eurasian area after crossing the Beringian landbridge and was afterwards dispersed all over Eurasia (Perini et al., 2010; Koufos, 2022). The family made its first appearance in the Eurasian area with the genus *Eucyon* (Perini et al., 2010); the first record of the family in Europe is considered to be in the Late Miocene of Spain, with the species *Eucyon cipio* (Rook, 2009), whereas the earliest occurrence of the family in Greece is dated back to the early Pliocene localities of Megalon Emvolon and Allatini with the genera *Nyctereutes* and *Eucyon* (Koufos, 1997, 2022). The Eurasian representatives of the family show a great number of taxa during the Pliocene and Pleistocene (Koufos, 2022). Most of the specimens collected from Greek fossiliferous localities that were identified as canids, are attributed

to the genera *Canis* and *Vulpes*, that are still present in the Greek fauna (Koufos, 2022).

***4.4* cf. *Canis* (*Xenocyon*) sp.** Kretzoi, 1938

**Material**
Postcranial: proximal extremity of left radius AT254

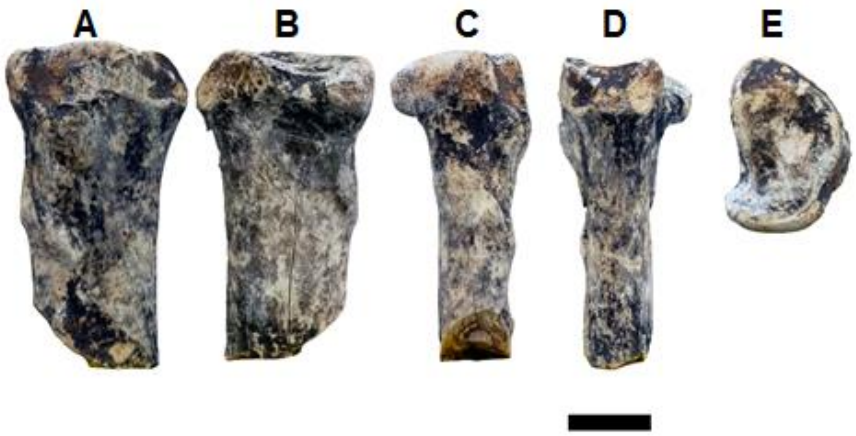


Figure 26: Proximal extremity of left radius AT254 from Aghia Kyriaki, attributed to cf. *Canis (Xenocyon)* sp. in A: posterior, B: anterior, C: lateral, D: medial and E: proximal view. Scale: 20mm.

**Description**
In proximal view (Fig. 28E), the outline of the proximal epiphysis (fovea capitus) is typical of a canid specimen. The anterior border of the proximal epiphysis is rather straight and mediolaterally elongated. The lateral border of the proximal epiphysis is curved, forming an anteroposterior orientated notch. The posterior edge of the proximal epiphysis is strongly curved, whereas it becomes almost straight in the medial half of the fovea capitulus, towards the medial edge. The medial edge of the fovea capitulus is curved but rather angular.
In anterior view (Fig. 28B), the medial part of the fovea capitulus is both mesiolaterally and proximodistally more developed than the lateral edge. Between the medial and the lateral edges of the proximal articulation, there is a concavity for the allocation of the ulna and the distal part of the humerus. In the lateral edge of the diaphysis, right distally of the proximal articulation, we observe a convexity, known as radial tuberosity. The diaphysis narrows right distally of the proximal epiphysis, and it remains relatively straight in all the preserved surface of the specimen.
In posterior view (Fig. 28A), the medial edge of the fovea capitus has a slight proximolateral to distomedial direction, meaning that it is “downturned”. The surface towards the lateral edge of the bone is covered in irregular convexities.
In medial view (Fig. 28D), the diaphysis appears slender, whereas in lateral view (Fig. 28C), the anteroposterior diameter of the lateral edge of the diaphysis is longer than the medial edge.

**Measurements**

The basic measurements of the specimen AT254 from Aghia Kyriaki are given in the Table 8.

Table 8: Basic measurements (DT proximal and DAP proximal) of the proximal epiphysis of radius attributed to *Canis* sp. from Aghia Kyriaki. Measurements in mm.

| ID code | Locality | DT proximal (Breadth) | DAP proximal (Depth) |
|---|---|---|---|
| AT(lost code) | Aghia Kyriaki | 22.48 | 14.92 |

**Comparison**

The morphology of the specimen, with the curved lateral border and the posterior edge of the proximal epiphysis in proximal view, is typical of Canini representatives. At the same time, the big size of the specimen excludes the possibility that it could belong to the genera *Vulpes*, *Nyctereutes* or other small or mid sized Canidae.

Figure 27: Morphological comparison of Canids. From left to right: Specimen from Aghia Kyriaki, *Lycaon* sp. (ID number: OM7426) extant, *Canis lupus*– inverted photo (ID number: CIPA1505), extant, *Cuon* sp., extantPhotos from: https://www.archeozoo.org/ (2021) and Meloro and Louys (2014).

The proximal view of the proximal epiphysis of radius of *Lycaon* sp. (ID code: OM7426) (Fig. 29) is similar to the one of the specimen from Aghia Kyriaki: the medial part of the anterior edge of the proximal epiphysis tends to be straight, whereas the posterior edge of the proximal articulation is curved.

On the other hand, the medial part of the anterior edge of the proximal epiphysis of *Canis lupus* (ID number: CIPA1505) is clearly more rounded, thus different than the specimen from Aghia Kyriaki.

Finally, the proximal view of the proximal epiphysis of *Cuon* sp. shares some similarities with the specimen from Aghia Kyriaki, however, the notch formed between the medial and lateral sides of the anterior edge of the proximal epiphysis is more obtuse than the one in *Lycaon* sp. and the specimen from Aghia Kyriaki. Thus, we can conclude that the specimen from Aghia Kyriaki shares more morphological features in

common with the modern *Lycaon* sp., than with the modern wolf *Canis lupus*, or *Cuon* sp.

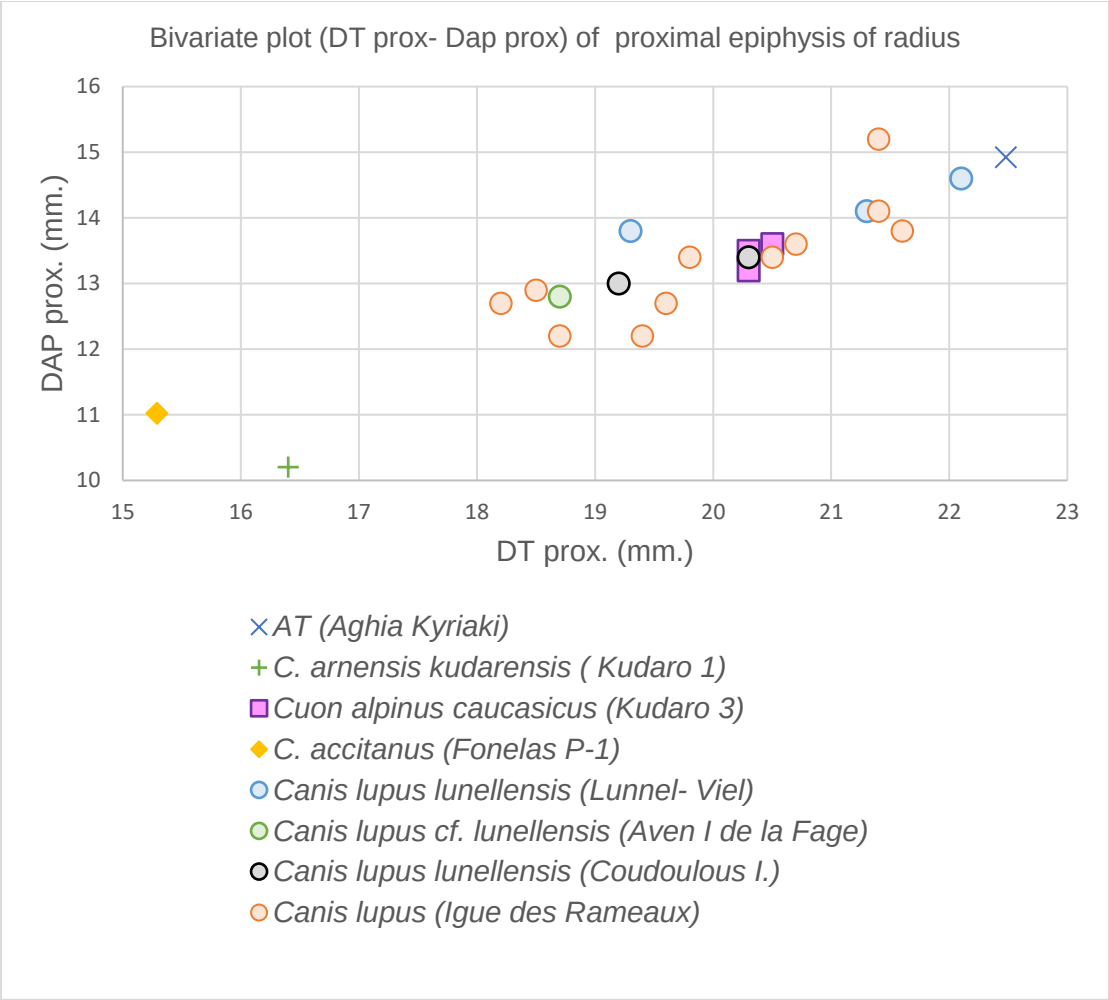


Figure 28: Bivariate plot of DT of proximal epiphysis and DAP of proximal epiphysis of the radius found in Aghia Kyriaki, as well as other radii specimens attributed to the taxa *C. arnensis kudarensis* from Kudaro 1, *Cuon alpinus caucasicus* from Kudaro 3, *Canis accitanus* from Fonelas P–1 and *Canis lupus* from Lunnel– Viel, Aven I de a Fage, Coudoulous I and Igue des Rameaux. Data from Baryshnkikov (2012), Garrido and Arribas (2008) and Boudadi– Maligne (2010) and Table 11.

Fig. 30, shows that the specimen from Aghia Kyriaki represent a large–sized Canid, in a size similar to *Canis lupus*.

*Lycaon* sp. is considered to have evolved from *Canis (Xenocyon) falconeri*, based on the size and morphological characteristics of the postcranial skeleton (Rook, 1994). Moreover, *Canis (Xenocyon) falconeri* is regarded to have a size similar to the one of modern wolves (Rook, 1994). Thus, taking into account the morphological similarities of the specimen from Aghia Kyriaki to *Lycaon* sp. and its big size– similar to the one of modern wolves, we can refer to it as cf. *Canis (Xenocyon)* sp.

**Discussion**

The genus *Canis* made its First Appearance at the Miocene– Pliocene boundary (~5.5 Ma) in North America (Masini and Torre, 1990; Rook and Torre, 1996a; Rook et al.,

2007; Wang and Tedford, 2007), however the geographical information about the origins of the genus is still a matter of debate (Holman Flower, 2014). As a matter of fact, there have been different hypotheses on the geographical origin of the genus, with some supporting a North American origin, as previously stated, and others supporting an Asian origin (Holman Flower, 2014). In any case, Sotnikova et al. (2002) suggested that the dispersal of the genus in the European area was the outcome of migration through Asia. The genus' earliest representative was attributed to the species *Canis davisi* Merriam, 1911 (Van Valkenburgh, 1988a; Rook and Torre, 1996a). However, the species showed more derived dental morphology (Tedford and Qui, 1996) and thus, was later removed from the genus *Canis* (Berta, 1987). Instead, it was incorporated in the genus *Eucyon* (Tedford and Qui, 1996) under the name of *E. davisi* Merriam, 1911 as the founder species of this genus (Holman Flower, 2014). *Canis lepophagus* Johnston, 1938, a species phylogenetically close to the extant coyote has been proposed as the first representative of the genus (Garrido and Arribas, 2008). Highly fragmented specimens belonging to a mid–sized *Canis* were found in two Late Turolian (9–3.5 Ma) localities of Spain (Concud and Los Mansuetos), and were originally identified as *Canis cipio* (Torre, 1979; Sotnikova and Rook, 2010). Although the species was later attributed to the genus *Eucyon* by Wang and Tedford (2007) it was afterwards related to *Canis etruscus* by Torre (1979) and Rook (1992) and finally attributed to *Canis michauxi* Martin, 1973 by Garrido and Arribas (2008).

According to Holman– Flower (2014), the early Villafranchian representatives of the genus *Canis* were *Canis* sp.*,* known from Vialette, the Middle– Villafranchian *Canis* cf. *senezensis* Martin, 1973 from Russia, though this identification is not certain (Sotnikova et al., 2002; Sotnikova and Rook, 2010), and *Canis* cf. *etruscus* from the site of Coste San Giacomo– Italy (2.2–2.1 Ma) (Rook and Torre, 1996a; Sardella and Palombo, 2007; Rook and Martinez–Navarro, 2010), that was later attributed to *Canis* sp. (Bellucci et al., 2014) (Holman– Flower, 2014 and reference therein). In fact, Cherin et al. (2014), amongst others (Azzaroli 1983; Azzaroli et al. 1988; Torre et al. 1992, 2001; Rook and Torre 1996a; Sardella and Palombo 2007; Rook and Martinez–Navarro 2010; Sotnikova and Rook 2010), supported that *Canis etruscus* made its first appearance in the late Vilafranchian.

After the so–called "Wolf– event" that took place during the middle–late Villafranchian transition, the canids were more spread in the European area, whereas the sporadic fossiliferous record of the early and middle Villafranchian canids suggests small canid populations at these times. During the late Villafranchian the first appearance of the early wolf *Canis etruscus* appears (Holman–Flower, 2014), along with the first occurence of *Canis arnensis* Del Campana, 1913 and *Canis (X.) falconeri* Forsyth–Major, 1877 in Western Europe (Tasso F.U.) (Azzaroli, 1983; Azzaroli et al., 1988; Gliozzi et al., 1997). Finally, specimens from the late Villafranchian localities of Seneze (France) and Slivnitsa (Bulgaria) were attributed to *Canis senezensis* and a form similar to it, respectively (Rook and Torre, 1996a; Sardella and Palombo, 2007; Sotnikova *et al.,* 2002). As far as the mid– sized canid species *Canis senezensis* is concerned (Bartolini–Lucenti and Rook, 2016), Sardella and Palombo (2007) considered a less derived form of *Canis arnensis*, whereas Garrido and Arribas (2008) regard it as synonymous to *Canis arnensis*, due to its anatomical and metrical similarity. Moreover, Garrido and Arribas (2008) rose the smallest– canid species *Canis accitanus* from the site of Fonelas P–1 in Spain (1.9–1.7 Ma). During the latest Villafranchian, the small sized canids occur for the first (Boudadi Maligne, 2010;

Petrucci et al., 2013) *Canis mosbachenis,* in the localities of Venta Micena (Martinez–Navarro et al., 2003) and Pirro Nord (Petrucci et al., 2013). Finally, *Canis apolloniensis* Koufos and Kostopoulos, 1997 is known only from the EpiVillafranchian locality of Apollonia 1, Greece (Koufos, 2022 and reference therein).

*Canis* (*Xenocyon*) sp. was originally described by Kretzoi, 1938, who used specimens from the locality of Gombastzog as type material of the genus (Rook, 1994). Since then, the genus has been recognized in several European localities. The subgenus *Xenocyon* includes the large–sized canid species *Canis (X.) falconeri* Forsyth Major, 1877 (Pons Moya, 1987; Rook, 1994), *Canis (X.) lycaonoides* Kretzoi, 1938 (Madurell–Malapeira et al., 2021) as well as the african species *Canis (X.) africanus* Pohle, 1928 and the Asian species *Canis (X.) antonii* Zdansky, 1924 (Rook, 1994). Although Pons Moya (1987) suggests the synonymy of *Canis (X.) lycaonoides* with *Canis (X.) falconeri*, Rook (1994), they suggest that the former is a derived form of the latter.

*Canis (X.) falconeri*, is a large– sized canid, with a size comparable to the one of the extant *Canis lupus* (Rook, 1994) The species can be distinguished by its synchronous species *Canis ex. gr. etruscus* and *Canis ex. gr. arnensis* due to its larger size and the morphology of its upper teeth (Rook, 1994). Madurell–Malapeira et al. (2021) support that the middle and late Villafranchian *Canis (X.) falconeri* (Bartolini–Lucenti and Spassov, 2022) was replaced by *Canis (X.) lycaonoides* at the second half of the late Villafranchian.

*Canis (X.) lycaonoides* was a large–sized Canid of an Early–Pleistocene Asian origin, that dispersed in the Old World (Martinez– Navarro and Rook, 2003; Bartolini– Lucenti et al., 2021). This hypercarnivorous species managed to be a common representative of the Eurasian and African faunal guilds, that lived in Europe until the late Early Pleistocene (Madurell– Malapeira et al., 2013; Bartolini–Lucenti et al., 2021) and even reached the north–eastern part of Russia and North America (Tedford et al., 2009).

The similar morphological traits of the forelimb of the extant *Lycaon* sp. and the extinct subgenus *Xenocyon*, led Rook (1993, 1994) to the suggestion that *Lycaon* sp. is a derived form of the *Canis (X.) falconeri* group. More recent research, including genetic evidence, leads to the general agreement that the extant *Lycaon pictus* has possibly derived from *Canis (Xenocyon) lycaonoides* (Stiner et al., 2001; Martinez–Navarro and Rook, 2003; Tedford et al., 2009; Madurell–Malapeira et al., 2013, 2021; Petrucci et al., 2013; Koufos, 2018; Bartolini–Lucenti et al., 2021). This is the reason why, in the worldwide bibliography, the group *Canis* (*Xenocyon*) is sometimes referred to as *Lycaon* (Madurell– Malapeira et al., 2021). Although the phylogeny and the geographical origin of the taxon is still disputed, Madurell– Malapeira et al. (2021) amongst others support the scenario accepted by most researchers for an Eurasian origin of the group, that later dispersed in Africa around 1.8 Ma (Rook and Martinez–Navarro, 2010; Madurell–Malapeira et al., 2013; Bartolini– Lucenti et al., 2021). It is notable that recently, Bartolini–Lucenti and Spassov (2022), suggested that the First Appearance Datum of the subgenus *Xenocyon* in Eurasia, in the locality Roca–Neya, France recently dated at 2.6 Ma.

The species *Canis (Xenocyon) falconeri* has been identified in, France (Bartolini–Lucenti and Spassov, 2022), Italy, Romania, Spain (Rook, 1994) and Israel (Gaudzinski, 2004). The species *Canis (Xenocyon) lycaonoides* has been identified in Slovakia, Spain, France, Germany, Hungary, Montenegro, Russia, Tajikistan, Italy, Israel as well as in the Greek localities of Apollonia 1 and Petralona Cave (Koufos, 2022).

**4.5 (?) Mustelidae indet.** Fischer von Waldheim, 1817

**Material**

Postcranial: left third metacarpal (AT l.c.1), first phalanx (AT l.c.4).


Figure 29: Left third metacarpal AT(l.c.1) in A: anterior, B: posterior, C: medial, D: lateral and left first phalanx AT(l.c.4) in E: lateral, F: anterior, G: posterior and H: proximal view. Scale bar: 20 mm.

**Description**

AT( l.c.1)

The complete third (?) right metacarpal has a slightly broken proximal epiphysis in the anteriolateral border (Fig. 31A, D).The medial border of the proximal epiphysis is straight with an anteroposterior direction: towards the posterior side, the medial border becomes slightly more converging towards the lateral part, whereas the articulation border forms a projection with a posteromedial direction. Accordingly, the lateral border of the proximal epiphysis has a straight morphology with an anterolateral to posteromedial direction. The anterior border of the proximal epiphysis is relatively straight, although broken in the anterolateral side, as formerly noted. The posterior border of the proximal epiphysis is characterized by two projections for the articulation with the carpal bones; the medial projection has a posteromedial direction, whereas the lateral projection has a posterolateral direction. In anterior view (Fig. 31A), the diaphysis of the bone is straight and becomes smoothly and gradually wider towards

the distal diaphysis. Right distally of the proximal epiphysis, we note a convexity of an irregular outline; the convexion is more elongated lateromedially than proximodistally, and it is located off–midline, towards the medial side of the bone. In posterior view (Fig. 31B), right below the proximal epiphysis a small– sized shallow notch appears with an inverted– triangle outline. The shape of the diaphysis is the same as described in anterior view. Proximally of the distal epiphysis several small sized convexions occur, possibly palaeopathological marks. In medial view (Fig. 31C), the proximal border of the proximal epiphysis is curved and higher towards the posterior side of the bone; The diaphysis is slender and straight, (Figure 31) and its anteroposterior diameter becomes gradually and smoothly shorter towards the distal epiphysis. The medial surface of the distal epiphysis shows slight signs of weathering. In lateral view (Fig. 31D), the proximal border of the proximal epiphysis is also curved, but has a more anterodistal to posteroproximal direction, than the one in the medial view. Right distally of the proximal epiphysis we note palaeopathological marks possibly attributed to the aging of the animal. The shape of the diaphysis is the same as observed in the medial view. In distal view, the anterior border of the distal epiphysis is curved, the medial and lateral borders of the epiphysis have an anterio–posteromedial and antero–posterolateral direction, accordingly, whereas the articulative projection of the distal epiphysis is straight and extended towards the posterior side of the bone.

(AT l.c.4)
Complete, first, possibly right phalanx. In anterior (Figure 31F) and posterior (Figure 31G) view, the diaphysis of the phalanx is straight and slender. In lateral (Figure 31E) and medial view, the phalanx appears to become slightly and gradually more slender from the proximal towards the distal epiphysis, resulting in its minimum anteroposterior diameter rightproximally of the distal epiphysis. In proximal view (Figure 31H), the proximal epiphysis is characterized by a facet, used for the allocation of the distal epiphysis of the (first) metapodial. In distal view, the distal epiphysis is characterized by two margins divided by a sagittal groove.

**Measurements**:
The measurements of the specimens AT(l.c.1) and AT(l.c.4) from Aghia Kyriaki, attributed to Mustelidae indet., are given in the table 9.

Table 9: Measurements of the specimens attributed to Mustelidae indet., from the locality of Aghia Kyriaki. Abbreviations in Table 8. Measurements in mm.

| Taxon | Locality | ID code | Anat/cal element | GL | Proximal epiphysis | | Diaphysis | | Distal epiphysis | |
|---|---|---|---|---|---|---|---|---|---|---|
| | | | | | DAP | DT | DAP | DT | DAP | DT |
| Mustelidae indet. | Aghia Kyriaki | AT (l.c.1) | Mc3 | 27.64 | 5.39 | 4.05 | 3.09 | 2.42 | 4.33 | 4.77 |
| Mustelidae indet. | Aghia Kyriaki | AT (l.c.4) | Phnx | 15.17 | 4.17 | 4.55 | 2.95 | 2.63 | 3.1 | 3.68 |

**Comparison**
The small size (Table 9) as well as morphology of the specimens (Fig. 31), allow us its attribution to the family Mustelidae. The mustelid material from Aghia Kyriaki is scarce;

the two available postcranial elements allow no safe attribution to a certain genus, especially after taking into account that the safest attribution of small sized carnivorans is based on cranial and dental remains.

**Discussion**

The family of Mustelidae Fischer von Waldheim, 1817 includes a variety of extinct and extant animals, that, despite their great diversification, share some common characteristics, such as: elongated and slender body, short skull and facial region, short– five– digit legs, non–retractile claws, as well as the absence of both the upper and lower third molar (Koufos, 2022). The first appearance of the family can be dated back to the Oligocene or Middle Miocene of the Old World however their ancestry is still not clarified (Orlov, 1968; Wund, 2018; Koufos, 2022). In fact, there is a debate regarding the origin and phylogenetics of the Family (Koufos, 2022), as different research methods have provided conflicting hypotheses.

In Greece Mustelidae can be dated back to the Early/ Middle Miocene, with the genus *Proputorius* (Koufos, 2022). The presence of mustelid representatives in the Greek area (both continental Greece and islands) is constant from the Miocene till nowadays, however, the Pliocene and Pleistocene fossiliferous record indicates that the mustelid species were fewer than the Neogene ones (Koufos, 2022). During the Villafranchian and Epi– Villafranchian of Greece, the family is represented by the taxa *Baranogale* cf. *helbingi* in Dafnero 1 (middle Villafranchian– MN17), *Meles thorali* in Vatera F (middle Villafranchian– MN17), *Meles dimitrius* in Gerakarou 1 (late Villafranchian– MNQ18) and Apollonia 1 (EpiVillafranchian– MN20), *Pannonictis* sp. in Libakos (possibly late Villafranchian) and *Mustela* sp. in Ravin of Voulgarakis (EpiVillafranchian– MNQ 20) (Koufos, 2022).

Order: Artiodactyla Owen, 1848

**4.6 Ruminantia indet.** Scopoli, 1777

**Material**

Postcranial elements: two right femurs (AT01–AT05/AT09–AT13/AT15–AT17, AT680), two left femurs (AT675, AT679), femur (AT681), right talus (AT302), left talus (AT376), three calcanei (AT239, AT290, AT326), six proximal phalanges (AT214, AT218a, AT354, AT357, AT359, AT725), nine intermediate phalanges (AT145, AT244, AT288, AT342, AT611, AT620, AT665, AT672, AT722),

**Description**

Femurs

The femurs from Aghia Kyriaki, note a high percentage of cracking, however in all specimens, the height of the neck of the proximal epiphysis, before the medial condyle, seems to be relatively long. This morphological characteristic leads us to the conclusion that the femurs most probably belong to Artiodactyls, and especially Ruminants, rather than to Carnivores. The outline of the lesser trochanter of the femurs is oval shaped and has a proximodistal orientation (its proximodistal diameter is greater than its lateromedial one). The cavity between the head of the femur and the trochanter

major (trochanteric fossa) is relatively deep, oval shaped and wider towards the proximal end. The specimen appears to be slender. The proximal end of the femurs, proximally to the transverse level of the lesser trochanter, seems to be slightly bended towards the anterior surface. In the anterior verge of the medial view, distally of the transverse level of the trochanteric fossa, there is a curved prominence that proceeds towards the posterior verge, and then forms a straight fattening that reaches the mid of the diaphysis. The transverse outline of the diaphysis seems to be almost circular. Two complete heads of femur were also found (AT182, AT183). The specimen AT01–AT05/AT09–AT13/AT15–AT17 (Incomplete, proximal epiphysis and part of diaphysis of right femur) is relatively well preserved, highly fragmented in the anterior view. In proximal view, the head of the femur and the trochanter major (greater trochanter) are cracked/ missing. In anterior view, the surface of the bone is highly cracked, with most of the outer surface missing. In posterior view, the specimen lacks the major and the lesser trochanter, as well as the head of the femur, however the neck of the femur is notable. The specimen AT131 (proximal end of left femur), lacks the head but bears a cracked neck. In anterior view the specimen has a slight crack on the trochanter major, thus revealing the sponge bone.

AT376

Left small to mid– sized astragalus. The specimen is almost complete with several cracks, mainly in the lateral and medial surfaces. In anterior view, the specimen has a rectangular shape, with the lateral and medial side being more elongated than the proximal and distal sides (Lmax/ Wmax= 34.15/ 22.53= 1.52). The proximal trochleae are broken in the posterior surface: in anterior view, the two trochleae are broken in the posterior side. The two proximal trochlear ridges are parallel to the sagittal plane. The lateral distal trochlea is wider but seems to be shorter than the medial distal trochlea. The lateral surface of the specimen has a notable prominence between the proximal and distal epiphysis, along the anterior border and a relatively deep cavity between the anterior and posterior side.

AT302

Right, complete astragalus, notably well preserved. It is the biggest Ruminant astragalus of the locality. In anterior view, the shape of the specimens resembles a rectangular, with the lateral and medial side being more elongated than the proximal and distal sides (Lmax/ Wmax= 37.43/ 26.32= 1.42). the specimen is sturdy. In anterior view, the lateral condyle of the proximal articulation is taller and wider than the medial condyle of the proximal articulation. The two trochlear ridges are parallel to the sagittal plane. The intertrochlear notch is smooth, has an in–between width (not very narrow, not very wide) and ends distally in a relatively deep fossa. The lateral trochlea of the distal condyle is slightly wider and higher than the medial one. Both in the lateral and the medial surface, along the anterior borders, there are notable prominences, between the proximal and distal epiphysis. The lateral surface of the specimen has a relatively deep cavity between the anterior and posterior side.

CALCANEI

AT239

Right, almost complete calcaneum. The anterior process is cracked (broken). The anterior surface of the specimen is gradually curved and smooth. The lateral and

medial surfaces are more flattened whereas the posterior surface of the specimen is almost flat and cracked towards the proximal end. A shallow furrow runs along the dorsal margin of the sustentaculum talis, creating a small crest dorsally to that. In lateral view, the anterior surface seems to be curved/ arched, whereas the posterior surface is straight.
In the distal end view, the naviculo–cuboid articular facet and the anterior process are cracked. The medial facet, which works as the only surface for the articulation of the astragalus, is relatively oval shaped; in distal view, there is a deep rounded fossa between the medial facet and the anterior process. Medioposteriorly of the articular facet for the astragalus, there is a shelf, with an oblique lateral–medial direction, that ends in an acute angle in the medial surface. In anterior view, the outline of the shelf and the crest described earlier, is concave– semilunar shaped. The antero–posterior measurement of the tuber calcis (*19.30* mm) is less than the maximum antero–posterior measurement taken in the distal region (*26.14* mm).

AT262/AT290/AT341
Right calcaneum, almost complete. The specimen is in good condition– well preserved, with slight cracks, mainly in the proximal and distal ends. The proximal end is broken. The anterior surface of the specimen is slender and abruptly curved. The posterior surface of the specimen is slender but becomes wider towards the proximal end. The medial surface is almost flat, whereas the lateral one is relatively more curved than the medial one.

Proximal phalanges
The proximal phalanges AT214, AT218a, AT354, AT357, AT359, AT725 from the locality of Aghia Kyriaki all show typical characteristics of the order Artiodactyla: the proximal epiphysis is characterized by an anteroposterior valley, known as the abaxial sesamoid facet that divides the abaxial metapodial facet and the interdigital facet.

Intermediate phalanges
The intermediate phalanges AT145, AT244, AT288, AT342, AT611, AT6320, AT655, AT672 and AT722 all bear the typical characteristics of intermediate phalanges of the order Artiodactyla: in proximal view, a sagittal ridge divide the (projected) abaxial and the interdigital tubercles.

**Measurements**
The measurements of the specimens from Aghia Kyriaki attributed to Ruminantia indet. are given in the tables 10 and 11.

Table 10: Measurements of proximal phalanges from the locality of Aghia Kyriaki, attributed toArtiodactyla indet. Abbreviations in Table 8. Measurements in mm.

| ID code | Site | Total length | Proximal epiphysis | | Diaphysis | | Distal epiphysis | |
|---|---|---|---|---|---|---|---|---|
| | | | DT | DAP | DT | DAP | DT | DAP |
| AT214 | Aghia Kyriaki | 48,67 | 14,18 | 16,96 | 8,72 | 11,2 | 13 | 10,83 |

| | | | | | | | | |
|---|---|---|---|---|---|---|---|---|
| AT218a | Aghia Kyriaki | | 19,33 | | | | | |
| AT354 | Aghia Kyriaki | | 17,29 | 20,25 | | | | |
| AT357 | Aghia Kyriaki | 44,71 | 13,26 | 16,7 | 11,45 | 10,98 | 12,83 | 12 |
| AT359 | Aghia Kyriaki | | 19,94 | 23,35 | | | | |
| AT725 | Aghia Kyriaki | 30,79 | | | | | 12,65 | 11,92 |

Table 11: Measurements of intermediate phalanges from the locality of Aghia Kyriaki, attributed to Artiodactyla indet. Abbreviations in Table 8. Measurements in mm.

| ID code | Site | Total length | Proximal epiphysis | | Diaphysis | | Distal epiphysis | |
|---|---|---|---|---|---|---|---|---|
| | | | DT | DAP | DT | DAP | DT | DAP |
| AT145 | Aghia Kyriaki | | 12,66 | 10,2 | | | | |
| AT244 | Aghia Kyriaki | 29,81 | 16,57 | 14,7 | 12,66 | 9,06 | 15,37 | 12,45 |
| AT288 | Aghia Kyriaki | | | | | | 15,57 | 12,18 |
| AT342 | Aghia Kyriaki | 32,64 | 18,73 | 18,52 | 13,65 | 13,23 | 15,49 | 16,95 |
| AT611 | Aghia Kyriaki | 24,72 | 13,48 | 11,09 | 10,68 | 7,31 | 11,91 | 10,67 |
| AT620 | Aghia Kyriaki | 29,21 | 16,13 | 13,75 | 12,56 | 8,54 | 15,51 | 13,22 |
| AT665 | Aghia Kyriaki | | | | | | 14,74 | 12,52 |
| AT672 | Aghia Kyriaki | | | | | | 17,59 | 14,02 |
| AT722 | Aghia Kyriaki | 27,87 | 16,28 | 12,15 | 11,85 | 6,93 | 14,83 | 11,24 |

**4.7 Cervidae indet.** Goldfuss, 1820

**Material**
Postcranial elements: two left humeri (AT366, AT228)

**Description**
Humeri: The distal epiphysis of the specimens AT366 and AT228 consists of two epitrochleae, divided by one groove and one crest, located slightly lateral to the distal articulation midline. The medial margin of the trochlea is proximodistally higher than the lateral, and consequently, in anterior view, the trochlea tapers laterally. In anterior view of the distal end of the specimen, the outline of the medial condyle is slightly curved. There is no synovial fossa present on the anterior surface of the medial condyle.
The specimen AT366 is a distal epiphysis and part of the diaphysis of a left humerus, bearing an almost complete trochlea and fragmented medial and lateral epicondyles

in posterior view. The specimen is generally well preserved, with a few cracks mainly in the distal epiphysis. The specimen AT228 is a highly fragmented distal epiphysis and part of diaphysis of a left humerus, similar to AT366. The distal epiphysis of the specimen AT228 is fragmented in the distal and lateral surface.

**Measurements**

The measurements of the specimens from Aghia Kyriaki (AT366, AT228) attributed to Cervidae indet, are given in the Table 12.

Table 12: Basic measurements (DAP and DT) of the distal epiphysis of the humeri AT366 and AT228 from Aghia Kyriaki. Measurements in mm.

| ID code | Locality | DAP distal | DT distal |
|---|---|---|---|
| AT366 | Aghia Kyriaki | 24.65 | 32.56 |
| AT228 | Aghia Kyriaki | | 31.03 |

**Comparison**

The specimens AT228, AT366 bear the typical morphological characteristics of Cervidae indet. humeri: the distal epiphysis consists of two epitrochleae, divided by one groove and one crest, located slightly lateral to the distal articulation midline (Heintz, 1970) The medial margin of the trochlea is proximodistally higher than the lateral, and consequently, in anterior view, the trochlea tapers laterally.

**4.8 *Metacervocerus* sp.** Dietrich 1938

**Material**

Postcranial: complete right tibia, AT293/AT306/AT311/AT312

**Description**

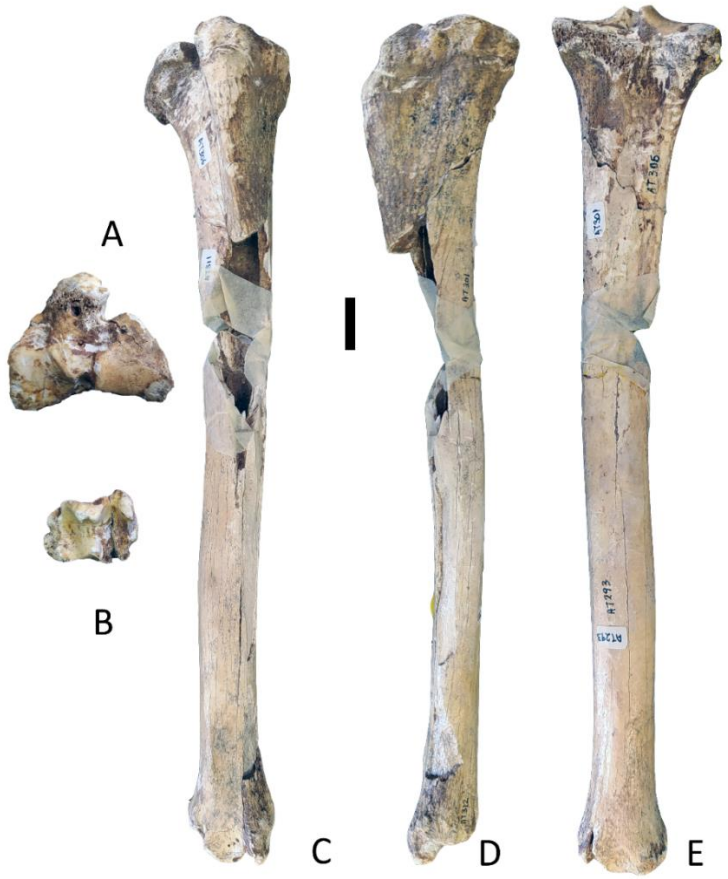


Figure 30: AT293/AT306/AT311/AT312, right tibia from the locality of Aghia Kyriaki, attributed to the taxon *Metacervocerus* sp.., in A: proximal, B: distal, C: anterior, D: medial and E: posterior views.

AT293/AT306/AT311/AT312

An almost complete right tibia, with slight breaks and cracks is preserved. The diaphysis is slender and slightly sinuous (Fig. 32 C–E); it creates a subtle curvature towards the lateral side, at the lower (distal) third of the specimen.

The proximal epiphysis of the specimen is consisted by a medial and a lateral condyle, that are divided in proximal view by an anteroposterior canal. In proximal view (Fig. 32A), the medial border of the medial condyle is almost straight from the posterior part till approximately the mid of the anteroposterior diameter of the tibia, with an anteroposterior direction, whereas the medial border of the specimen from the middle of the anteroposterior diameter of the tibia towards the anterior side, is narrower and it forms a concavity leading to the convex anterior edge of the tibia. Although slightly broken, the anteromedial edge of the lateral condyle of the proximal epiphysis is rather rounded than angular. The mediolateral length of the lateral condyle is larger than the one of the medial condyle. Also, the anterior edge of the proximal epiphysis, as well

as the anterolateral border of the lateral condyle are slightly broken, thus the outline of the muscular sulcus is not clear. However, this outline seems to be rather angular than concave.

In anterior view (Fig. 32C), the tibial crest tuberosity is slightly cracked and broken, especially towards the edges. Its proximodistal dimension is longer than the mediolateral one. Neither notch nor groove is found on the tibial crest. Approximately one fourth of the anterior surface of the diaphysis is missing.

In posterior view (Fig. 32E), the surface right distally of the proximal epiphysis is broken, thus the ligament tubercule is absent. However, it seems to be rather off–centered, towards the medial part of the diaphysis. The lateral edge of the diaphysis is strong and rather angular towards the proximal side but it becomes more circular towards the distal part. Two strong almost parallel muscular ridges are present in the diaphysis, starting from the proximal part of the diaphysis and ending up less prominent in the distal part, with a proximolateral to distomedial direction. The medial articular groove seems to be broken, with the breakage being present in the diaphysis, right proximally of the distal epiphysis, too.

In lateral view, the bone being rather concave towards the anterior surface.

In distal view (Fig. 32B), the distal epiphysis consists of two parallel articular grooves, with an anteroposterior direction: the lateral and the medial articular grooves, as well as two facets on the lateral edge of the epiphysis for the attachment of the distal fibula (lateral malleolus): one anterior and one posterior facet. The medial articular facet has a crack parallel to the sagittal axis of the bone, and when seen on distal view, it also has a crack on the posterior edge. The anterior facet is almost drop–like shaped, and its anteroposterior dimension (9.55 mm.) is greater than its medio–lateral one (4.92 mm.). The posterior facet is almost rounded, and medio–laterally larger (7.62 mm.) than the anterior facet. The lateral edge of the lateral articular groove is straight and parallel to the groove. The anterior portion of the edge angles sharply toward the midline.

**Measurements**

The measurements of the specimen AT293/AT306/AT311/AT312 from Aghia Kyriaki, attributed to *Metacervocerus* sp. are given in the Table 13.

Table 13: Measurements of the specimen AT293/AT306/AT311/AT312, according to Van den Dreisch (1976) and Sorbelli et al. (2021). Abbreviations in these pubications, accordingly. Measurements in mm.

| ID code | Locality | GL | LI | BP (DT prox.) | DAP prox | SD | CD | DEEAW |
|---|---|---|---|---|---|---|---|---|
| AT293/ AT306/ AT311/ AT312 | Aghia Kyriaki | 315.3 | 295 | *57.81* | *47.62* | *23.03* | 19.47 | 22.76 |
| | | **DEAW** | **DEAT** | **MFT** | **MFW** | **DEW (DT dist.)** | **DET (DAP dist.)** | |
| | | 31.06 | *20.84* | *12.77* | 6.51 | 35.25 | 25.84 | |

**Comparison**

The specimen AT293/AT306/AT311/AT312 shows the typical morphology of a Cervidae tibia: slender and slightly sinuous diaphysis, thus will be compared to various Pleistocenic Cervid taxa.

Table 14: Measurements of the total length of the tibias for the specimen AT293/AT306/AT311/AT312 from Aghia Kyriaki, as well as for the taxa *Croizetoceros ramosus*, *Metacervocerus rhenanus*, *Eucladocerus* sp., *Haploidoceros mediterraneus* and *Capreolus capreolus*. Measurements from: Heintz (1970), Cregut Bonnoure and Tsoukala (2017), Garrido (2014), Croitor (2006), Croitor et al. (2008), Sanz et al. (2013) and Mirzoyan and Manaseyran (2008).

| Taxon | Locality | ID code | Length | | |
|---|---|---|---|---|---|
| | | | N | min-max | mean |
| | Aghia Kyriaki | AT293/AT306/ AT311/AT312 | 1 | | 315.3 |
| *Croizetocerus ramosus* | La Puebla de Valverde | | 1 | | 259 |
| *Croizetocerus ramosus* | Saint Vallier | | 3 | 274–290 | 282 |
| *Metacervocerus rhenanus perolensis* | Peyrolles | | 2 | 267–275 | 271 |
| *Metacervocerus rhenanus philisi* | Seneze | | 26 | 290–343 | 318.27 |
| *Metacervocerus rhenanus valliensis* | Saint Vallier | | 4 | 289–322 | 309.5 |
| *Eucladoceros* sp. | Seneze | | 22 | 331–413 | 368.9 |
| *Eucladoceros* sp. | La Puebla de Valverde | | 1 | | 420 |
| *Eucladoceros* sp. | Saint Vallier | | 1 | | 423 |
| *Haploidoceros mediterraneus* | Lunel– Viel | LV1–9–2220 | 1 | | 275 |
| *Haploidoceros mediterraneus* | Lunel– Viel | LV1–5–4880 | 1 | | 270 |
| *Haploidoceros mediterraneus* | Lunel– Viel | LV1–9–1951 | 1 | | 282 |
| *Haploidoceros mediterraneus* | Cova del Rinoceront | CR–I–3204 | 1 | | 291 |
| *Haploidoceros mediterraneus* | Cova del Rinoceront | CR–I–3320 | 1 | | 298 |
| *Haploidoceros mediterraneus* | Cova del Rinoceront | CR–I–3255 | 1 | | 301 |
| *Capreolus capreolus* | Shirakavan | | 1 | | 195 |

Following the metrical comparison in Table 14, the total length of the specimen AT293/AT306/AT311/AT312 (315.3 mm) is well within the range of *Metacervocerus*, larger than *Croizetocerus* and *Capreolus* and significantly smaller than *Eucladoceros*.

Table 15: Basic measurements of the proximal epiphysis of the tibia (DAP prox, DT prox) for the specimen AT293/AT306/AT311/AT312 from Aghia Kyriaki, as well as the taxa *Haploidoceros mediterraneus* and *Capreolus capreolus*. Measurements from Sanz et al. (2013) and Mirzoyan and Manaseyran (2008).

| Taxon | Locality | ID code | DAP prox. | | | DT prox | | |
|---|---|---|---|---|---|---|---|---|
| | | | N | min-max | mean | N | min-max | mean |
| | Aghia Kyriaki | AT293/AT306/ AT311/AT312 | 1 | | *47.62* | 1 | | *57.81* |
| *Haploidoceros mediterraneus* | Lunel– Viel | LV1–5–4880 | | | | 1 | | 59 |
| *Haploidoceros mediterraneus* | Lunel– Viel | LV1–9–1951 | | | | 1 | | 61.1 |
| *Haploidoceros mediterraneus* | Cova de Rinoceront | CR–I–3320 | 1 | | 56 | 1 | | 56 |
| *Haploidoceros mediterraneus* | Cova de Rinoceront | CR–I–3255 | | | | 1 | | 63 |
| *Haploidoceros mediterraneus* | Cova de Rinoceront | CR–I–2067 | 1 | | 61 | 1 | | 59 |
| *Capreolus capreolus* | Shirakavan | | | | | 1 | | 39 |

The DT proximal of the specimen AT293/AT306/AT311/AT312 from Aghia Kyriaki (*57.81* mm.) is similar in size to those of *Haploidoceros mediterraneus* , and significantly larger than the one of *Capreolus capreolus*. However, The DAP prox of the specimen from Aghia Kyriaki is smaller than the one of *Haploidoceros mediterraneus* and *Capreolus capreolus* (Table 15).

Table 16: Basic measurements of the distal epiphysis (DAP dist and DT dist) of the specimen AT293/AT306/AT311/AT312 from Aghia Kyriaki, as well as the taxa *Croizetoceros ramosus*, *Metacervocerus rhenanus*, *Metacervocerus pardinensis*, *Eucladoceros* sp. *Haploidoceros mediterraneus* and *Capreolus capreolus*. Measurements from Heintz (1970), Cregut Bonnoure and Tsoukala (2017), Garrido (2014), Croitor (2006), Croitor et al. (2008), Sanz et al. (2013) and Mirzoyan and Manaseyran (2008).

| Taxon | Locality | ID code | DAP dist. | | | DT dist. | | |
|---|---|---|---|---|---|---|---|---|
| | | | N | min-max | mean | N | min-max | mean |
| | Aghia Kyriaki | AT293/ AT306/ AT311/ AT312 | 1 | | 25.84 | 1 | | 35.25 |

| | | | | | | | | |
|---|---|---|---|---|---|---|---|---|
| *Croizetoceros ramosus* | La Puebla de Valverde | | 7 | 22.5–24 | 23.1 | 5 | 28.5–29.5 | 29.1 |
| *Croizetoceros ramosus* | Saint Vallier | | 17 | 22.5–24.5 | 23.8 | 16 | 27.5–32.5 | 29.7 |
| *Croizetoceros ramosus* | Villaroya | | 17 | 22.5–26 | 23.7 | 18 | 28–32 | 29.8 |
| *Croizetoceros ramosus* | Etouaires | | 13 | 24–26.5 | 25 | 13 | 30–33 | 31.5 |
| *Croizetoceros ramosus* | Milia | MIL 663 D | | | | 1 | | 28.9 |
| *Croizetoceros ramosus* | Milia | MIL 1219 D | 1 | 23 | | 1 | | 31.4 |
| *Croizetoceros ramosus* | Milia | MIL 1209 D | 1 | 20.9 | | 1 | | 26.4 |
| *Croizetoceros ramosus* | Milia | MIL 1849 D | 1 | 24.9 | | 1 | | 31.2 |
| *Croizetoceros ramosus* | Milia | MIL 1141 S | 1 | 22.6 | | 1 | | 30.2 |
| *Croizetoceros ramosus* | Milia | MIL 1383 S | 1 | 25.6 | | 1 | | 33.7 |
| *Croizetoceros ramosus* | Milia | MIL 1543 D | 1 | 22.4 | | 1 | | 30.3 |
| *Croizetoceros ramosus fonelensis* | Fonelas P–1 | FP1–2001–0084 | 1 | 21.42 | | 1 | | 28.54 |
| *Metacervocerus rhenanus perolensis* | Peyrolles | | 4 | 23.5–28 | 25.37 | 5 | 28.5–31.5 | 30.3 |
| *Metacervocerus rhenanus philisi* | Seneze | | 33 | 27–33 | 30.71 | 33 | 33.5–40 | 36.43 |
| *Metacervocerus rhenanus* | Chillac | | 1 | | 32 | 1 | | 36 |
| *Metacervocerus rhenanus valliensis* | Saint Vallier | | 16 | 27.5–31.5 | 29.28 | 15 | 32–37.5 | 34.53 |
| *Metacervocerus pardinensis* | Etouaires | | 1 | | 27.5 | 2 | 33–34 | 33.5 |
| *Metacervocerus pardinensis* | Vialette | | 13 | 27–31.5 | 29.11 | 14 | 32.5–37 | 34.53 |
| *Eucladoceros* sp. | Peyrolles | | 2 | 31.5–37.5 | 34.5 | 2 | 43–48.5 | 45.75 |
| *Eucladoceros* sp. | Seneze | | 29 | 35–45.5 | 39.81 | 29 | 43.5–56 | 47.96 |

| | | | | | | | | |
|---|---|---|---|---|---|---|---|---|
| *Eucladoceros* sp. | La Puebla de Valverde | | 6 | 41–43.5 | 42.33 | 6 | 48.5–56 | 50.5 |
| *Eucladoceros* sp. | Saint Vallier | | 15 | 38.5–47 | 43.9 | 15 | 41–56 | 52.63 |
| *Eucladoceros* sp. | Roccaneyra | | 2 | 40.5–44 | 42.25 | 2 | 49–51.5 | 50.25 |
| *Eucladoceros* sp. | Fonelas P–1 | FP1–2001–0158 | 1 | | 46.9 | 1 | | 61.21 |
| *Metacervocerus rhenanus philisi* | Fonelas P–1 | FP1–2001–0369 | 1 | | 32.32 | 1 | | 38.15 |
| *Metacervocerus rhenanus* | Ceyssaget | Cey–10272 | 1 | | 27 | 1 | | 34 |
| *Haploidoceros mediterraneus* | Lunel–Viel | LV1–9–2220 | 1 | | 30.4 | 1 | | 40 |
| *Haploidoceros mediterraneus* | Lunel–Viel | LV1–5–4880 | 1 | | 29.7 | 1 | | 39.4 |
| *Haploidoceros mediterraneus* | Lunel–Viel | LV1–9–1951 | 1 | | 31.1 | 1 | | 39 |
| *Haploidoceros mediterraneus* | Cova de Rinoceront | CR–I–3204 | 1 | | 29 | 1 | | 36 |
| *Haploidoceros mediterraneus* | Cova de Rinoceront | CR–I–3320 | 1 | | 29 | 1 | | 37 |
| *Haploidoceros mediterraneus* | Cova de Rinoceront | CR–I–3255 | 1 | | 29 | 1 | | 38 |
| *Haploidoceros mediterraneus* | Cova de Rinoceront | CR–I–2067 | 1 | | 31 | 1 | | 36 |
| *Capreolus capreolus* | Shirakavan | | | | | 1 | | 24 |

The distal epiphysis of the specimen AT293/AT306/AT311/AT312 from Aghia Kyriaki (25.84, 35.25) is comparable in size to the smaller forms of *Metacervocerus rhenanus* (Philisi), larger than *C. ramosus*.and smaller than *Eucladoceros* sp. (Table 16) Combining all theaforementioned metrical data, we can say that both the total length as well as the DAP and DT of the distal epiphysis of the specimen AT293/AT306/AT311/AT312 from Aghia Kyriaki fall into the range of *Metacervocerus* sp. Thus, we can attribute the specimen to the genus *Metacervocerus*.

**Discussion**

The genus *Metacervocerus* was represented in Europe by two different species: *Metacervocerus pardinensis* Croizet & Jobert, 1828 and *Metacervocerus rhenanus* 1904 (Croitor, 2018). The genus *Cervus* (*Metacervoceros*) Dietrich 1938 was established with the type species *Cervus pardinensis* Croizet & Jobert, 1828 for the small sized, simple three–pointed antlered cervids of the Late Pliocene. However, the exact systematic position of the cervids with these characteristics is under debate. Whereas the *Metacervocerus* was elevated to the generic level by Samson et al. (1970), De Vos et al. (1955) suggested that *Metacervocerus pardinensis* and *Metacervocerus rhenanus* should be attributed to the genus *Cervus*, and Pfeiffer (1999) attributed them to the genus *Dama*. However, the primitive skull morphological characteristics of *Metacervocerus rhenanus* cannot include it in the genera *Dama* or *Cervus* (Croitor, 2018). On the contrary, Di Stefano and Petronio (2002) included the two species of *Metacervocerus* in the modern *Rusa*, a suggestion that Croitor (2018) does not support, based on the cranial morphology.

*Metacervocerus pardinensis* Croizet and Jobert, 1828 is a small cervid with an estimated weight of 60 kg that was first described from the Pliocene fauna of Perrier–Les Etouaires, France (Pomel, 1853; Heintz 1970; Croitor, 2018). The older fossils attributed to this species come from the late Ruscinian (MN15) faunas of Moldova (Croitor and Stefaniak, 2009), Bulgaria (Spassov, 2005), Brasov– Romania (Radulesco et al., 2003) and Poland (Stefaniak 1995, 2015). According to Croitor (2018), the youngest remains of the species are reported from the faunas of Etouaires (France) and the Red Crag Nodule Bed, England (MN16b) (Lister, 1999), as well as MN16a faunas in Romania (Radulesco et al. 2003; Radulesco 2005) and Slovakia (Sabol, 2003). Moreover, an antler specimen from the Late Pliocene of Azerbaijan, described by Alekperova (1964) as *Cervus (Rusa)* sp., is regarded to be similar to *M. pardinensis* by Croitor (2018).

*Metacervocerus rhenanus* Dubois, 1904 is a middle–sized deer with a rather complicated nomenclatural history, since each European sample collection was considered taxonomically distinct and thus was named differently (Athanassiou, 2022). The species was included in the genus of *Metacervocerus* by Croitor and Bonifay (2001). Synonym species to *Metacervoceros rhenanus* are *Cervus (Axis) rhenanus* Dubois, 1904, *Cervus philisi* Schaub, 1941, *Cervus perolensis* Azzaroli, 1952 and *Cervus ischnoceros* Boeuf, Geraads and Guth, 1992, with *Cervus philisi* being the most often used name, as the rich mid–sized deer samples from the localities of Saint Vallier, Seneze and Chillac were attributed to that (Viret 1954; Heintz 1970; Boeuf 1983; Valli 2004; Athanassiou, 2022). According to Athanassiou (2022), the taxon is split into four different subspecies, based on the locality they were found in: *M. rhenanus valliensis* Heintz, 1970 (Saint Vallier), *M. rhenanus philisi* Schaub, 1941 (Seneze), *M. rhenanus rhenanus* Dubois, 1904 (Tegelen), and *M. rhenanus perolensis* Azarroli, 1952 (Peyrolles).

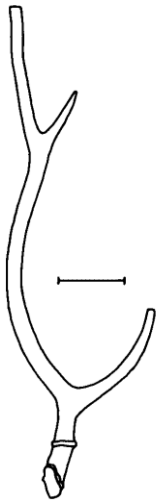

Figure 31: Holotype of *Metacervocerus rhenanus*: Ha –15–777, left antler described by Dubois in 1904 and 1905. Figure from Spaan (1992).

The type material (holotype) of the species was defined on the left antler Ha–15–777, described by Duboiis in 1904 and 1905 (Fig. 33), and the type locality of the species is the Lower Pleistocene (MN18) site of Clays of Tegelen in the Netherlands (Athanassiou, 2022).
According to Athanassiou (2022), the species is the most abundant deer in Villafranchian aged faunas. Moreover, Croitor (2018) states that the species was present during the Early Pleistocene, with its first occurrence in the fauna of Saint Vallier, France (2.5 Ma) and its last occurrence in Vallonet (0.9 Ma). *M. rhenanus* was present in Spain, France, Netherlands, Romania and Greece (Croitor and Bonifay, 2001), whereas no proofs of its existence have yet been found in the Italian Peninsula (Croitor, 2018). In Greece, samples from the Villafranchian faunas of Volakas, Dafnero, Sesklo, Gerakarou, Tsiotra Vryssi and Tourkobounia are attributed to the species (Kostopoulos, 1996; Athanassiou, 2022), and also possibly those of Kos (Athanassiou, 2022). Thus, the biochronological range of the species in Greece is limited to the biozones MNQ17–18 and possibly MNQ19.

**4.9 *Croizetoceros ramosus*** Croizet & Jobert, 1828.

**Material**
Teeth: maxillar fragment, with M1 and empty tooth case of M2 (AT188).

Postcranial elements: distal epiphysis of right tibia (AT205), distal epiphysis of left tibia (AT218b), one right astragalus (AT198), left astragalus (AT367).

**Description**

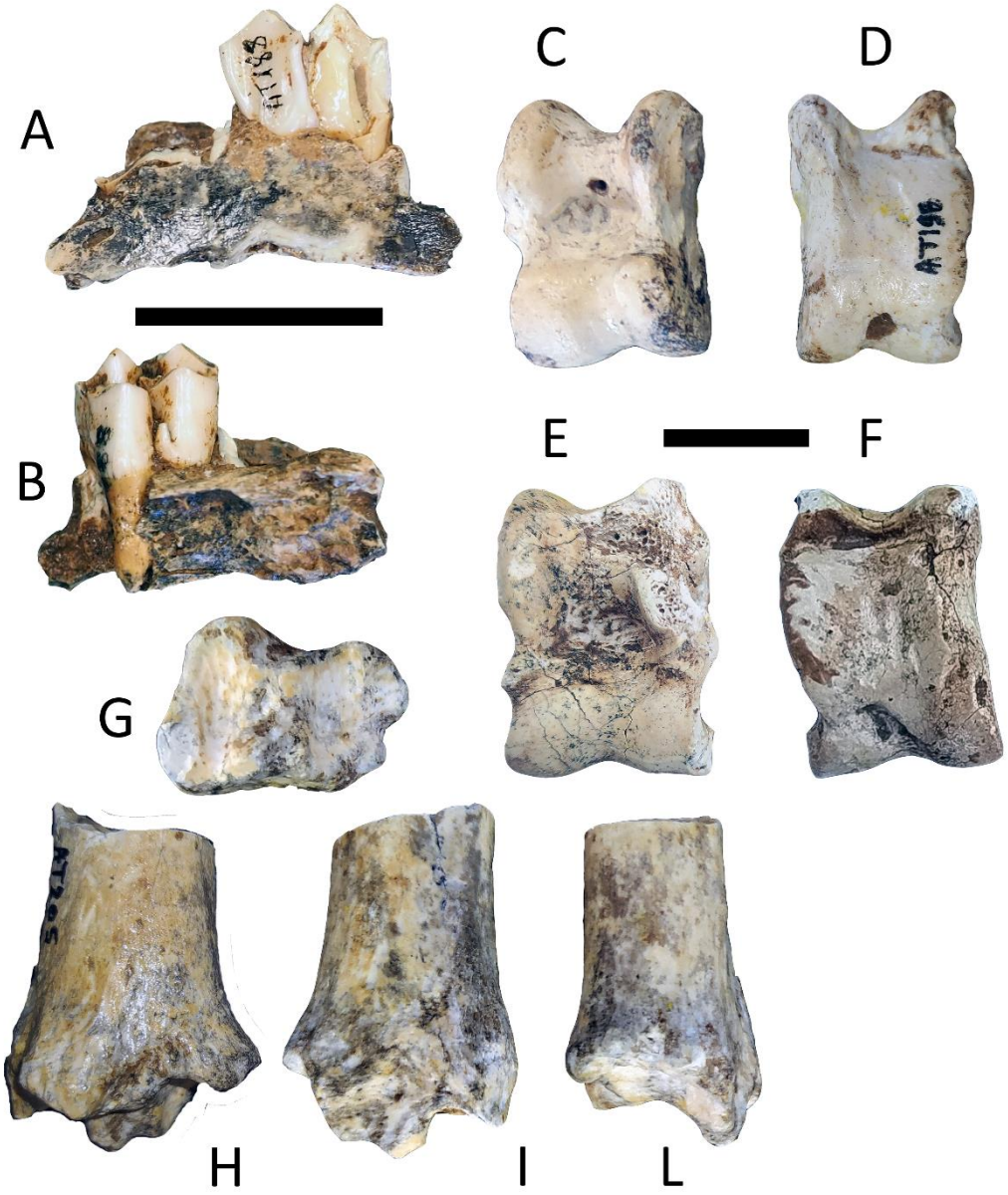


Figure 32: Specimens from the locality of Aghia Kyriaki, attributed to *C. ramosus*: maxillar fragment with M1 and empty tooth case of M2 (AT188) in A: buccal and B: lingual view, right astragalus (AT198) in C: anterior and D: posterior views, left astragalus (AT367) in E: anterior and F: posterior view, right tibia (AT205) in G: distal, H: posterior, I: anterior and L: lateral views. Scale bar: 20mm.

AT188

The maxillary fragment AT188 bears only M1, while M2, is broken in the base of the tooth (Fig. 34 A,B). The parastyle of M1 is slightly broken. The metastyle is well developed and has a slight posterolingual direction, in the occlusal view. The mesostyle is remarkably strong from the base of the buccal side until the edge of the occlusal surface, being the most prominent element of the outer wall of the tooth. Both the paracone and the metacone are projected towards the lingual side of the occlusal

surface, with the former having a buccolingual direction and the latter having a rather more posterobuccal to anterolingual direction. The entostyle is developed, and it is tangential to the hypocone.

Tibias

In distal view (Fig. 34G), the posterior facet is subtriangular and larger than the subtriangular– almost rounded anterior facet. In distal view, the lateral edge of the lateral articular groove is straight and parallel to the groove. The anterior portion of the edge angles sharply toward the midline. Immediately above the anterior fibular facet on the lateral surface, there is a raised tubercle. In anterior view, the medial malleolus is thin and is the same height as the spine. There are only few muscular ridges, confined to proximal half of the shaft. The specimen AT218b is has a slightly cracked anterior facet in distal view. The specimen AT205 is a distal epiphysis of a right tibia.

Astragali

In dorsal view, the specimens have a rectangular shape (Fig. 34), with the lateral and medial side being more elongated than the proximal and distal side. The two proximal trochlear ridges are parallel to the sagittal plane. In proximal view, the lateral trochlea of the proximal articulation seems to be higher but less wide than the medial one. The intertrochlear notch is wide and smooth and ends distally in a deep fossa. The distal trochleae are more clearly different in size than the proximal trochlea: in anterior view, the lateral condyle of the distal trochlea is higher and clearly wider than the medial condyle. The intertrochlear notch of the distal trochlea is narrower and shallower than the one of the proximal trochlea. In lateral view, there is a prominence between the proximal and distal epiphysis, along the anterior border.

The specimen AT198 is a right astragalus of rectangular shape (Lmax/ Wmax= 31.4/ 20.39= 1.54). AT198 is complete, with slight cracks mainly in the medial and lateral view. In proximal view, the lateral trochlea of the proximal articulation is broken towards the posterior side. The specimen AT367 is a an almost complete, left astragalus with several cracks due to weathering (stage 1– Behrensmeyer, 1978). In anterior view, the specimen has a rather rectangular shape, with the lateral and medial side being more elongated than the proximal and distal side. However, it seems to be more squared than the specimen AT198 (AT367: Lmax/Wmax= 34.15/ 23.46= 1.46). In proximal view, the lateral condyle of the proximal articulation is broken in the anterior side, whereas the medial condyle has a small crack distal–laterally.

**Measurements**

The basic measurements of the specimens from Aghia Kyriaki attributed to *Croizetoceros ramosus* are given in the Tables 17–19.

Table 17: Basic measurements (occlusal length and occlusal width) of the M1 tooth AT188 from Aghia Kyriaki. Measurements in mm.

| ID code | Site | Occlusal length (mm) | Occlusal width (mm) |
|---|---|---|---|
| AT188 | Aghia Kyriaki | 12.05 | 11.37 |

Table 18: Basic measurements (DT and DAP) of the distal epiphysae of the tibias AT218b and AT205 from Aghia Kyriaki. Abbreviations in Table 8. Measurements in mm.

| ID code | Site | DT distal (mm) | DAP distal (mm) |
|---|---|---|---|
| AT218b | Aghia Kyriaki | 28.52 | 23.42 |
| AT205 | Aghia Kyriaki | 29.01 | 20.27 |

Table 19: Measurements of astragali AT198 and AT367 from Aghia Kyriaki, attributed to the species *C. ramosus*. Measurements in mm.

| ID code | Locality | L. lat. | L. med. | L. min. | DT artic prox. | DT prox. | DAP max. | DT min. | DT dist. |
|---|---|---|---|---|---|---|---|---|---|
| AT198 | Aghia Kyriaki | 31.67 | 30.75 | 25.38 | 19.2 | 20.36 | 18.09 | 17.68 | 19.86 |
| AT367 | Aghia Kyriaki | 34.12 | 32.28 | 27.42 | 20.21 | 23.23 | 18.77 | 19.98 | 22.03 |

**Comparison**

The basic measurements on the occlusal surface of the preserved tooth, M1 (length, width) of the specimen AT188, as well as of other Cervidae of the Villafranchian, can be seen in the Table 20.

Table 20: Basic measurements of the occlusal surface of the M1 tooth of the specimen AT188 from Aghia Kyriaki, as well as of the Villafranchian taxa of *C. ramosus, M. rhenanus, Eucladoceros* sp. and *Arvernoceros ardei* from various localities. Measurements in mm. Data from Heintz (1970) and Kostopoulos (1996).

| Taxon | Site | Length | | | Width | | |
|---|---|---|---|---|---|---|---|
| | | N | Min–max | Mean | N | Min–max | Mean |
| AT188 | Aghia Kyriaki | 1 | | 12.05 | 1 | | 11.37 |
| *Croizetoceros ramosus* | Seneze | 2 | 14.5 | 14.5 | 2 | 14 | 14 |
| *Croizetoceros ramosus* | Coupet | 4 | 11.5–14.5 | 13.37 | 4 | 13.5–14.5 | 14.25 |
| *Croizetoceros ramosus* | La Puebla de Valverde | 25 | 11.5–16 | 13.78 | 24 | 13.5–15 | 14.14 |
| *Croizetoceros ramosus* | Saint Vallier | 28 | 11.5–15 | 13.78 | 27 | 12.5–15.5 | 14.01 |
| *Croizetoceros ramosus* | Pardines | 5 | 13.5–15 | 14.2 | 5 | 13.5–15.5 | 14.6 |
| *Croizetoceros ramosus* | Villaroya | 22 | 13–16 | 14.5 | 22 | 13.5–16 | 15.02 |
| *Croizetoceros ramosus* | Etouaires | 20 | 12.5–14.5 | 13.67 | 20 | 13.5–15.5 | 14.45 |

| | | | | | | | |
|---|---|---|---|---|---|---|---|
| *Croizetoceros ramosus* | Vialette | 2 | 13–13.5 | 13.25 | 2 | 15.5–16 | 15.75 |
| *Croizetoceros ramosus* | Volakas | 1 | 14.10 | 14.10 | 1 | 13.7 | 13.7 |
| *Croizetoceros ramosus* | Gerakarou | 17 | 12–15.8 | 14.17 | 17 | 12.8–15.1 | 13.71 |
| *M. rhenanus perolensis* | Peyrolles | 8 | 14.5–17.5 | 15.93 | 9 | 16–17.5 | 16.72 |
| *M. rhenanus philisi* | Seneze | 36 | 14.5–19.5 | 16.81 | 35 | 16–19 | 17.42 |
| *M. rhenanus* | Chillac | 1 | 17 | 17 | 1 | 18 | 18 |
| *M. rhenanus* | Coupet | 1 | 15.5 | 15.5 | 1 | 18.5 | 18.5 |
| *M. rhenanus valliensis* | Saint Vallier | 30 | 14–17 | 15.2 | 30 | 145–18.5 | 16.56 |
| *M. pardinensis* | Etouaires | 2 | 16–17 | 16.5 | 2 | 19.5 | 19.5 |
| *Eucladoceros sp.* | Peyrolles | 2 | 21.5–26 | 23.75 | 2 | 23–24 | 23.5 |
| *Eucladoceros sp.* | Seneze | 35 | 20–26.5 | 23.3 | 34 | 20.5–25.5 | 22.85 |
| *Eucladoceros sp.* | Coupet | 1 | 21.5 | 21.5 | 1 | 21.5 | 21.5 |
| *Eucladoceros sp.* | La Puebla de Valverde | 4 | 24.25 | 24.62 | 3 | 22.5 | 22.5 |
| *Eucladoceros sp.* | Saint Vallier | 20 | 19–26.5 | 23.47 | 17 | 22.5–25 | 23.41 |
| *Eucladoceros sp.* | Pardines | 2 | 19–25.5 | 22.25 | 2 | 24.5 | 24.5 |
| *Arvernoceros ardei* | Villaroya | 2 | 22–24 | 23 | 2 | 23–25.5 | 24.25 |
| *Arvernoceros ardei* | Etouaires | 12 | 19–22 | 20.2 | 12 | 20–23.5 | 21.91 |

Note 1: The species attributed to *Metacervocerus* were originally described as "*Cervus*" by Heintz (1970). However, according to modern bibliography, the species *C. perolensis*, *C. philisi* and *C. pardinensis* are all attributed to the genus "*Metacervocerus*". Thus, *M. rhenanus perolensis* from Peyrolles belongs to the ex. group *Cervus perolensis*, *M. rhenanus*, *M. rhenanus philisi* and *M. rhenanus valliensis* from Seneze, Chillac and Saint Vallier accordingly belong to the ex. Group *Cervus philisi*. Last, *M. pardinensis* from Etouaires belong to the ex. Group *Cervus pardinensis*.

In the Table 20, we observe that the upper first molars of the species *Croizetoceros ramosus* are smaller (both in occlusal length and width) than the ones of the genus *Metacervocerus*, which are also smaller than those of *Eucladoceros* and *Arvernoceros ardei.* The measurements of the specimen AT188 (12.05, 11.37) (in mm.) fall into the range of *Croizetoceros ramosus* (11.5–16, 12.5–16) (in mm.), and especially to the

Saint Vallier population of this species with the occlusal width of the specimen being slightly smaller than the aforementioned range.

Table 21: Basic measurements of the distal epiphysis of tibias (DAP and DT) for the specimens AT218 and AT205 from Aghia Kyriaki, as well as for specimens attributed to *Croizetoceros ramosus* from the localities of La Puebla de Valverde (Spain), Saint Vallier (France), Villaroya (Spain), Etouaires (France), Milia (Greece) and Fonelas P–1 (Spain). Measurements from: Heintz (1970) and Cregut– Bonnoure & Tsoukala (2017). Measurements in mm.

| Taxon | Site | DT distal | | | DAP distal | | |
|---|---|---|---|---|---|---|---|
| | | N | Min–max | Mean | N | Min–max | Mean |
| AT218 | Aghia Kyriaki | 1 | | 28.52 | 1 | | 23.24 |
| AT205 | Aghia Kyriaki | 1 | | 29.01 | 1 | | 20.27 |
| *Croizetoceros ramosus* | La Puebla de Valverde | 5 | 28.5–29.5 | 29.1 | 7 | 22.5–24 | 23.1 |
| *Croizetoceros ramosus* | Saint Vallier | 16 | 27.5–32.5 | 29.7 | 17 | 22.5–24.5 | 23.8 |
| *Croizetoceros ramosus* | Villaroya | 18 | 28–32 | 29.8 | 17 | 22.5–26 | 23.7 |
| *Croizetoceros ramosus* | Etouaires | 13 | 30–33 | 31.5 | 13 | 24–26.5 | 25 |
| *Croizetoceros ramosus* | Milia | 7 | 26.4–33.7 | 30.28 | 6 | 20.9–25.6 | 23.25 |
| *Croizetoceros ramosus* | Fonelas P–1 | 1 | 28.54 | | 1 | 21.42 | |

The distal tibias from Aghia Kyriaki AT205 and AT218 are closer proportionally to the taxon *Croizetoceros ramosus*, from the locality of Fonelas P–1, than to other cervid taxa (Table 21).

Table 22: Table of measurements (total– maximum length and DT distal of astragalus) of the specimens AT198 and AT367 from Aghia Kyriaki, as well as the taxa *Croizetoceros ramosus*, *Metacervocerus rhenanus* and *Metacervocerus pardinensis*. Measurements from Heintz (1970). Measurements in mm. Numbers in italics are appropriate measurements.

| Taxon | Locality | ID code | Length | | | DT distal | | |
|---|---|---|---|---|---|---|---|---|
| | | | N | min-max | mean | N | min-max | mean |
| | Aghia Kyriaki | AT198 | 1 | 31.67 | 31.67 | 1 | 19.86 | 19.68 |
| | Aghia Kyriaki | AT367 | 1 | *33.75* | *33.75* | 1 | 23.62 | 23.62 |
| *C. ramosus* | Coupet | | 10 | 30.5-37.5 | 33.3 | 10 | 18.5-23.5 | 20.8 |
| *C. ramosus* | La Puebla de Valverde | | 10 | 33.5-36.5 | 34.8 | 10 | 20.5-22.5 | 21.4 |
| *C. ramosus* | Saint Vallier | | 34 | 33.0-38.5 | 36.8 | 35 | 20.5-24.5 | 23 |

| | | | | | | | | |
|---|---|---|---|---|---|---|---|---|
| *C. ramosus* | La Roche-Lambert | | 1 | | 36.5 | 1 | | 23 |
| *C. ramosus* | Villaroya | | 6 | 36.5-38.0 | 37.2 | 7 | 20.0-23.5 | 22.3 |
| *C. ramosus* | Etouaires | | 5 | 35.0-40.5 | 37.8 | 6 | 21.5-24.5 | 23.2 |
| *M. rhenanus perolensis* | Peyrolles | | 2 | 39.0-40.0 | 39.5 | 2 | 24.0-25.0 | 24.5 |
| *M. rhenanus philisi* | Seneze | | 50 | 41.0-49.5 | 45.52 | 55 | 25.5-31.5 | 28.26 |
| *M. rhenanus* | Coupet | | 4 | 41.0-46.5 | 42.75 | 4 | 24.5-29.0 | 26 |
| *M. rhenanus valliensis* | Saint Vallier | | 3 | 41.0-47.5 | 43.56 | 34 | 24.5-29.0 | 26.77 |
| *M. pardinensis* | Etouaires | | 6 | 41.0-48.5 | 45.33 | 6 | 25.5-31.0 | 28.16 |
| *M. pardinensis* | Vialette | | 22 | 41.0-49.0 | 44.27 | 27 | 24.5-28.5 | 26.9 |

The maximum length range of the astragalus of *Croizetoceros ramosus* is 30.5–40.5 mm (Table 22), whereas the one of *Metacervocerus* sp. is larger. Accordingly, the DT distal range of *C. ramosus* (18.5–24.5 mm) is smaller than the one of *M. rhenanus* (24–31.5 mm.) and *M. pardinensis* (24.5–31 mm.). Thus, both the length and the DT dist. of the specimens AT198 and AT 367 are placed within the ranges of *Croizetoceros ramosus* and closer to the smallest forms of *Croizetoceros ramosus*, eg. the ones of Coupet.

Thus, by its size, we may attribute theAghia Kyriaki small cervid taxon to the species *Croizetoceros ramosus*.

**Discussion**

According to Kostopoulos (1996), the main combinations of deer–like taxa of West Europe during the Villafranchian are the following: Upper Villafranchian (Seneze): *Croizetoceros ramosus*, *Metacervocerus rhenanus philisi* (ex. Group *"Cervus" philisi philisi* (Croitor, 2018*)*), *Eucladoceros ctenoides* (ex. group *Eucladoceros senezensis senezensis)*, *Libralces gallicus* (attributed to the genus *Alces*, according to Croitor (2018)), middle Villafranchian (Saint Vallier): *Croizetoceros ramosus medius*, *Metacervocerus rhenanus valliensis* (ex. Group *"Cervus" philisi valliensis*), *Eucladoceros senezensis vireti* and Lower Villafranchian (Etouaires): *Croizetoceros ramosus ramosus, Metacervoceros pardinensis (ex. Group "Cervus" pardinensis,* according to Croitor, 2018)*, C. perrieri/ Arvernoceros ardei*.

The type species of the genus *Croizetoceros* Heintz, 1970 is *Cervus ramosus* Croizet and Jobert, 1828. The genus *Croizetoceros* is represented by a single species, *Croizetoceros ramosus,* thus, it is monophyletic/ monotypic (Athanassiou, 2022). The species was originally defined on an antler fragment by Croizet and Jobert (1828),

however since no specimen from the collection of Natural History Museum in Paris fitted in the description of the holotype, Heintz (1970) set a neotype of the species (Fig. 35B). The type locality of the species is the Upper Pliocene Les Etouaires, France (MN16b) (Athanassiou, 2022).

Synonyms to this species are *Cervus cladocerus* Pomel, 1853, *Cervus polycladous* Gervais, 1859, *Cervus cylindrocerus* Dawkins, 1878 as well as the genera *Anoglochis* Croizet and Jobert, 1826, *Polycladus* Pomel, 1853 and *Cylindrocerus* Teilhard de Chardin and Piveteau, 1930 (Heintz, 1970; Athanassiou, 2022). Its biochronology ranges from the Pliocene to the Early Pleistocene (MN16– MN18), and it lived in Western and Southern Europe (Croitor, 2018; Athanassiou, 2022). It is a small sized deer, with an estimated weight of approximately 50–55 kg., with long and complex antlers, a relatively high positioned first tine and several crown tines with a small distance in between them. These tines grow only in the rostral side of the beam (Croitor, 2018; Athanassiou, 2022).

According to Heintz (1970), the number of tines of a completely grown antler can range from six to eight (Fig. 35A). These characteristics are unique and split *Croizetoceros* representatives from their contemporary genera (Athanassiou, 2022). In general, the frontal area of *Croizetoceros ramosus* is wide; the area between the pedicles is almost flattened, whereas caudally to them it narrows (Athanassiou, 2022). The derived dentition always presents constantly molarized p4s (Heintz, 1970). Another species from the Pliocene (MN15) locality of Serrat d'en Vacquer, named *Croizetoceros preramosus* is known only by dental elements and no antlers (Dong, 1996), thus the attribution of this mid– sized species into *Croizetoceros* sp. is uncertain (Athanassiou, 2022).

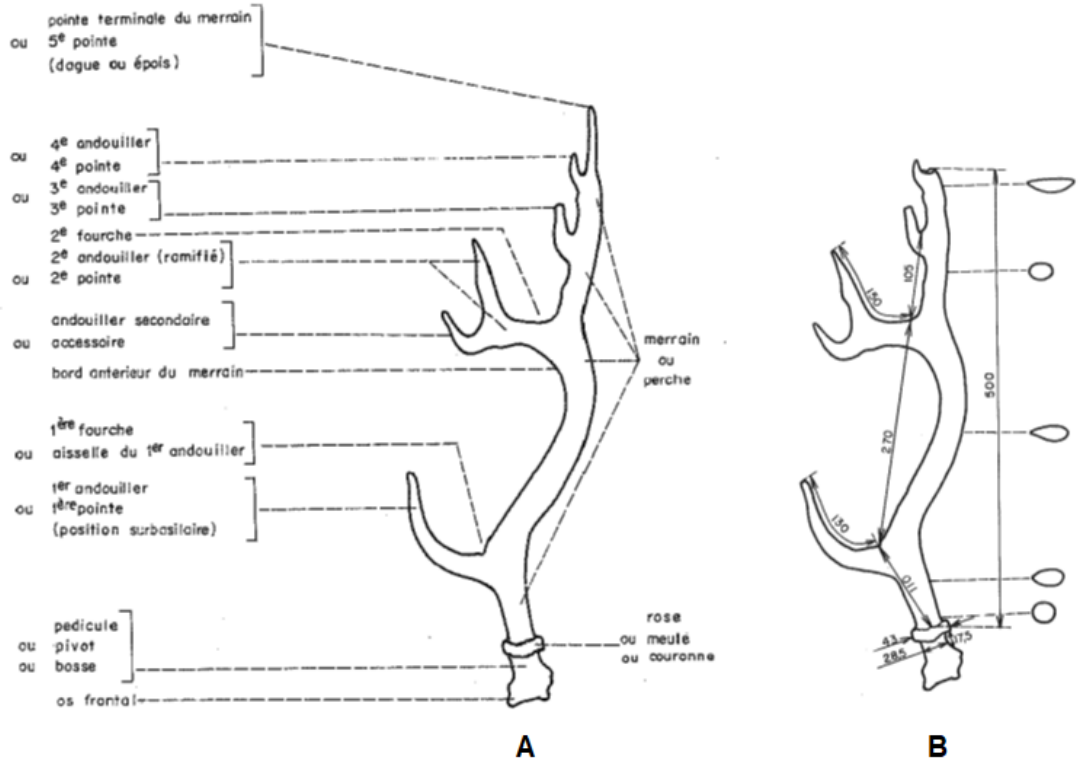


Figure 33: A: Sketch of the lateral– medial ("Latero–interne") view of a right antler from Les Etouaires and its basic characteristics. Figure from Heintz (1970). B: Neotype of *Croizetoceros*

*ramosus*, as set by Heintz (1970). Right antler from Les Etouaires in latero–internal (lateromedial?) view. Sketch from Heintz (1970).

The species was originally defined on an antler fragment by Croizet and Jobert (1828), however since no specimen from the museum collection fitted in the description of the holotype, Heintz (1970) set a neotype of the species (Figure 35B). The type locality of the species is the Upper Pliocene locality of Les Etouaires, France (MN16b) (Athanassiou, 2022).

The geographical range of the species shows that *C. ramosus* covers all the Mediterranean areas from Spain to Greece from the late Rusinian (MN15) to the late Villafranchian (MN18) and it is a characteristic species of the Villafranchian faunas of west Europe (Kostopoulos, 1996).

Table 23: biostratigraphic table of *Croizetoceros ramosus* in the European area. Table from Kostopoulos (1996), modified.

| | **France** | **Spain** | **Italy** | **Greece** |
|---|---|---|---|---|
| Upper Villafranchian | *C. r. minor*<br><br>Seneze, Coupet, Chillac | | | *C. r. gerakarensis*<br><br>Gerakarou |
| middle Villafranchian | *C. r. medius*<br><br>Saint Vallier, Saint Vidal, R. Lambert | *C. r. pueblensis*<br><br>La Puebla de Valverde | | |
| Lower Villafranchian | *C. r. ramosus*<br><br>Etouaires, Vialette | *C. r. villaroyensis*<br><br>Villaroya | *C. r. (ramosus)*<br><br>Montopoli | |

As far as *C. ramosus* is concerned, there are six supspecies noted during the whole Villafranchian in France, Italy, Spain and Greece (Table 23) (early Villafranchian: *C. r. ramosus, C. r. villaroyensis*, middle Villafranchian: *C. r. medius, C. r. pueblensis*, late Villafranchian: C*. r. minor, C. r. gerakarensis*) (Heintz, 1970, De Giuli and Heintz, 1974, Kostopoulos, 1996); it is noted that the size of *C. ramosus* is generally decreased from the early towards the late Villafranchian, however different sizes of the species can appear in isochronous localities, possibly due to two different evolutionary trends (Heintz, 1970; 1974, Heintz and Aguirre, 1976, Brunet and Heintz, 1984, Kostopoulos, 1996). The size of *C. r. ramosus* is larger than the one of *C. r. medius*, that is larger than the one of *C. r. minor* and *C. r. pueblenensis*, whereas *C. r. minor* and *C. r. pueblenensis* are larger than *C. r. gerakarensis* (Kostopoulos, 1996). It is also noted that the only Greek subspecies, *C. ramosus gerakarensis* is smaller than the representatives of the species from West European localities, whereas it also bears different morphological traits: a shorter and more distally positioned first tine as well as

a shorter premolar row (Kostopoulos, 1996; Kostopoulos and Athanassiou, 2005; Athanassiou, 2022).
In Greece, *C. ramosus* specimens have been found in the MN16a aged locality of Milia, the Early Pleistocene localities of Kos Island and Kastritsi, the MN17 aged localities of Volakas and Sesklo and the MNQ18 aged locality of Gerakarou (Athanassiou, 2022).

Order Artiodactyla Owen, 1848
Suborder Ruminantia Scopoli, 1777
Superfamilia: Bovoidea Gray, 1821
Family: **Bovidae** Gray, 1821

**4.10 Bovidae indet.** Gray, 1821

**Material**
Postcranial elements: one right distal epiphysis of humerus (AT685).

**Description**
The distal epiphysis consists of two epitrochleae, divided by one large groove and one crest. The intertrochlear groove is positioned approximately in the midline of the distal articulation, whereas the crest is positioned slightly lateral to the midline of the distal articulation, characteristics present in the Bovidae family (Heintz, 1970). The medial margin of the trochlea is proximodistally higher than the lateral, and consequently, in anterior view, the trochlea tapers lateralward. In anterior view of the distal end of the specimen, the outline of the medial condyle is slightly curved. There is no synovial fossa present on the anterior surface of the medial condyle. The coronoid fossa is on the anterior surface immediately above the distal condyles and is an elongated mediolateral depression. The lateral surface of the shaft immediately above the lateral epicondyle is smooth. Viewed posteriorly, the junction of the two margins of the olecranon fossa creates an abrupt proximal edge of the fossa. The lateral trochlear pit is rounded, large and relatively deep.
The specimen AT119 (part of distal epiphysis of a left humerus), is highly fragmented. The trochlea is almost complete, whereas in posterior view the medial and lateral epicondyles are fragmented.

**Measurements**
The measurements of the specimen AT119 from Aghia Kyriaki are given in the Table 24.

Table 24: Basic measurements (DAP, DT) of the sdistal epiphysis of the humerus AT119 from Aghia Kyriaki. Measurements in mm.

| ID code | Locality | DAP (mm) | DT (mm) |
|---|---|---|---|
| AT119 | Aghia Kyriaki | 21.15 | 31.56 |

**Comparison**
Thedistal epiphysis of humerus AT119 from Aghia Kyriaki is compared to various Bovidae representatives from the Pleistocene of Europe in the Fig. 36.


Figure 34: Bivariate plot of basic measurements (DT and DAP) of the distal epiphysis of the humerus of AT119 from Aghia Kyriaki, as well as specimens attributed to the taxa *G. borbonica, G. torticornis, G. m. meneghinii, G. soriae* and *H. merlae* from various European localities. Data from: Andres Rodrigo (2011).

In the Fig. 36, we observe that the specimen AT119 is slightly bigger than *Gazella* sp. and smaller than *Gazellospira torticornis*. However, the aforementioned metrical analysis is not enough for the attribution to a certain genus. Thus, we can attribute the specimen AT119 to a small sized Bovid, slightly bigger than *G. borbonica*.

**Discussion**

The Bovidae (Gray, 1821) family is regarded to be monophyletic group (Hassasin and Douzery, 1999; Marcot, 2007; Hassasin et al.,2012; Bibi et al., 2009; Kostopoulos, 2021), divided into two subfamilies by both morphological and molecular criteria (Vrba and Schaller 2000; Matthee and Davis 2001; Marcot 2007; Groves and Grubb 2011;

Hassanin et al. 2012; Bibi 2013; Yang et al.,2013): Bovinae and Antilopinae. The former subfamily consists of the boselaphines, bovines and tragelaphines, whereas the latter includes the remaining bovids, mostly known as aego donts, as well as bovids with dental characteristics that do not refer to goat morphology (Vrba and Schaller, 2000; Hassasin and Douzery, 1999; Bibi et al, 2009; Kostopoulos, 2021). However, the phylogenetic relationships and the taxonomy of the family, have been a field of debate for a long time (Hernandez Fernandez and Vrba, 2005), thus resulting in mismatches in the palaeontological bibliography. This is the reason why, Cregut–Bonnoure (2007) distinguishes Caprinae Gill, 1872 and Antilopinae Baird, 1857 as two different subfamilies.

**4.11 cf. *Gazellospira* torticornis** Aymard, 1854

Dental elements: left upper M3 (AT356), upper M2 (AT187), upper M1 (AT284).

Postcranial elements: two left (AT119, AT325) humeri.

**Description:**

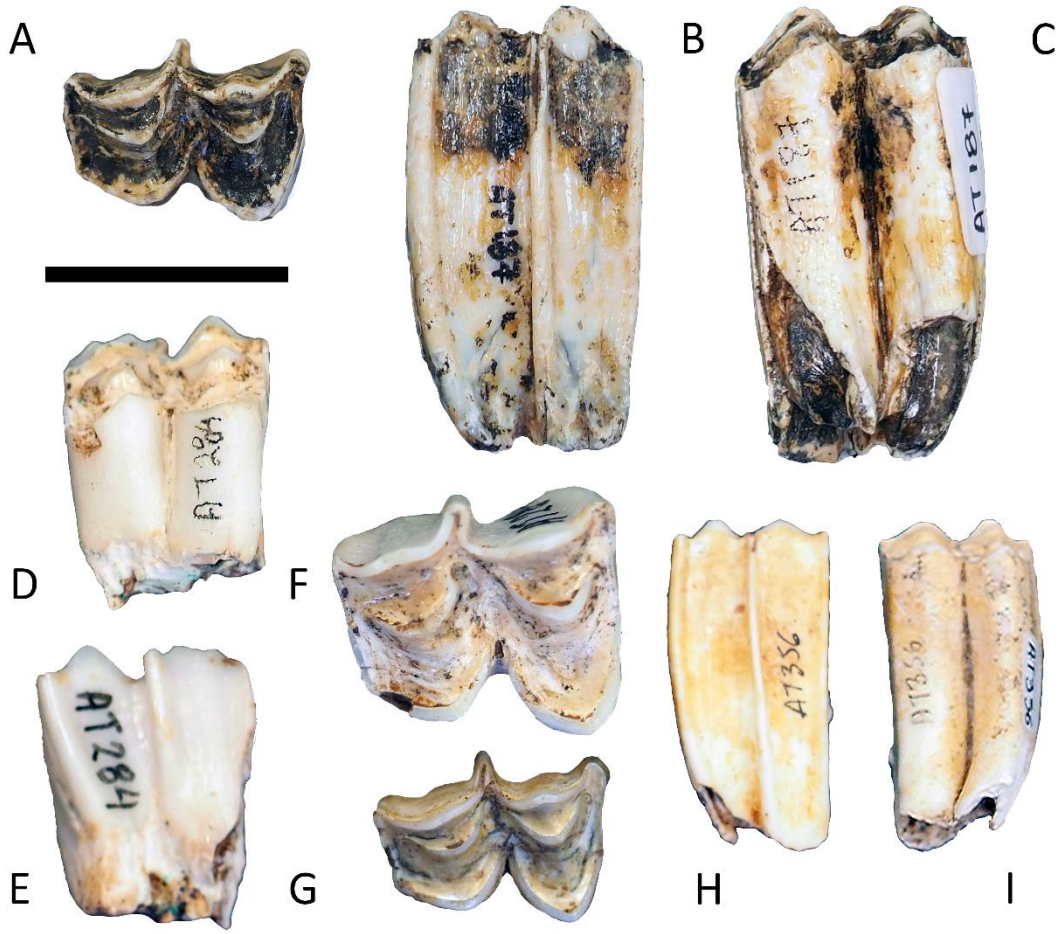


Figure 35: Bovidae indet. Specimens from Aghia Kyriaki. Upper M2 (AT187) in A: occlusal, B: buccal and C: lingual view, upper M1 (AT284) in D: lingual, E: buccal and F: occlusal view and upper M3 (AT356) in G: occlusal, H: buccal and I: lingual view. Scale bar: 20mm.

AT284

Upper right M1. Strongly worn. The two lobes are of different buccolingual dimensions. The tooth is broken at the base thus the root is not preserved. In buccal view (Fig. 37E), the parastyle and metastyle (although the latter missing of the basal portion) are diverging occlusally. The mesostyle gets more developed and prominent from the base towards the occlusal part of the tooth. The parastyle is more pointed than the metastyle. The parastyle is straight. The metacone is worn and broken, whereas the paracone is less worn and more acute. In occlusal view (Fig. 37F), the parastyle is cilidrican and it is more developed than the metastyle. The metastyle has a rather sharp triangular shape. The mesostyle, which is the most developed style, has a circular outline and bends towards the anterior surface. The protocone is subtriangular although with with smooth edges, whereas the hypocone is more rounded. In anterior view, the lingual side is straight, whereas the buccal side is slightly convex. The enamel islets inside the protocone and hypocone are crescent–moon–shaped,

AT187

Almost complete, highly fragmented upper right M2. The two lobes are of different buccolingual dimensions. In buccal view (Fig. 37B), the parastyle runs from the base towards the occlusal surface of the tooth with a curved outline that diverges from the base. The metastyle, on the contrary, is straight and vertical. The mesostyle is strongly protruding buccally and is cracked from the upper third of the tooth, towards the upper–occlusal part. The metacone is slightly curved, whereas the paracone is more developed, buccally, and curved. In lingual view (Fig. 37C), the hypocone is pointed and more buccolingually extended than the rather smooth and circular protocone. The linguodistal edge of the hypocone is strong and forms an obtuse angle. In anterior view, the buccolingual dimension of the tooth is larger in the base of the tooth than in the occlusal surface. The buccal part of the tooth is convex, whereas the lingual part of the tooth is concave. In occlusal view (Fig. 37A), the posterior lobe is longer (anterioposteriorly) and narrower (buccolingually) than the anterior lobe. The parastyle develops buccolingually with an almost circular outline. The metastyle is buccoposteriorly extended, tending towards the posterior side with a circular to rather triangular outline. The mesostyle is is the stronger style with a sharp triangular shape. The protocone is bending towards the lingual side. The hypocone is cilindrical and its posterolingual border forms an angle. Both of the enamel islets have a smooth crescent–moon outline.

AT356

Right upper M3. The tooth is morphologically identical to AT187.

It differs for a smaller size and few minor characters including: a more pointed protocone with a anterioposterior compression of the lobe and a slightly more developed parastyle.

Humeri

The distal epiphysis consists of two epitrochleae, divided by one large groove and one crest. The intertrochlear groove is positioned approximately in the midline of the distal articulation, whereas the crest is positioned slightly lateral to the midline of the distal articulation, characteristics present in the Bovidae family (Heintz, 1970). The medial margin of the trochlea is proximodistally higher than the lateral, and consequently, in

anterior view, the trochlea tapers lateralward. In anterior view of the distal end of the specimen, the outline of the medial condyle is slightly curved. There is no synovial fossa present on the anterior surface of the medial condyle. The coronoid fossa is on the anterior surface immediately above the distal condyles and is an elongated mediolateral depression. The lateral surface of the shaft immediately above the lateral epicondyle is smooth. Viewed posteriorly, the junction of the two margins of the olecranon fossa creates an abrupt proximal edge of the fossa. The lateral trochlear pit is rounded, large and relatively deep.

The specimen AT325 (distal epiphysis and distal part of diaphysis of left humerus) is characterized by a broken epicondyle and a broken distal part of the medial condyle. The specimen AT685 (distal epiphysis of a right humerus), is characterized by a cracked/ broken posterior part of the lateral epitrochlear, when viewed in the distal view.

**Measurements**

The measurements of the specimens from Aghia Kyriaki attributed to cf. *Gazellospira torticornis*, are given in the Tables 25 and 26

Table 25: Basic measurements of the occlusal surface of dental elements AT356, AT187, AT284 from the locality of Aghia Kyriaki, attributed to Bovidae indet. Measurements in mm.

| ID code | Site | Anatomical element | Occlusal length (mm.) | Occlusal width (mm.) |
|---|---|---|---|---|
| AT356 | Aghia Kyriaki | M3 | 19.58 | 13.58 |
| AT187 | Aghia Kyriaki | M2 | 20.05 | 14.23 |
| AT284 | Aghia Kyriaki | M1 | 16.96 | 15.04 |

Table 26: Basic measurements (DAP, DT) of the distal epiphysis of the humeri AT685 and AT325 from Aghia Kyriaki. Measurements in mm.

| ID code | Locality | DAP (mm) | DT (mm) |
|---|---|---|---|
| AT685 | Aghia Kyriaki | 37.27 | 44.4 |
| AT325 | Aghia Kyriaki | 35.88 | 47.08 |

**Comparison**

The specimens from Aghia Kyriaki are compared to various Bovidae representatives from the Pleistocene of Europe (Heintz, 1970), in the Fig. 38–40.

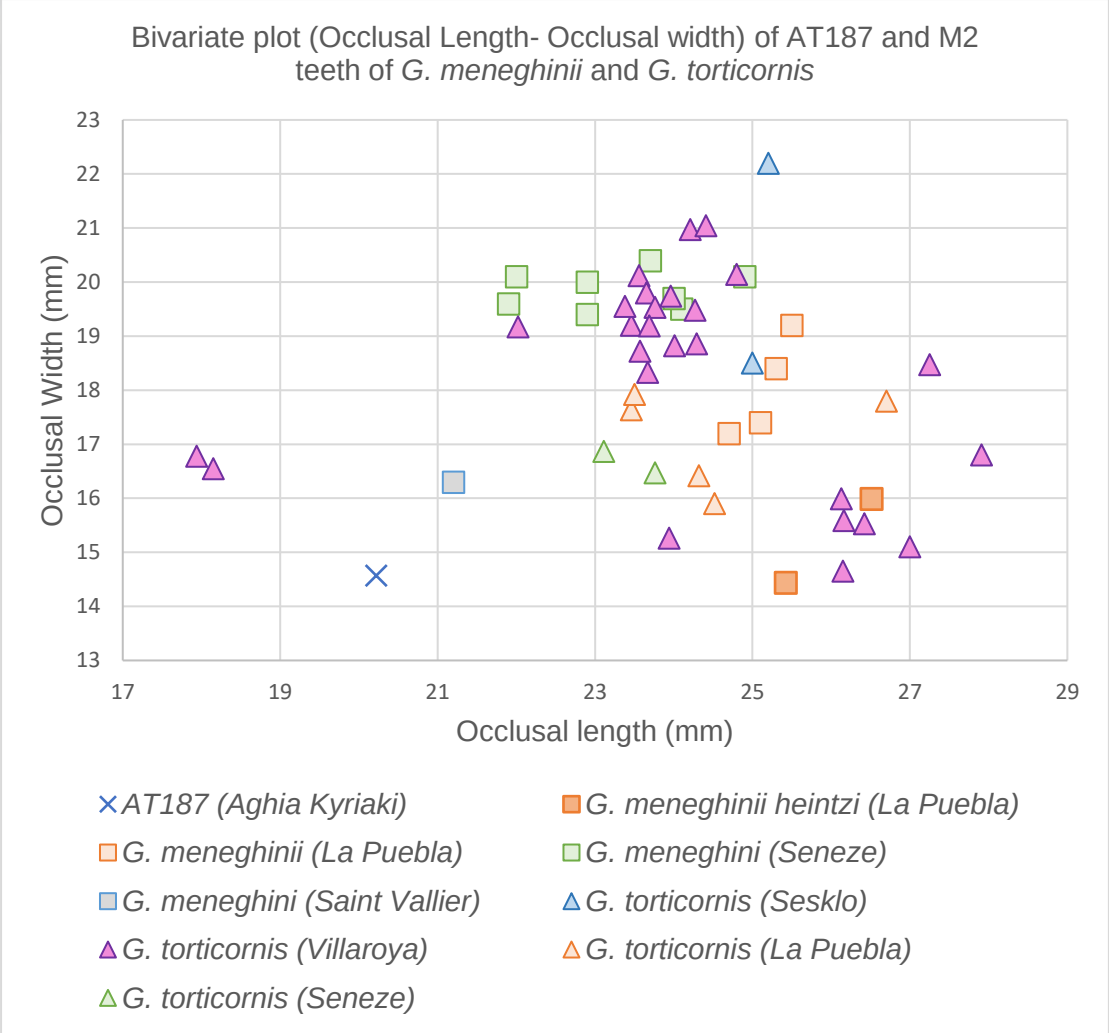


Figure 36: Bivariate plot of occlusal length and occlusal width of the specimen AT187 as well as M2 teeth specimens of the taxa *G. meneghinii* and *G. torticornis* from various localities. Data from: Andres– Rodrigo (2011), Athanassiou (1996) and Cregut– Bonnoure and Valli (2004).

In the Fig. 38, we observe that there is an overlap among the M2 measurements of *G. meneghinii* and *G. torticornis*, with *G. torticornis* having a larger range of occlusal length. Thus, the two taxa can not be easily distinguished by the occlusal length and width of their M2 teeth. The specimen AT187 is placed towards the lowest values of both taxa.

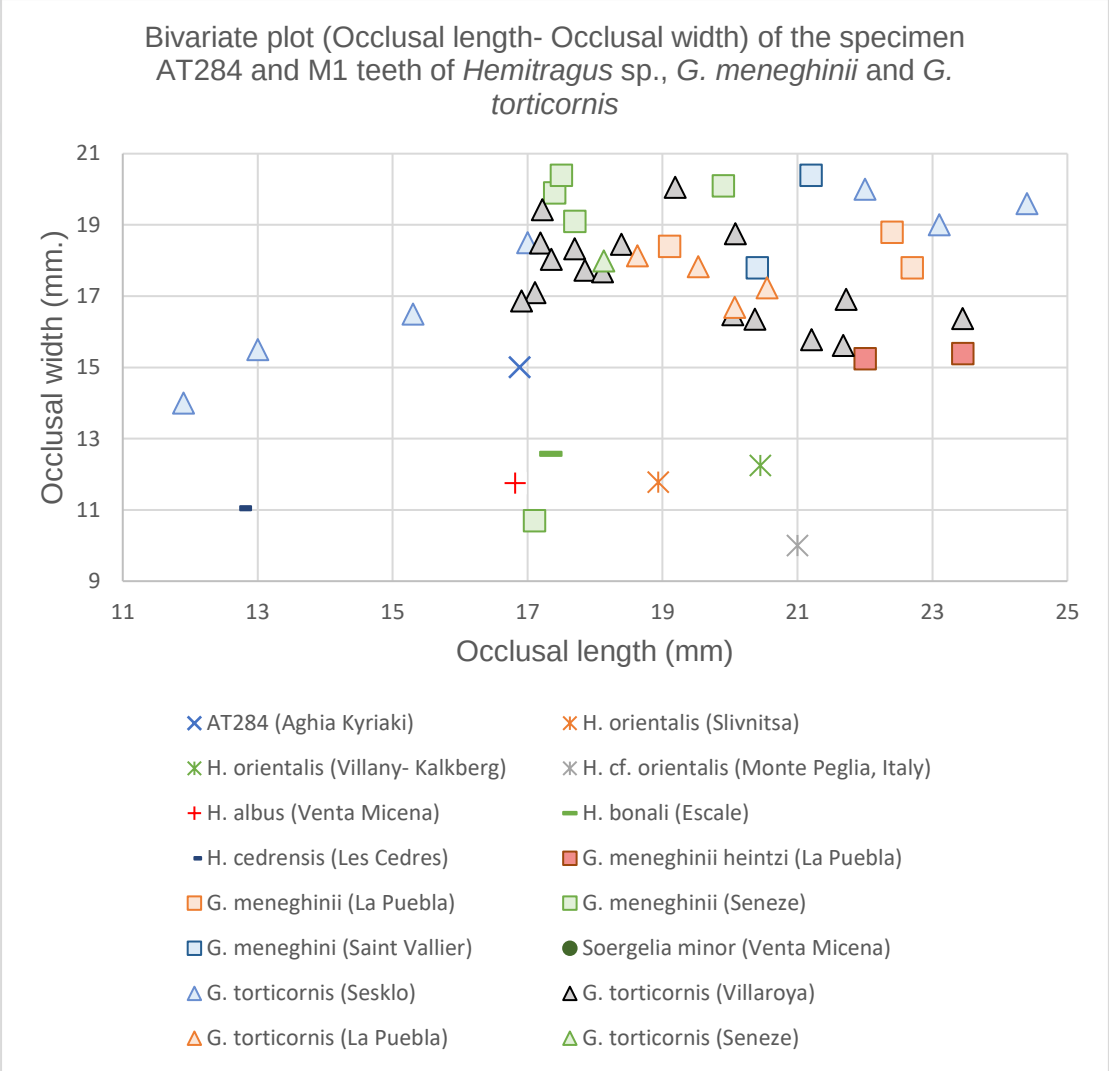


Figure 37: Bivariate plot (occlusal length– occlusal width) of the specimen AT284 from Aghia Kyriaki as well as M1 specimens of *Hemitragus* sp., *G. meneghinii* and *G. torticornis* specimens from various localities. Data from: Andres– Rodrigo (2011), Cregut– Bonnoure and Valli (2004) and Athanassiou (1996).

In the Figure 39, we observe that measurements of the specimen AT284 from Aghia Kyriaki, are amongst the ones of *Hemitragus* sp., *G. meneghinii* and *G. torticornis*. Thus, no clear metrical attribution can be made to the specimen. Moreover, the number of specimens (only one) is not enough for an attribution to a certain taxon. However, the morphology of the tooth allows us its attribution to the family of Bovidae.

Despite the metrical proportions of the teeth, certain morphological characteristics of the specimens AT284, AT187 and AT356 like the broader parastyle than mesostyle, the lack of central islet, as well as the posterior lobe of the m3 that does not extend towards the base, in buccal view, are all indicative of the taxon *Gazellospira* sp. Thus, we can attribute the teeth AT284, AT187 and AT356 to cf. *Gazellospira* sp.

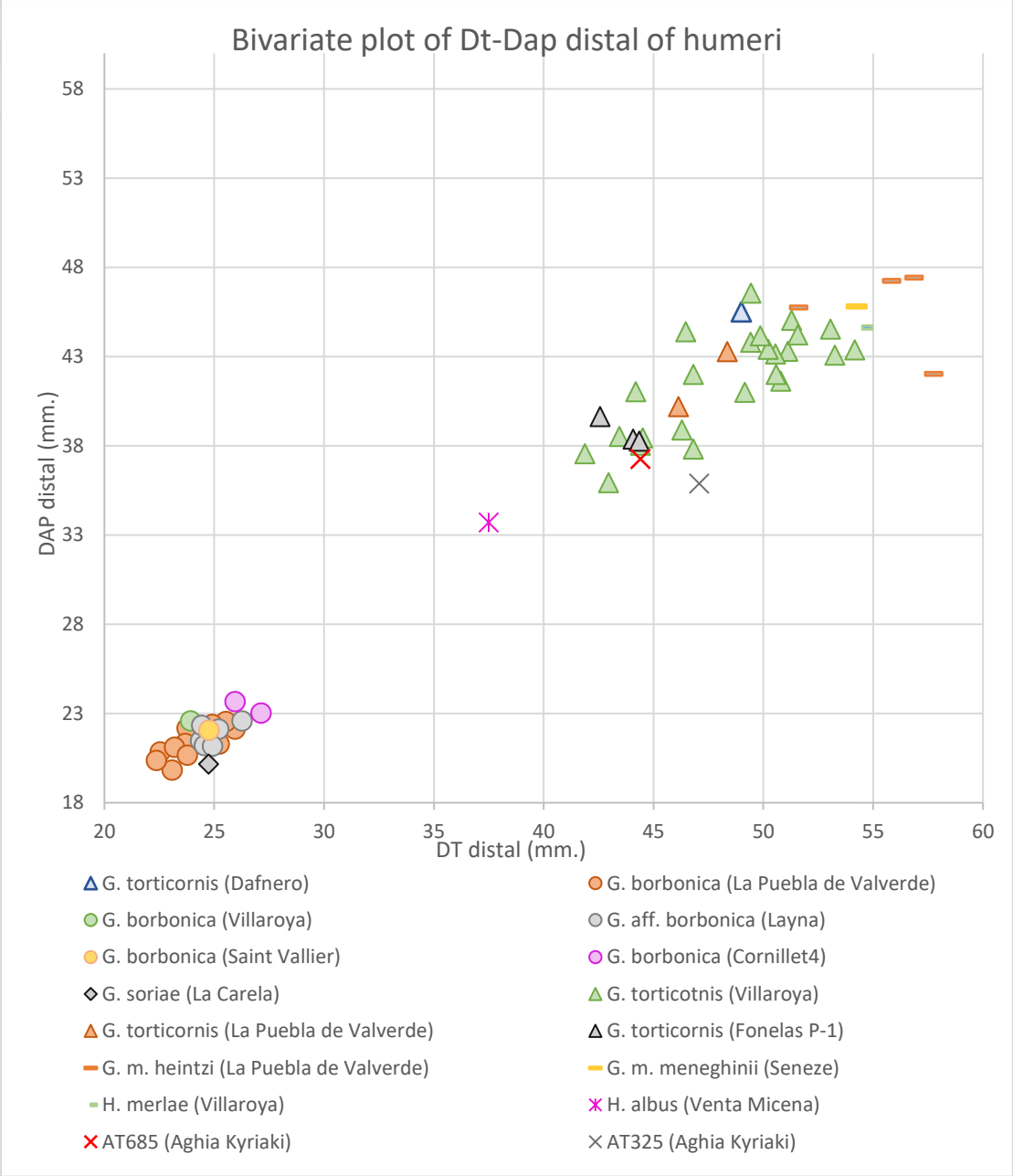


Figure 38: Bivariate plot of basic measurements (DT and DAP) of the distal epiphysis of the humerus of the specimens AT325 and AT685 from Aghia Kyriaki, as well as specimens attributed to the taxa *G. borbonica, G. torticornis, G. m. meneghinii, G. soriae* and *H. merlae* from various European localities. Data from: Andres Rodrigo (2011).

The specimens AT325 and AT685 share similar metrical proportions with specimens of *Gazellospira torticornis* from Villaroya, and Fonelas P–1. Thus, we could attribute these two specimens to cf. *Gazellospira torticornis*.

**DIscussion**

*Gazellospira torticornis* is a small sized and the most frequently found bovid in Villafranchian localities of Europe (Duvernois and Guerin, 1989). Their size is slightly larger than the one of great–sized gazelles (Guvernois and Guerin, 1989). The

biochronological range of the species, according to Rook and Martinez–Navarro (2010) is approximately 2.5– 1.8 Ma.

*G. torticornis* has been found in the Villafranchian localities of Roccaneyra, Pardines, Villaroya, Seneze, Olivola, Val d'Arno, Villany and Erpfingen (Kurten, 2007), as well as the Greek Villafranchian localities of Dafnero 1,2,3, Sesklo, Volax, Vatera, Pyrgos, Karnezaiika and possibly Gerakarou (Kostopoulos, 2022).

Based both on morphological and metrical data, the dental specimens AT187, AT284, AT3256, as well as the humeri AT325 and AT685 can be attributed to the species cf. *Gazellospira torticornis*.

Bovidae Gray, 1821
Caprinae Gill, 1872
Rupicaprini Simpson, 1945

**4.12 Rupicaprini indet.** Simpson, 1945 (**cf. *Procamptoceras brivatense*** Schaub, 1923)

**Material**
Dental elements: right hemimandible with m3–p3 (AT216), lower molars (AT189, AT190).

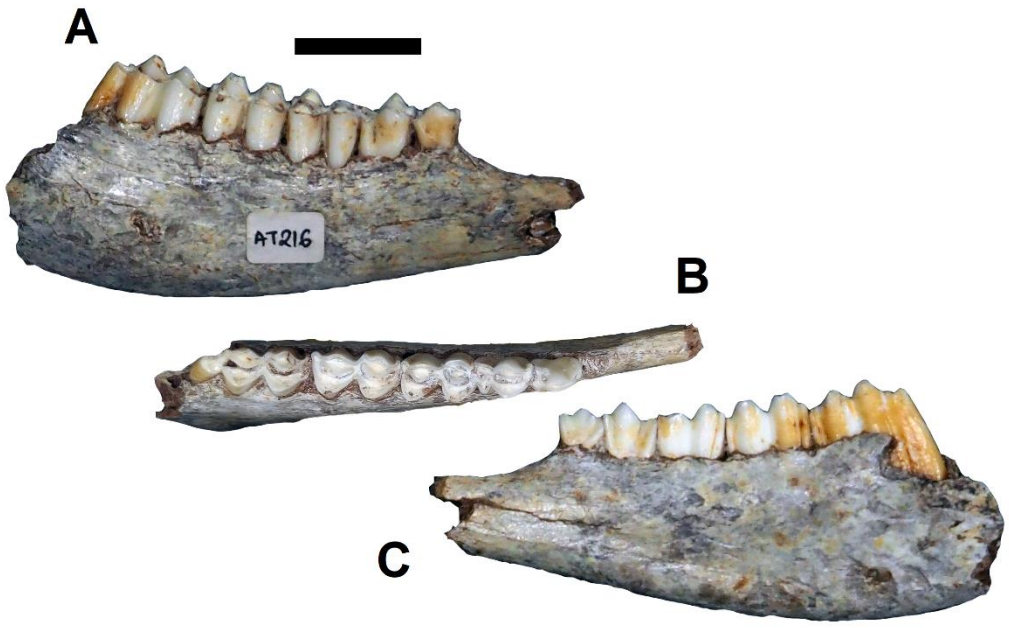


Figure 39: Right hemimandible AT216 from the locality of Aghia Kyriaki, attributed to Rupicaprini indet. In A: buccal, B: occlusal and C: lingual view. Scale bar: 20mm.

AT216
Incomplete right hemimandible of small sized Bovidae, with m3, m2, m1, p4 and p3 (Fig. 41). The specimen is well preserved, with very few, slight superficial cracks. The teeth are in excellent preservation status. The mandible is broken on the anterior portion, anteriorly of the mental foramen and on the posterior part, just posteriorly to the m3. The mandibular corpus strongly and quickly deepens below the molars.

m3: The posterior lobe is slightly wider at the base of the tooth, thus the anterior and mesial edges of the tooth are converging occlusally. The talonid is strongly converging towards the anterior portion of the tooth. The hypoconulid and the entoconulid are small, with the entoconulid being slightly more developed proximodistally. The entoconid is well developed in the occlusal surface, whereas in the lingual view, it is triangular shaped, from the base towards the occlusal surface of the tooth. The entostylid, which is located between the entoconid and the entoconulid is well developed and quite wide in the lingual view, with a slight widening trend from the base towards the occlusal surface of the tooth. The metaconid is developed but broken towards the occlusal surface. The lingual surface of the metaconid is curved, but with a slight triangular tendency. The mesostylid is strong. The anterior cingulid is less developed than the mesostylid.

m2: in buccal view, the entostylid is straight, strongly developed, whereas the parastylid is slightly convex and less developed. The anteroposterior dimension of the entostylid is greater than the one of the parastylid. The entoconid is broken closer to the occlusal side, and it is convex. The metaconid is broken transversally, in an anteroposterior direction. It is convex and more anteroposteriorly developed than the entoconid. The metastylid is developed in the distal part of the anterior lobe. In lingual view, a weak pli caprin is developed in the anterior part of the tooth. The hypoconid is more convex than the protoconid. In occlusal view, the entostylid is slightly linguodistally extended and has a circular outline. The parastylid is less developed and more pointed than the entostylid. The metastylid has a triangular outline and it is more transposed towards the anterior lobe. The metaconid is more circular/ more convex than the entoconid, and less anteroposteriorly extended. The protoconid is more convex than the hypoconid, whereas both the hypoconid and the protoconid tend to have a buccodistal direction.

m1: the m1 shares the same morphological characteristics as the m2, with the main difference being that the parastylid is slightly developed.

p4: molarized. An almost square shaped protoconid, and a strongly developed hypoconid. The metaconid is almost parallel to the protoconid, and weakly connected with the entoconid (the posterior valley as a groove); the entoconid is strongly developed. Strong parastylid+pacaconid complex (as a strong anterior style)

p3: the protoconid, metaconid and hypoconid are slightly developed. The entoconid is of mediocre development. The proprotoconoulidocristid is strongly/ sharply extended towards the lingual side and it forms a deep anterior valley. Strong anterior stylid.

**Measurements:**

The measurements of the dental elements from Aghia Kyriaki attributed to Rupicaprini indet. are given in the Tables 27–28.

Table 27: Basic measurements (LO: occlusal length, WO: Occlusal width) of the teeth of the specimen AT216 from Aghia Kyriaki, attributed to Rupicaprini indet. Measurements in mm.

| ID code | Site | m3 | | m2 | | m1 | | p4 | |
|---|---|---|---|---|---|---|---|---|---|
| | | LO | WO | LO | WO | LO | WO | LO | WO |
| AT216 | Aghia Kyriaki | 15.27 | 6.55 | 13.1 | 6.85 | 10.54 | 6.5 | 8.46 | 5.62 |
| | | p3 | | m1–m3 | | p3–p4 | | | |

| | | LO | WO | LO | LO |
|---|---|---|---|---|---|
| | | 7.58 | 4.53 | 42.17 | 15.46 |

Table 28: basic measurements (occlusal length and occlusal width) of the lower molars (AT189 and AT190) (m1 or m2) from the locality of Aghia Kyriaki, attributed to Rupicaprini indet. Measurements in mm.

| ID code | Site | Occlusal Length | Occlusal width |
|---|---|---|---|
| AT189 | Aghia Kyriaki | 13.95 | 5.81 |
| AT190 | Aghia Kyriaki | 12.53 | 5.73 |

**Comparison**

The specimen AT216 is characterized by a weak pli– caprin, until the base of the molars, characteristics present in certain Caprinae representatives. Moreover, the last lobe of the m3 of the Aghia Kyriaki specimen widens towards the base (Fig. 41). Thus, morphologically, the specimen AT216 is clearly attributed to Caprinae.

Parparousi et al. (2021) in their preliminary taxonomical results of the site attributed the specimen AT216 to *Gazella borbonica*, due to its metrical characteristics. However, its morphological characteristic, as aforementioned, allow its attribution to Caprinae.

According to Cregut– Bonnoure (2007), the Caprinae subgroup consists of the tribes Rupicaprini Simpson, 1945, Ovibovini Gray, 1872, Ovini Cregut– Bonnoure, 2002 and Caprini Gray, 1821.

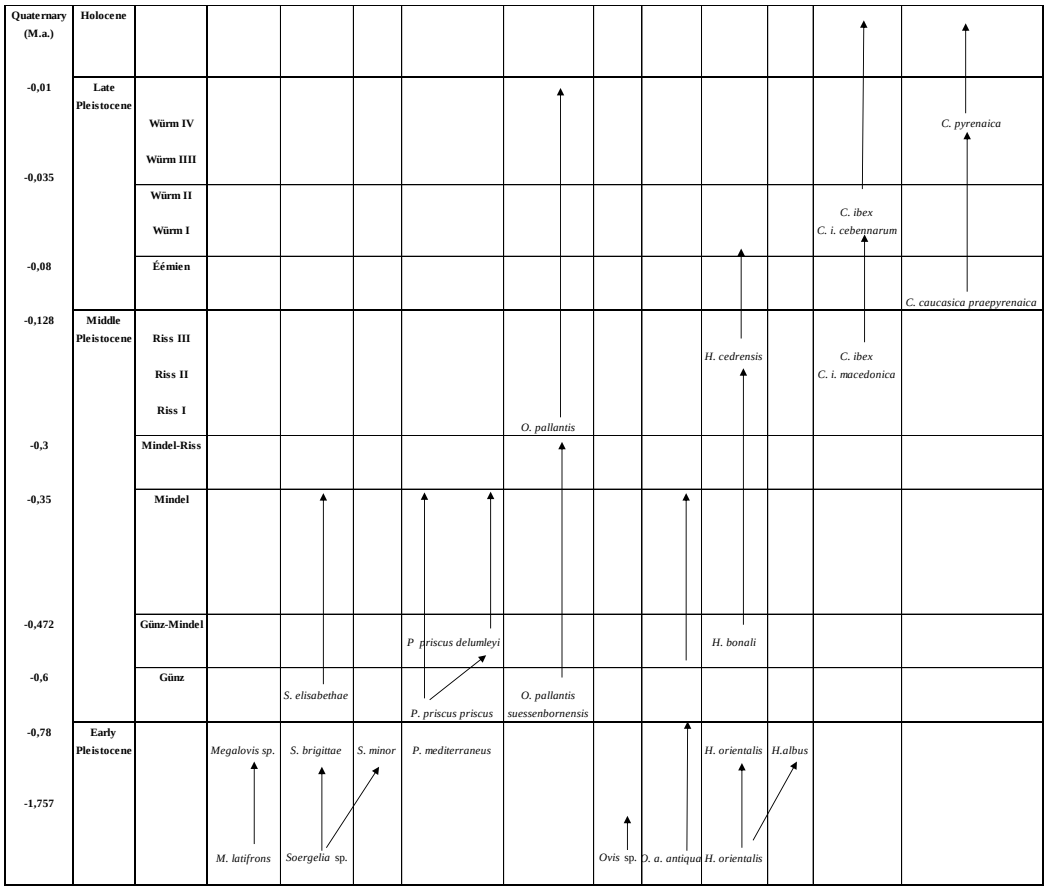

Figure 40: Biochronological distribution of the Ovibovini, Caprini and Ovini in the Western Europe. Figure by Cregut– Bonnoure (2020), modified (translated in English).

According to Cregut– Bonnoure (2007), the only two genera of the tribe Caprini that inhabited Europe during the Pleistocene are the genera *Hemitragus* Hodgson, 1841 and *Capra*, Linne,1758. The specimen AT216 has a less molarized p4 and a longer p3 than the representatives of Caprini indet. Thus, we cannot attribute it to Caprini. On the other hand, the latter two characteristics appear in the Rupicaprini. representatives. Fernandez and Cregut– Bonnoure (2006) suggest that the Rupicaprini representatives in the MNQ18 locality of Kozarnica (Bulgary) are *Procamptoceras* cf. *brivatense* and *Rupicapra* sp. Despite the phylogeny of certain Bovid taxa being a matter of dispute, *Procamptoceras brivatense* and *Pliotragus* sp. are now attributed to the tribe of Rupicaprini (Duvernois and Guérin, 1989; Crégut–Bonnoure and Guérin, 1996; Fernandez and Cregut Bonnoure, 2006), along with *Rupicapra* sp. (Fernandez and Cregut– Bonnoure, 2006).

Table 29: Table of basic measurements of total length and total width of the occlusal surface of teeth m3**–**p3, as well as occlusal length of the molar and the premolar teeth rows of the specimen AT216 from Aghia Kyriaki, *Procamptoceras brivatense* from the localities of Seneze, Le Coupet, Olivola, Vllany and Csarnota and *Pliotragus* sp. from the locality of Seneze. Data from: Duvernois and Guerin (1989). Measurements in mm.

| Taxon | | AT216 | *Procamptoceras brivatense* | *Pliotragus* sp. |
|---|---|---|---|---|
| Locality | | Agha Kyriaki | Various sites* | Seneze |
| p4–p3 | LO (min–max) | | 16.5–26 | 30–33.5 |
| | LO (mean) | 18.1 | 21.3 | 31.6 |
| | N | 1 | 2 | 4 |
| m3–m1 | LO (min–max) | | 50–57 | 16.5–79 |
| | LO (mean) | 53.5 | 54.2 | 77.5 |
| | N | 1 | 3 | 3 |
| p3 | WO total (min–max) | | | 12–13.5 |
| | WOtotal (mean) | 4.4 | 8 | 12.5 |
| | LO (min–max) | | | 14–15.5 |
| | LO (mean) | 7.46 | 12 | 14.8 |
| | N | 1 | 1 | 4–5 |
| p4 | WO total (min–max) | | 6.5–8 | 10–13 |
| | WOtotal (meanO | 6.88 | 7.3 | 11.4 |
| | LO (min–max) | | 9–13 | 16–19.5 |
| | LO (mean) | 9.65 | 10.8 | 18.2 |
| | N | 1 | 3 | 5 |
| m1 | WO total (min–max) | | 9–10.5 | 13–15 |
| | WOtotal (mean) | 8.21 | 9.8 | 14.1 |
| | LO (min–max) | | 12–15 | 18–22 |
| | LO (mean) | 12.53 | 13.5 | 19.8 |
| | N | 1 | 2 | 4–5 |
| m2 | WO total (min–max) | | 9.5–11 | 14–17 |
| | WOtotal (mean) | 9.2 | 10.2 | 15.3 |

| | | | | |
|---|---|---|---|---|
| | LO (min–max) | | 15–18.5 | 21–25 |
| | LO (mean) | 15.22 | 16.9 | 22.7 |
| | N | 1 | 5 | 5–6 |
| m3 | WO total (min–max) | | 8–11 | 13–15.5 |
| | WO total (mean) | 8.72 | 9.5 | 14.3 |
| | LO (min–max) | | 23.5–31 | 29–38 |
| | LO (mean) | 23.65 | 26.2 | 33.7 |
| | N | 1 | 5 | 6 |

Table 30**:** Table of basic measurements of total length and total width of the occlusal surface of the m3 tooth of *Rupicapra* sp. representatives from the localities of Kozarnika, Arago, Le Portel**–**Ouest and Les Gras. Data of the dimensions of other teeth of the taxon were not available. Data from: Fernandez and Cregut**–**Bonnoure (2006). Measurements in mm.

| Taxon | *Rupicapra* sp. | *R*. cf. *pyrenaica* | *R*. *pyrenaica* | *R*. *rupicapra* |
|---|---|---|---|---|
| Locality | Kozarnika | Arago | Le Portel–Ouest | Les Gras |
| m3 | | 5.7–7.2 | 4.6–6.8 | 5.7–7.3 |
| | 7 | 6.45 | 5.7 | 6.4 |
| | | | 16.9–17.1 | 16–19.1 |
| | 19 | 18.3 | 17 | 17.34 |
| | 1 | 1–2 | 2 | 9–10 |

In the Tables 29 and 30, we observe that the specimen AT216 is metrically close to both *Procamptoceras brivatense* and *Rupicapra* sp. prepresentatives. Despite the lack of bibliography concerning *Rupicapra* sp., we can observe that the m3 tooth of AT216 has slightly largerr dimensions than the Rupicapra sp. from Kozarnika, Arago, Le Portel–Ouest and Les Gras. On the other hand, the morphology of the m3 tooth AT216 resembles the one of *Rupicapra* sp.: the metaconid and the entoconid are significantly developed on the lingual side and the pli–caprin extends till the upper part of the tooth. The posterior lobe of the m3 is thinner towards the occlusal surface.

Moreover, in the Table 29 we observe that the proportions of AT216 generally fit better the ones of *Procamptoceras brivatense*, although the p3 tooth is smaller than the one of *Procamptoceras*, both in anteroposterior (length) and buccolingual (width) dimensions of the occlusal surface. We note that the alveolar length of the p3 teeth of *Procamptoceras brivatense* varies from 7.5–9.5 mm, with a mean value of 8mm, thus approaching the alveolar length of the p3 tooth of the specimen AT216 from Aghia Kyriaki (7.32mm). The morphology of the teeth resembles the one of *Procamptoceras*, since, amongst others, the p4 is consisted by two lobes divided by a deep vertical valley on the labial view. The paraconid and metaconid are merged.

Thus, both the chronological frame, and the morphometrical characteristics of the specimen AT216 are in accordance with the ones of *Procamptoceras brivatense*, thus we can safely attribute the specimen to Rupicaprini indet, cf. *Procamptoceras brivatense*.

**Discussion**

*Procamptoceras* is a monospesific genus, with *Procamptoceras brivatense* being the type species of the genus (Fernandez and Cregut–Bonnoure, 2006). The species made its first appearance at the beginning of the middle Villafranchian (MNQ17) and

its last appearance until the end of the late Villafranchian (MNQ18) (Fernandez and Cregut–Bonnoure, 2006). However, Cregut–Bonnoure (2007) suggests that Procamptocareas brivatense was present in the European Pleistocene faunas from MNQ17 till the first part of MNQ20. The species, also referred as chamois antelope, is a small goat–like chamois with weird horns (Kurten, 2007). Despite its anatomical charactersare indicative of a close phylogenetic relationship to the goats, morphological characters as the slender limb bones and the head held forward are indicative of its closer relationship with the chamois (Kurten, 2007). *Procamptoceras brivatense* has a size between the gazelle and antelope of the Villafranchian faunas (Kurten, 2007) and is regarded to be the smallest antilope of the Villafranchian period, with its size being slightly bigger than the one of chamois (Fernandez and Cregut–Bonnoure, 2006). Specimens attributed to the species have been found in the Villafranchian localities of Perrier–Roccaneyra, Montousse5, Le Coupet, Seneze (France), Olivola (Italy), Almejnara 1 en Castellon (Spain), Beremond 4, Csarnota 1, Nagyharsananyhegy 4, Villany 3 (Hungary), Volax and Vassiloudi (Greece) and Slivnitsa (Bulgaria) (Fernandez and Cregut–Bonnoure, 2006 and reference therein; Kurten, 2007 and reference therein).

Caprini Gray, 1821

**4.13 *Hemitragus* sp.** Hodgson, 1841

**Material**

Craniodental elements: right hemimandible with m3–p3 teeth and empty alveolar cavity of p2 (AT215/185), lower p4 (AT427), lower p3 (AT658).

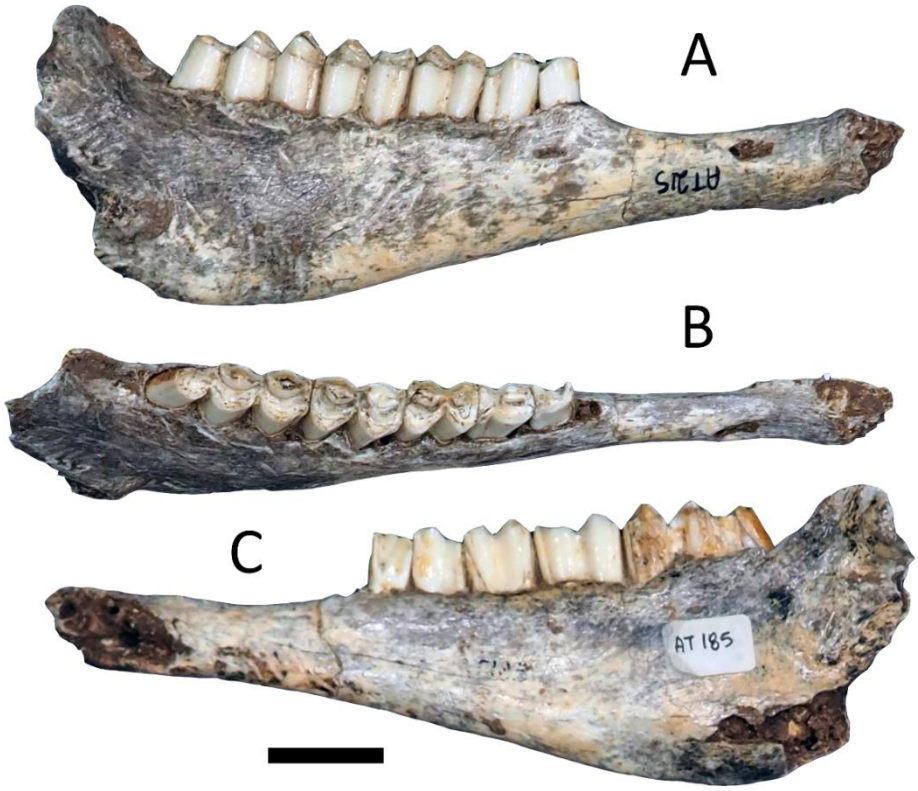


Figure 41: Right hemimadible AT185/AT215 from the locality of Aghia Kyriaki, attributed to *Hemitragus* sp., in A: buccal, B: occlusal and C: lingual view. Scale bar: 20 mm.

Postcranial material: Left metacarpal (AT286), right metacarpal (AT319/ AT335).


Figure 42: Metacarpals from the locality of Aghia Kyriaki, attributed to *Hemitragus* sp. Upper: left metacarpal AT286 and lower: right metacarpal AT319/335 in anterior view. Scale: 20mm.

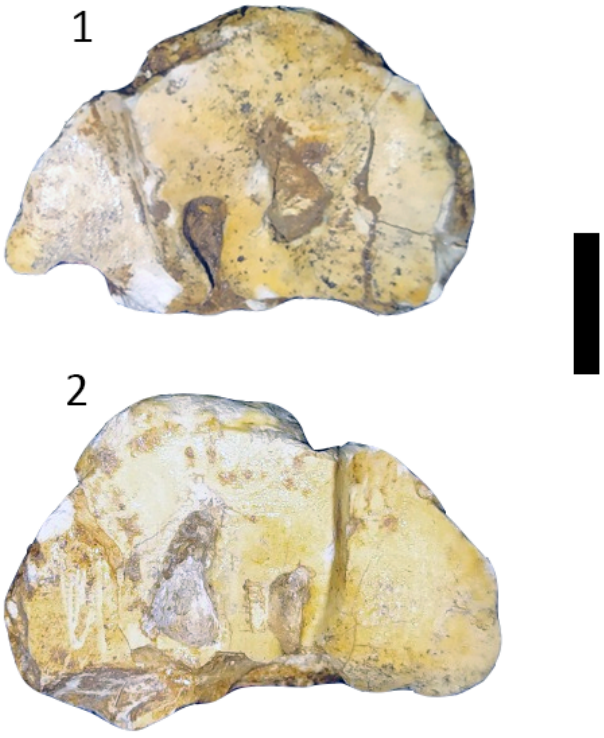


Figure 43: Metacarpals from Aghia Kyriaki attributed to *Hemitragus* sp. in proximal view. 1: AT286, 2; AT315/339. Scale bar: 20mm.

**Description**

AT215+185

Hypsodontic tooth lobes, whose size does not change significantly from the base to the occlusal surface (Fig. 43).

m3: strong pli– caprin (goat fold), almost curved hypoconulid, triangular protoconid and hypoconid, with tendency to curve. The hypoconid has a slightly smaller linguo–bucal breadth than the protoconid. Mild metaconid and entoconid, slightly developed entoconulid and clearly developed mesostylid.

m2: strong pli–caprin, less developed than the one of the m3 and more extended towards the buccal side. The protoconid and the hypoconid are triangularly shaped, with a tendency to curve, more triangular– shaped than the ones of the m3. Mild metaconid and entoconid, but stronger than the ones of the m3. The entoconid is stronger than the metaconid. Mild entostylid and strong mesostylid (The mesostylid is bigger than the entostylid).

m1: absence of pli–caprin. Triangular– shaped cross–section of protoconid and hypoconid, hypoconid stronger/ more developed than the protoconid. The metaconid and the entoconid are slightly developed. The mesostylid and the entostylid are moderately developed, with the entostylid being developed throughout the whole lingual surface, whereas the mesostylid starts to develop from the mid of the lingual surface towards the occlusal surface.

p4: completely molarized. Almost square shaped protoconid, weakly developed hypoconid. The metaconid closes the lingual wall of the teeth and contacts the strongly developed entoconid.

p3: very short; the protoconid, metaconid and hypoconid are slightly developed. The entoconid is of mediocre development. The proprotoconoulidocristid is strongly/ sharply extended towards the lingual side and it forms a deep anterior valley.

AT286

A complete left metacarpal (Fig. 44). The bone is in good state of preservation, with several cracks, mainly on the diaphysis and the distal epiphysis. The proximal epiphysis displays a D–shaped to triangular outline in proximal view. The proximal epiphysis consists of one lateral and one medial articular facet, divided by one high crest with an orientation from the posterior towards the lateral side of the anterior surface of the epiphysis. The lateral articular facet, when seen from the proximal view, is broken palmary. The medial articular facet is larger and located in a higher plane than the lateral one. In proximal view, the medial articular facet (facet for the capitatotrapezoid) has a trapezoid outline (Fig. 45 –1). At the posterior margin of the crest that separates the two proximal facets we note one inverted drop– like shaped nutrient foramen. Also, the medial articular facet has a small drop–like synovial fossa, located medially to the nutrient foramen. The posteroproximal nutrient foramen is line shaped and located within a deep rough/ridged depression, that does not extend on the posterior portion of the diaphysis, which is in general flat. In anterior view, the diaphysis is slender and extends a little mediolaterally towards the distal epiphysis. Near the distal end there seems to be no vascular groove on the anterior part of the diaphysis. In cross– section view at midshaft, the posterior surface is flattened. The nutrient foramen both in the anterior and in the posterior surface of the diaphysis are oval shaped. In the posterior surface of the diaphysis, right below the nutrient foramen

towards the distal epiphysis there is an arched/curved, rounded surface. On the distal epiphysis, the two condyles are converging. The condyles in lateral view do not appear to be posteriorly tilted. The epicondyles are S–shaped. In posterior view, pits can be found on either side of both of the sagittal ridges at the epiphysis of the condyles, meaning that there are four pits in total. The lateral and medial trochlear pits are deep.

AT319/ AT335

The specimen AT319 consists of a proximal epiphysis and part of the diaphysis of a right metacarpal. The specimen AT335 is a broken distal epiphysis of a right metacarpal. It is considered that the specimens AT319 and AT335 belong to the same right metacarpal bone, thus from now on they will be referred as AT319/AT335. The specimen AT319/AT335 is characterized by old cracks right above the distal epiphysis, as well as on the diaphysis, towards the distal side. Morphologically, the specimen AT319/AT335 is similar to the specimen AT286. However, in proximal view the lateral articular facet is complete and of triangular–like shape, and the medial articular facet is slightly broken posteriorly.

**Measurements**

Th measurements of the specimens from Aghia Kyriaki attributed to *Hemitragus* sp., are given in the Tables 31–32.

Table 31: Basic measurements (LO: occlusal length, WO: Occlusal width) of the teeth of the specimen AT185/215 from Aghia Kyriaki, attributed to *Hemitragus* sp. Measurements in mm. Numbers in italics are approximate measurements.

| ID code | Site | m3 | | m2 | | m1 | | p4 | |
|---|---|---|---|---|---|---|---|---|---|
| | | LO | WO | LO | WO | LO | WO | LO | WO |
| AT185/ 215 | Aghia Kyriaki | 23.65 | 8.72 | 15.22 | 9.2 | 12.53 | 8.21 | 9.65 | 6.88 |
| | | p3 | | m1–m3 | | p3–p4 | | | |
| | | LO | WO | LO | | LO | | | |
| | | 7.46 | 4.4 | 53.5 | | *18.1* | | | |

Table 32: Basic measurements of the metacarpals from Aghia Kyriaki. Attributed to *Hemitragus* sp. Abbreviations in table 8. Measurements in mm.

| ID code | Site | GL | DT prox. | DAP prox. | DT diaph. | DAP diaph. | DT dist. | DAP dist. |
|---|---|---|---|---|---|---|---|---|
| AT286 | Aghia Kyriaki | 149.4 | 34.78 | 24.35 | 22.57 | 17.6 | 40.39 | 22.29 |
| AT335 | Aghia Kyriaki | | | | | | 40.26 | 22.15 |
| AT319 | Aghia Kyriaki | | 35.37 | 24.34 | 20.98 | 17.15 | | |

**Comparison**

The specimen AT185/AT215 is characterized by a strong pli– caprin, until the base of the molars, characteristics not present neither in *Capra* sp., *Ovis ammon antiqua* or *Pseudocapra primaeva*, but present in *Hemitragus* sp. (Fig. 46). Moreover, the last lobe of the m3 of the specimen is slightly divergent in the base, another characteristic of *H. albus* and *H. cedrensis* that is missing in *Capra* sp. Also, the lower m1 of the

specimen is characterized by the formation of “en coup de pouce” (an oval shaped central valley in the buccal view of the m1 teeth), another characteristic present in *Hemitragus* sp. but absent in *Capra* sp. representatives (Cregut–Bonnoure, 2020). Finally, the absence of bulging in the labial base of the second lobe of the p3 and p4 of AT185/AT215 is also characteristic of *Hemitragus* sp. but not of *Capra* sp.

| | *Hemitragus* | | | | *Capra* | | | *Ovis ammon* | *Pseudocapra* |
|---|---|---|---|---|---|---|---|---|---|
| | *orientalis* | *albus* | *bonali* | *cedrensis* | *caucasica* | *pyrenaica* | *ibex* | *antiqua* | *primaeva* |
| **Lower molars** | | | | | | | | | |
| Pli caprin | | | | | | | | | |
| until the base | + | + | + | + | + | + | + | + | - |
| only in the upper part | - | - | - | - | - | - | - | - | + |
| strong | + | + | + | - | - | - | - | - | + |
| slightly marked | - | - | - | + | + | + | + | + | - |
| **m3** | | | | | | | | | |
| Last lobe | | | | | | | | | |
| very straight | - | + | + | - | + | + | + | - | - |
| curvilinear | + | - | - | - | - | - | - | + | - |
| variable shapes/ outlines | - | - | - | - | - | - | - | - | + |
| divergent in the base | - | - | + | - | + | + | + | - | - |
| slightly diverged in the base | - | + | - | + | - | - | - | - | + |
| narrowed at the base | - | - | - | - | - | - | - | + | - |
| **m1** | | | | | | | | | |
| Depressed lingual base "en coup de pouce" | + | + | + | + | - | - | - | - | - |
| **Lower premolars** | | | | | | | | | |
| Base labiale du lobe 2° lobe | | | | | | | | | |
| bulging/ swollen | ? | - | - | - | + | + | + | - | ? |

Figure 44: Morphological characteristics of lower molars and premolars of Caprini and Ovini representatives (*H. orientalis, H. albus, H. bonali, H. cedrensis, C. caucasica, C. pyrenaica, C. ibex, O. ammon antiqua, P. primaeva*). Modified table (translated in English) by Cregut–Bonnoure (2020).

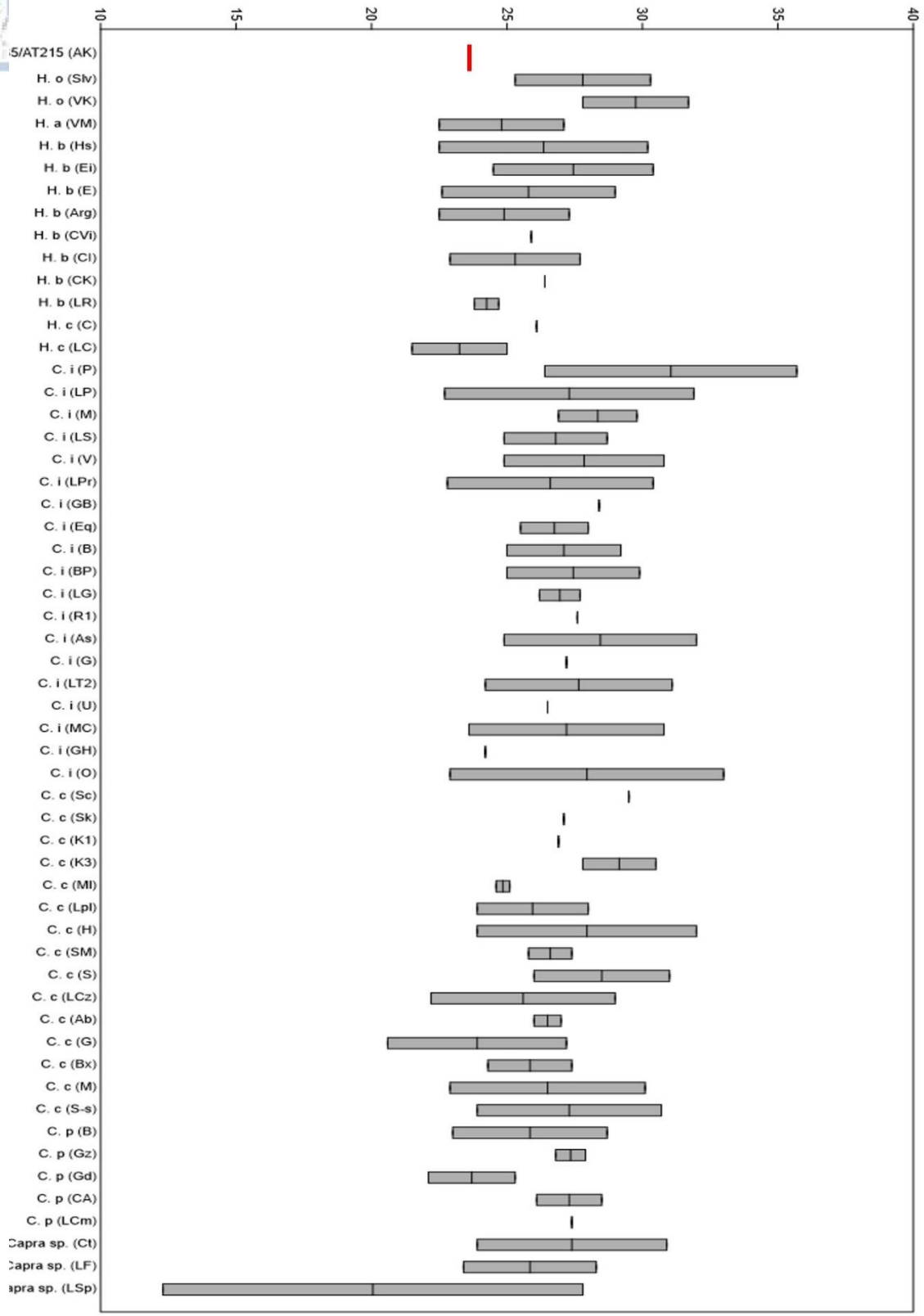


Figure 45: Boxplot showing min–max and median values of occlusal length of m3 of the specimen AT185/AT215 from Aghia Kyriaki, as well as *Hemitragus* sp. and *Capra* sp. and their representatives from various localities. Abbreviations: H. o stands for *H. orientalis*, H. a for *H. albus*, H. b for *H. bonali*, H. c for *H. cedrensis*, C. I for *C. ibex*, C. c for *C. caucasica*, C. p for *C. pyrenaica*, AK for Aghia Kyriaki, Slv for Slivnitsa, VK for Villany– Kalkberg, VM for Venta

Micena, Hs for Hundsheim, Ei for Escale (isolated teeth), E for Escale (on mandibles), Arg for Arago, CVi for Cueva Victoria, Cl for Aldene– couche I, CK for Aldene– couche K, LR for Les Rameaux, O3 for Orgnac 3, C for Cimay, LC for Les Cedres, P for Petralona, LP for Les Pecheurs, M for Mialet, LS for La Sartanette, V for Valescure, LPr for Les Peyrards, GB for Grette Basse, Eq for Eqyi, B for Bayol, BP for Baume Perigaud, LG for Les Gras, R1 for Rainaudes I, As for Adaouste– sommet, G for Gramari, LT2 for Le Tai 2, U for Unang, MC for Monte Cucco, GH for Gamssulzen Hohle, O for Observatoire, Sc for Sacublia, Sk for Sakajia, K1 for Koudaro I, K3 for Koudaro III, Ml for Moula, Lpl for Le Portel, H for Hortus, LV for La Vacheresse, SM for Saint Marcel– d'Ardeche, S for Soulabe, LCz for Le Crouzade, Ab for Adaouste– base, G for Gibraltar, Bx for Bouxes, M for Montferrand, S–s for Soulabe– sommet, B for Belvis, Gz for Gazel, Gd for Gedre, CA for Cueva del Agua, LCm for Le Colombier, Ct for Le Cottier, LF for Le Figuier and LSp for La Salpetriere. Data from Cregut– Bonnoure (2020).

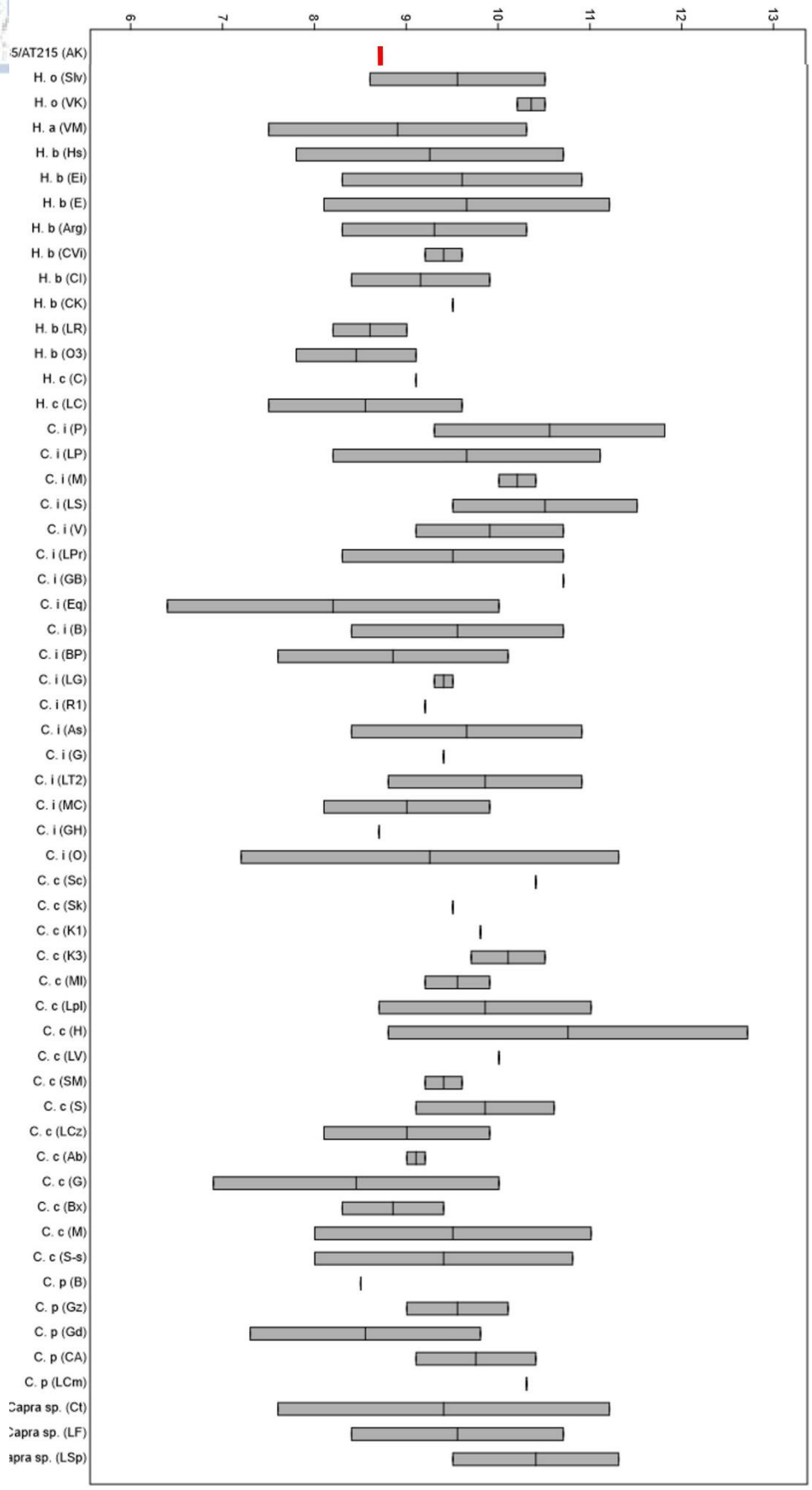

Figure 46: Boxplot showing minimum, maximum and median values of occlusal width of m3 of the specimen AT185/AT215 from Aghia Kyriaki, as well as *Hemitragus* sp. and *Capra* sp. and its representatives from various localities. Abbreviations: H. o stands for *H. orientalis*, H. a for *H. albus*, H. b for *H. bonali*, H. c for *H. cedrensis*, C. I for *C. ibex*, C. c for *C. caucasica*, C. p for *C. pyrenaica*, AK for Aghia Kyriaki, Slv for Slivnitsa, VK for Villany– Kalkberg, VM for Venta Micena, Hs for Hundsheim, Ei for Escale (isolated teeth), E for Escale (on mandibles), Arg for Arago, CVi for Cueva Victoria, Cl for Aldene– couche I, CK for Aldene– couche K, LR for Les Rameaux, O3 for Orgnac 3, C for Cimay, LC for Les Cedres, P for Petralona, LP for Les Pecheurs, M for Mialet, LS for La Sartanette, V for Valescure, LPr for Les Peyrards, GB for Grette Basse, Eq for Eqyi, B for Bayol, BP for Baume Perigaud, LG for Les Gras, R1 for Rainaudes I, As for Adaouste– sommet, G for Gramari, LT2 for Le Tai 2, U for Unang, MC for Monte Cucco, GH for Gamssulzen Hohle, O for Observatoire, Sc for Sacublia, Sk for Sakajia, K1 for Koudaro I, K3 for Koudaro III, Ml for Moula, Lpl for Le Portel, H for Hortus, LV for La Vacheresse, SM for Saint Marcel– d'Ardeche, S for Soulabe, LCz for Le Crouzade, Ab for Adaouste– base, G for Gibraltar, Bx for Bouxes, M for Montferrand, S–s for Soulabe– sommet, B for Belvis, Gz for Gazel, Gd for Gedre, CA for Cueva del Agua, LCm for Le Colombier, Ct for Le Cottier, LF for Le Figuier and LSp for La Salpetriere. Data from Cregut– Bonnoure (2020).

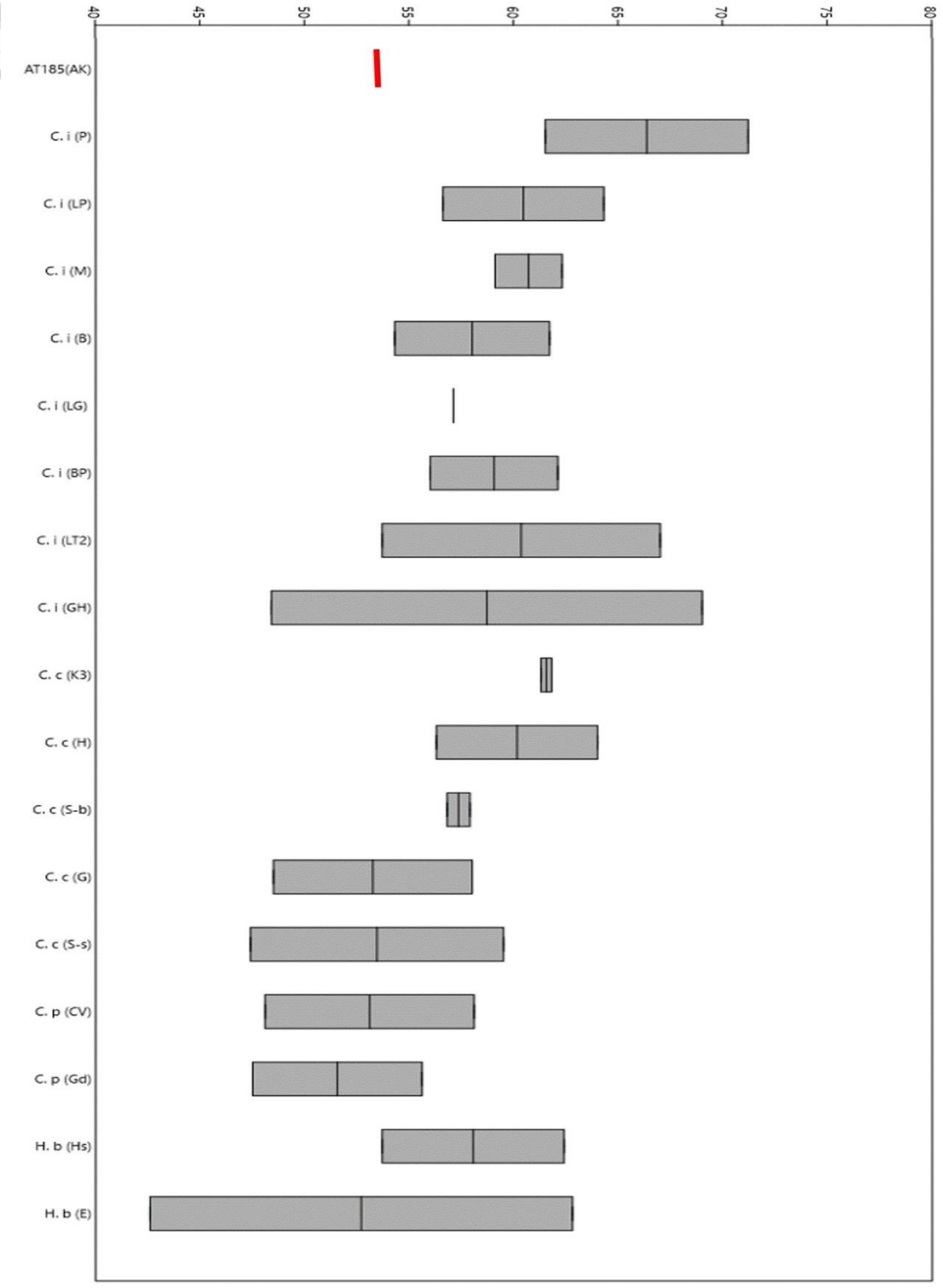


Figure 47: Boxplot table of the min– max and median value of m1–m3 tooth row (in mm.) for the specimen AT185/AT215 from Aghia Kyriaki as well as *C. ibex*, *C. caucasica*, *C. pyrenaica* and *H. bonali* from various localities. Abbreviations: C. I stands for *C. ibex*, C. c for *C. caucasica*, C. p for *C. pyrenaica*, H. b for *H. bonali*, P for Petralona, LP For Les Pecheurs, B for Bayol, LG for Les Gras, BP for Baume Perigaud, LT2 for Le Tai 2, GH for Gamssulzen Hohle, K3 for Kudaro III, H for Hortus, Sb for Soulabe– base, G for Gibraltar, S–s for Soulabe– sommet, CV

for Cueva del Valle, Gd for Gedre, Hs for Hundsheim and E for Escale. Data from Cregut–Bonnoure (2020).

In the Fig. 47 and 48, accordingly, we observe that the occlusal length and width of m3 of the specimen AT185/AT215 from Aghia Kyriaki belongs to the respective range of both *Hemitragus* sp. and *Capra* sp., as the two genera are overlapping.

Fig. 49 shows that the length of the molar row of the mandible AT185/AT215 from Aghia Kyriaki is within the range of both *Capra* sp. from various localities and *Hemitragus bonali* from the locality Escale.

Table 33: Table of measurements (Total length, DT proximal, DT distal) of metacarpals, for the specimens AT286, AT319/335 from Aghia Kyriaki and *Hemitragus* sp. representatives from various localities. Data from Cregut– Bonnoure (2020).

| Taxon | Locality | Total length | | | DT proximal | | | DT distal | | |
|---|---|---|---|---|---|---|---|---|---|---|
| | | Mean | Min-Max | N | Mean | Min-Max | N | Mean | Min-Max | N |
| AT286 | Aghia Kyriaki | 149.4 | 149.4 | 1 | 34.78 | 34.78 | 1 | 40.39 | 40.39 | 1 |
| AT319/335 | Aghia Kyriaki | | | | 35.37 | 35.37 | 1 | 40.26 | 40.26 | 1 |
| *H. orientalis* | Csarnota 2 | | | | 33.2 | 33.2 | 1 | 40.6 | 40.6 | 1 |
| *H. orientalis* | Slivnitsa | | | | | | | 36.7 | 35-38.6 | 2 |
| *H. albus* | Venta Micena | 152.21 | 146.6-157.8 | 2 | 30.2 | 30.2 | 1 | 33.21 | 32.7-33.8 | 3 |
| *H. bonali* | Hundsheim | 146.02 | 139.6-151 | 13 | 34.09 | 32.2-36.5 | 15 | 38.29 | 35.6-44.2 | 15 |
| *H. bonali* | Escale | 139.29 | 129.8-152 | 41 | 33.03 | 28.4-40.4 | 71 | 37.4 | 31.5-43.7 | 35 |
| *H. bonali* | Arago | | | | | | | 39.16 | 36.7-41.6 | 3 |
| *H. bonali* | Koudarol | | | | | | | 47 | 47 | 1 |
| *H. bonali* | Aldene | | | | | | | 38.9 | 38.9 | 1 |
| *H. bonali* | Les Rameaux | 151.77 | 151.7-151.8 | 2 | 32.08 | 29.8-33.6 | 5 | 34 | 34 | 2 |
| *H. cedrensis* | Cimay | | | | 30.02 | 26.9-32.5 | 4 | 34 | 34 | 1 |

| | | | | | | | | | | |
|---|---|---|---|---|---|---|---|---|---|---|
| *H. cedresnsis* | Les Cedres | | | | 30.2 | 30.2 | 1 | 34.8 | 34.8 | 1 |

In the Table 33, it appears that the total length of the specimens from Aghia Kyriaki is within the range of *H. albus* and *H. bonali*, however there are no data for other *Hemitragus* representatives, i.e., *H. orientalis* and *H. cedrensis*. As far as the DT proximal of the specimens from Aghia Kyriaki is concerned, it is within the range of *H. albus* and *H. bonali* but larger than the one of *H. orientalis*, *H. cerdensis* and *H. bonali* from Les Rameaux. Finally, the DT distal of the two specimens from Aghia Kyriaki is within the range of *H. bonali*, close to the one of *H. orientalis* but larger than the one of *H. albus* and *H. cedrensis.*

| | ***Capra*** | ***Hemitragus*** | ***Ovis*** |
|---|---|---|---|
| **Metacarpal** | | | |
| Proximal articulation | | | |
| Facet for the unciform | | | |
| curvilinear outline | - | + | - |
| trapezoid outline | + | - | - |
| triangular outline | - | - | + |
| overflows on the palmar face | - | - | + |
| Facet for the capitato-trapezoid | | | |
| curvilinear outline | + | - | - |
| trapezoid outline | - | + | - |
| rectangular outline | - | - | + |
| Proximo-palmar tuberosities | | | |
| symmetric | + | - | + |
| medial more developped than the lateral | - | + | - |

Figure 48: Morphological characteristics of the proximal articulation of metacarpals of the taxa *Capra* sp., *Hemitragus* sp. and *Ovis* sp. Table from Cregut– Bonnoure (2020), modified (translated in English).

The morphological characteristics of the proximal articulation of the specimens AT286 and AT319 from Aghia Kyriaki, such as the curvilinear outline of the facet for the unciform, the trapezoid outline of the facet for the capitato–trapezoid and the more developed medial than lateral proximopalmar tuberosity (Fig. 45), are all diagnostic of the genus *Hemitragus* sp. (Fig. 50),

In conclusion, although the dental metrical data of the specimen from Aghia Kyriaki cannot allow a precise attribution of the studied speciemns as *Capra* or *Hemitragus*, the dental morphological characteristics along with the proportionas and morphology of the available metacarpals allow us referring the taxon to as *Hemitragus* sp. Moreover, the morphological traits of the proximal epiphysis of the metacarpals of Aghia Kyriaki, are typical of the taxon *Hemitragus* sp.

Thus, we can safely attribute the specimens AT185/AT215 and ATAT286 and AT319 to the taxon *Hemitragus* sp., based on their morphometrical characteristics.

**Discussion**

According to Cregut–Bonnoure (2007), the only two genera of the tribe Caprini that inhabited Europe during the Pleistocene are the genera *Hemitragus* Hodgson, 1841 and *Capra*, Linne,1758.

The genus *Hemitragus* is represented by four different species during the Pleistocene of Europe (Fig. 51): *Hemitragus orientalis* Cregut–Bonnoure & Spassov, 2002, *Hemitragus albus* Moya–Sola, 1987, *Hemitragus bonali* Harlé & Stehlin, 1913 and *Hemitragus cedrensis* Cregut– Bonnoure, 1989.

| | **CHRONOLOGY** | *Hemitragus* | | | |
|---|---|---|---|---|---|
| | | *orientalis* | *albus* | *bonali* | *cedrensis* |
| **Quaternary**<br><br>**(M.a.)** | **Late Pleistocene**<br><br>**Éémien & Würm ancien** | | | | Bau de l'Aubesier (H)<br>Saint–Marcel d'Ardèche (U) |
| **–0,128** | **Middle Pleistocene** | | | Koudaro I<br>Grotte XIV<br>Combe Grenal | Les Cèdres<br>Bau de l'Aubesier (I, J) |
| | **Riss** | | | La Fage<br><br>Abri Vaufrey<br>Baume Bonne<br>Orgnac 3 (2,3 & 4)<br>Coudoulous I<br>Aldène (G, H) | Rigabe (I, J)<br><br>Cimay |
| **–0,3** | **Mindel–Riss** | | | Balaruc VII<br>Orgnac 3 (7)<br>Les Rameaux<br>Aldène (I, X3) | |
| **–0,35** | **Mindel** | | | Aldène (K)<br>Terra Amata<br>Arago<br>Cueva Victoria<br>Bérigoule | |

| | | | | | |
|---|---|---|---|---|---|
| | | | | Grotte Harlé<br>Grotte de l'Église<br>Grotte XIV<br>Pech de l'Azé II<br>Escale<br>Hundsheim | |
| **–0,472** | **Günz–Mindel** | | | Wesbury–<br>sub–Mendip | |
| **–0,6** | **Günz** | | | | |
| **–0,78**<br><br><br><br><br><br><br>**–1,757** | **Early Pleistocene** | Soleilhac<br><br>Appolonia I<br><br>Le Vallonnet<br><br><br><br>Slivnitsa<br>Villany–<br>Kalkberg<br>Csarnota 2 | Fuente Nueva 3<br>Venta Micena<br>Barranco Léon | | |

Figure 49: Chronological expansion of the taxon *Hemitragus* sp. in the European area during the Late Pliocene– Pleistocene, and table of localities in which each species was identified in. Figure by Cregut– Bonnoure (2020), translated in English.

*Hemitragus* sp. made its first appearance in the eastern Europe in the MN17, with the large– sized species *Hemitragus orientalis* in the localities Csarnota 2 and Villany 3 (Schaub, 1932; Cregut–Bonnoure, 2007). Specimens of the species *Hemitragus orientalis* have been identified in the Upper Pliocene locality of Csarnota 2 (Hungary), as well as in the –Lower Pleistocenen localities of Villany– Kalkberg– Nord (Hungary) and Slivnitsa (Janossy, 1986; Spassov and Cregut– Bonnoure, 1999; Cregut–Bonnoure, 2020). Also, possibly evolved representatives of the same genus? have been found in late Lower Pleistocene localities, like Appolonia I (Greece), Vallonnet and Soleilhac (France) (Bout, 1976; Bonifay et Bonifay, 1983; Cregut Bonnoure, 2020). Moreover, specimens from the locality of Volos, Greece attributed to *Hemitragus* cf. *bonali* (Meulen and Kolfschoten, 1968; Kostopoulos et al., 2002; Athanassiou, 2002), would rather be attributed to *Hemitragus orientalis*, because of the age of the locality (Cregut–Bonnoure, 2020). Specimens from the Villafranchian localities of Collepardo and Colegordo in Italy have been attributed to the species *Hemitragus* cf. *stehlini* (Gliozzi et al., 1997; Alberdi et al., 1998); however, Cregut Bonnoure (2020) suggests that since *H. stehlini* is a synonym of *H. bonali* (more recent species), it is unlikely that the identification of the specimens was correct, thus a proper revision of the material

could attribute these specimens to the Villafranchian species *H. orientalis*. Thus, the biochronological range of the species ranges from the Late Pliocene to the Early Pleistocene (Cregut– Bonnoure, 2020) (see figure Hemitragus chronology with sites).
*H. albus* was found in Venta Micena, Spain; Moya Sola (1987) originally attributed it to the species *Capra alba* by Moya– Sola (1987). According to Cregut– Bonnoure (2007), *H. albus* was a small– sized species, endemic to the Spanish area. After the attribution of the species to the genus *Hemitragus*, Cregut– Bonnoure suggests that all species attributed to *C. alba* should follow the attribution to *H. albus*; Thus, the species is found in Venta Micena (Moya– Sola, 1987), Barranco Léon (Agusti et al., 1987), Fuente Nueva 2 (Moyà–Solà & Menendez, 1986), Fuente Nueva 3 (Turcq et al., 1996), Guadiz–Baza (Moyà–Solà & Menendez, 1986). Thus, the species was fairly spread in Western Europe during the Early Pleistocene (Fig. 51).
*H. bonali* was the most common found species of the genus in the Western Europe. no data support its presence in Eastern Europe (Cregut– Bonnoure, 2007). According to Cregut Bonnoure (2007), the species has been identified from specimens in the MNQ 22 localities of Hundsheim (Daxner, 1968), Escale (Bonifay, 1974–1975), Arago (Cregut– Bonnpoure, 1979), Cueva Victoria (Cregut–Bonnoure, 1999), Pech–de–l'Azé II (Martini–Jacquin 1984 a), grotte Harlé (Harlé & Stehlin, 1913), grotte de l'Église (Laville et al., 1972), grotte XIV (Guadelli, 1994), Aldène (Couche K ; Bonifay, 1989), Terra Amata (Mourer–Chauviré & Renault–Miskovsky, 1980), Bérigoule (Crégut–Bonnoure, 2002 b); Moreover, Cregut Bonnoure (2002) attributes the specimens studied and described by Sanchez Chillon (1977) as *Capra*, to *H. bonali*. The species is also present in more recent localities, such as the MNQ 23 localities of Aldene, Balaruc VII (Cregut– Bonnoure, 1988), Orgnac 3 (Aouraghe, 1992), Igue des Rameaux (Cregut Bonnoure, 2002) and the MNQ 24 localities of Aldene, Abimes de la Fage (Cregut– Bonnoure, 2002), Combe Grenal (Delpech & Prat, 1995), Coudoulous I (Jaubert et al. 1999), Orgnac 3 (Couche 2, 3, 4), Payre II (Lamarque, 1996), Baume Bonne (Psathi, 1996), Abri Vaufrey (Delpech, 1988), possibly La Pineta (Peretto et al., 1983), as well as in a few Iberian localities e.g. Galeria Pesada (Brugal, 2004). The last occurence of the species was noted in the end of the MNQ 24, in the locality of Koudaro 1 (Cregut– Bonnoure and Baryshnikov, 2005).
The last European species, *H. cedrensis*, is regarded to be an endemic species inhabiting solely in the southern area of France during the Middle and the Late Pleistocene (Cregut– Bonnoure, 2007, 2020). As a matter of fact, the species has been identified in the Middle Pleistocene localities of Les Cedres, Rigabe (Cregut–Bonnoure, 1989), Le bay de l' Aubesier (Fernandez, 2001, 2006) and Cimay and the Upper Pleistocene localities of Saint Marcel de l'Ardeche (Cregut–Bonnoure, 1989), Arago (Rivals, 2002, 2005) and Bau de l' Aubesier (Cregut–Bonnoure, 2020) (Fig. 51). Thus, we can conclude that the only representatives of the genus *Hemitragus* that inhabited Eastern Europe, are *H. orientalis* and *H. bonali*, with *H. orientalis* being the only species identified in the Greek area to date (Fig. 12) (Apollonia I– described in Kostopoulos 1996; Cregut Bonnoure, 2020).

**4.14 Chiroptera indet.** Blumenbach, 1779

**Material**
Dental: one canine (ATchir1), one upper P4 (ATchir2) and one lower molar (ATchir3).

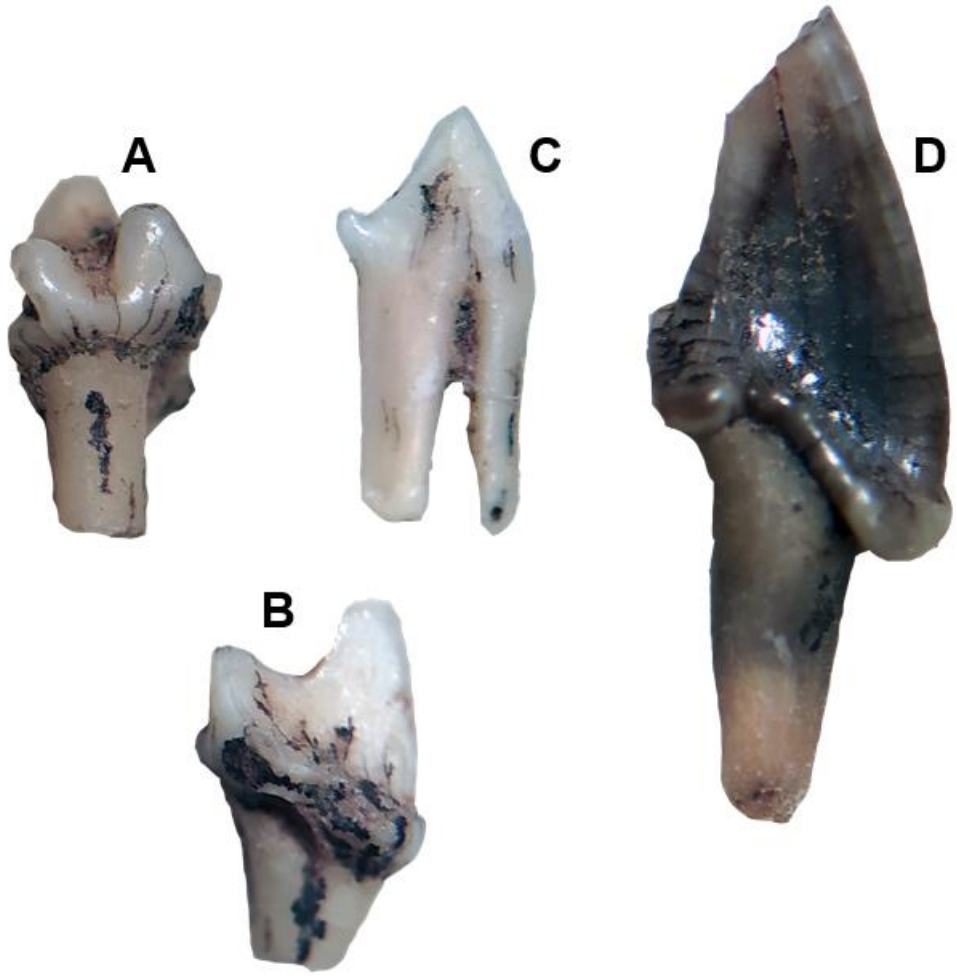


Figure 50: Dental elements from Aghia Kyriaki attributed to Chiroptera indet: A, B: lower molar (ATchir3), C: upper P4 (ATchir2), D: canine (ATchir1)

**Description & Comparison**
The teeth display the typical characteristic of the Michrochiroptera family, i.e., a pronounced and well defined cingulum. The canine ATchir1 is fragmented towards the occlusal surface of the tooth and bears a strong cingulum in the base of the tooth (Figure 52D). The upper P4 (ATchir2) has a prominent, sharp point (Fig. 52C). The lower molar (ATchir3) bears three different cusps (Fig. 52A,B).

**Discussion**
The order Chiroptera Blumenbach, 1779 is the second most diverse order of extant mammals, with a worldwide distribution (Simmons, 2005a; 2005b). Fossil representatives of the order are not that common, due to their small and delicate skeleton (Gunnell and Simmons, 2005). The first appearance of the taxon is dated back to the Early Eocene, in the European locality of Coimbra District, Portugal, as

well as in other localities in North and South America, Africa, Asia and Oceania (Tabuce et al. 2009; Simmons et al. 2008; Tejedor et al. 2005; Sigé 1991; Ravel et al. 2011; Hand et al. 1994; Smith et al. 2007), thus had an almost global distribution (Piskoulis and Chatzopoulou, 2022). Smith et al. (2007) consider the dispersal of the taxon in the Early Eocene as a sudden, isochronous event. The delicate nature of the postcranial elements of the Chiroptera (excluding the humerus), is the reason why most of the fossil record includes dental elements and humeri (Piskoulis and Chatzopoulou, 2022). Although the phylogenetic origin of the taxon is debated, research focused on the topic supports the hypothesis that Chiroptera is a monophyletic order, with the common ancestor having the ability of flying (Gunnell and Simmons 2005; Teeling et al. 2005; Piskoulis and Chatzopoulou, 2022).

The earliest occurence of the order Chiroptera in the Greek area dates back to the early Miocene, at the locality of Lapsarna, Lesvos (Vasileiadou and Zouros 2012; Vasileiadou et al. 2017). Although the Greek fossil record of Chriropteran is scarce, it's chronological distribution dates from the Early Miocene to the Early/Middle Holocene (Piskoulis and Chatzopoulou, 2022). According to Piskoulis and Chatzopoulou (2022), all the localities with identified Chiroptera specimens are located East of the Pindus Mountain Range. It is notable that *Myotis alcathoe* von Helversen et al., 2001 is a species endemic to Greece (Piskoulis and Chatzopoulou, 2022).

Table 34: Table showing all widely– accepted Chiropteran families, after Gunnell and Simmons (2005), Miller–Butterworth et al. (2007), Simmons et al. (2008) and Lack et al. (2010). The Chiropteran families identified from the Greek fossil record are shown in bold letters. Table from Piskoulis and Chatzopoulou (2022).

| **Extinct families** | **Extant families** | | |
|---|---|---|---|
| Icaronycteridae | Pteropodidae | Emballonuridae | Furipteridae |
| Archaeonycteridae | **Rhinolophidae** | Myzopodidae | Natalidae |
| Palaeochiropteridae | Hipposideridae | Mystacinidae | Molossidae |
| Hassianycteridae | **Megadermatidae** | Phyllostomidae | **Vespertilionidae** |
| Tanzanycteridae | **Rhinopomatidae** | Mormoopidae | **Miniopteridae** |
| Philisidae | Craseonycteridae | Noctilionidae | Cistugidae |
| Onychonycteridae | Nycteridae | Thyropteridae | |

The family Vespertilionidae Gray, 1821 (Table 33) made its first appearance during the Early Eocene (Miller–Butterworth et al. 2007) and it is also identified in the Greek fossil record with the taxa *Samonycteris majori* Revilliod, 1922, *Myotis* Kaup, 1829, *Nyctalus lasiopterus*? Schreber, 1780, *Nyctalus leisleri* Kuhl, 1817, *Nyctalus noctule* Schreber, 1774, *Pipistrellus* Kaup, 1829, *Vespertilio murinus* Linnaeus, 1758, *Eptesicus* Rafinesque, 1820, *Barbastella barbastellus* Schreber, 1774 and *Plecotus* Geoffry, 1818 (Piskoulis and Chatzopoulou, 2022).

The three teeth bear the typical morphological characteristics of Chiroptera. Their morphological characteristics also seem to resemble the ones of the family Vespertilionidae, however the specimens need further analysis. Thus, they are attributed to Chiroptera sp.

**4.15 Arvicolidae indet.** Gray, 1821

**Material**

Eleven dental specimens (ATarv1, ATarv2, ATarv3, ATarv4, ATarv5, ATarv6, ATarv7, ATarv8, ATarv9, ATarv10, ATarv11)

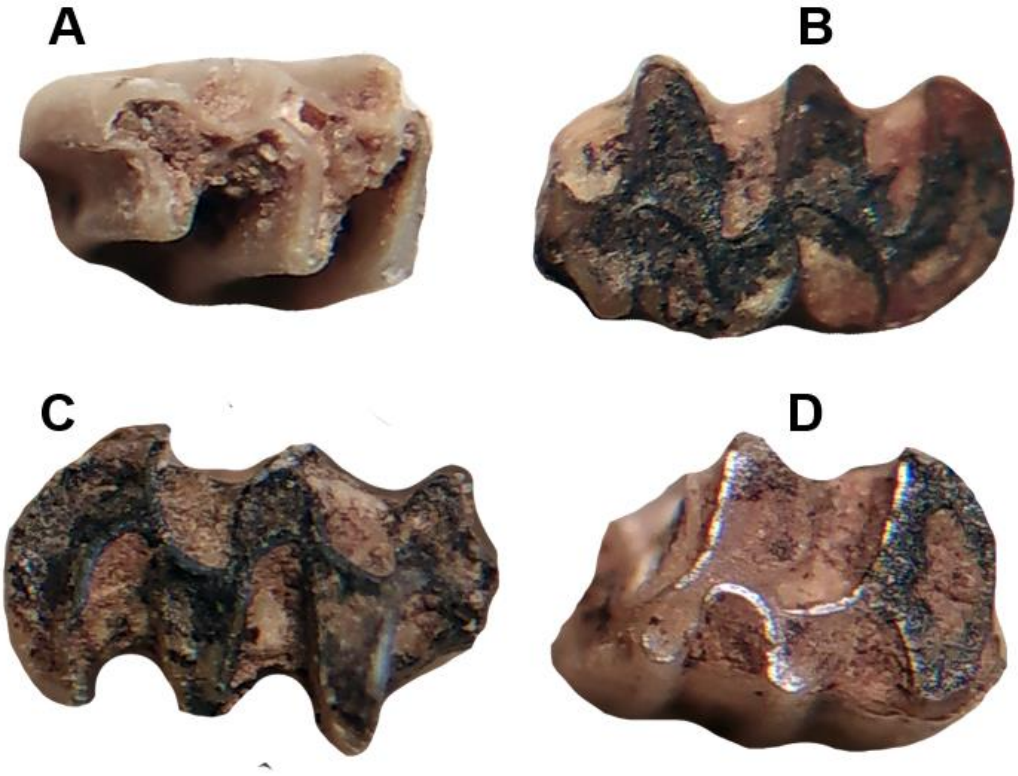


Figure 51: Dental elements from the locality of Aghia Kyriaki attributed to Arvicolidae indet. A: ATarv1, B: ATarv2, C: ATarv3, D: ATarv4 in occlusal view.

**Description**

All the dental specimens bear a prismatic occlusal surface with triangular shaped enamel ridges and inbetween valleys (Fig. 53).

**Discussion**

The family of Arvicolidae Gray, 1821 is a rodent family that made its first appearance during the Late Miocene, possibly in North America, however, it is not considered possible that the taxon originated there (Martin, 2008). Representatives of the family dispersed at higher latitudes during the Neogene (Martin, 2008), hence the taxon is present in Europe and N. America since then (Martin, 2008). Since skull remains are rarely found in the fossil record, the most characteristic features of the family, used for its taxonomy, are on dental and mandibular remains (Martin, 2008). A distinctive characteristic of the taxon is that the occlusal surface of the teeth of all representatives of Arvicolidae is planed and prismatic, with often triangular shaped enamel edges, the anticlines as well as their inbetween valleys, known as reentrant folds or synclines (Martin, 2008).

The teeth from Aghia Kyriaki are all characterized by a planed and prismatic occlusal surface, with triangular shaped enamel ridges and inbetween valleys (anticlines). According to Martin (2008), the exact same characteristics are typical of the family

Arvicolidae, thus, we can refer these specimens from the locality of Aghia Kyriaki to Arvicolidae indet.

## 5. BIOCHRONOLOGY

According to Koufos (2022), the family Canidae is the oldest carnivoran family of the fossil record, with the first specimens attributed to the taxon being late Eocene aged and it still bears extant representatives.

Rook (1994) suggests that the earliest appearance of *Canis (Xenocyon) falconeri* in Western Europe is estimated around 1.5–1.4 Ma (Kromdraai A and Olduvai bed II, accordingly), whereas its presence in Olduvai bed I, aged at 1.9 Ma is indicative of the dispersal of the species in Africa slightly earlier than in Western Europe. Rook and Martinez– Navarro (2010) state that the first appearance of the taxon in Europe is noted at around 1.8Ma. However, in their recent research, Bartolini–Lucenti and Spassov (2022) state that the FAD of the taxon in Europe is estimated at 2.6 Ma, in the French locality Roca–Neya. The taxon was later replaced by *Canis (Xenocyon) lycaonoides* during the second half of the late Villafranchian (Madurell–Malapeira et al., 2021).

As far as *U. etruscus* is concerned, Torres (1992) attributes its FAD in Villaroya, and Madurell–Malapeira et al. (2021) refer to the LAD of the species at 1.2 Ma.

The First Appearance of *Metacervocerus* sp. is attributed to the Late Ruscinian (MN15) faunas of Moldova (Croitor and Stefaniak, 2009), Bulgaria (Spassov, 2005), Brasov–Romania (Radulesco et al., 2003) and Poland (Stefaniak 1995, 2015), whereas, according to Croitor (2018) the last appearance of the genus is in Vallonet (0.9 Ma). The first appearance of the species *Croizetoceros ramosus* can be attributed in the Upper Ruscinian (MN15) with the species C*. ramosus pyrenaicus* (Heintz, 1970, Vislobokova, 1992, Vislobokova et al., 1993), whereas its last appearance is noted at the MN18, with the subspecies *C. ramosus minor* and *C. ramosus gerakarensis* (Kostopoulos, 1996).

The species *Procamptoceras brivatense* is typical of MNQ17–MNQ18 faunas, as it noted its first appearance at the beginning of the middle Villafranchian and its last appearance till the late Villafranchian (Fernandez and Cregut–Bonnoure, 2006). However, Cregut– Bonnoure (2007) states that the biochronological range of the species is from MNQ17 until the first part of MNQ20 (2.5–0.8Ma). *Hemitragus* sp. made its First Appearance in the eastern Europe at MNQ17, with the large– sized species *Hemitragus orientalis* in the localities Csarnota 2 and Villany 3 (Schaub, 1932; Cregut–Bonnoure, 2007), whereas the taxon is still represented by the modern species *Hemitragus jemlahicus.*

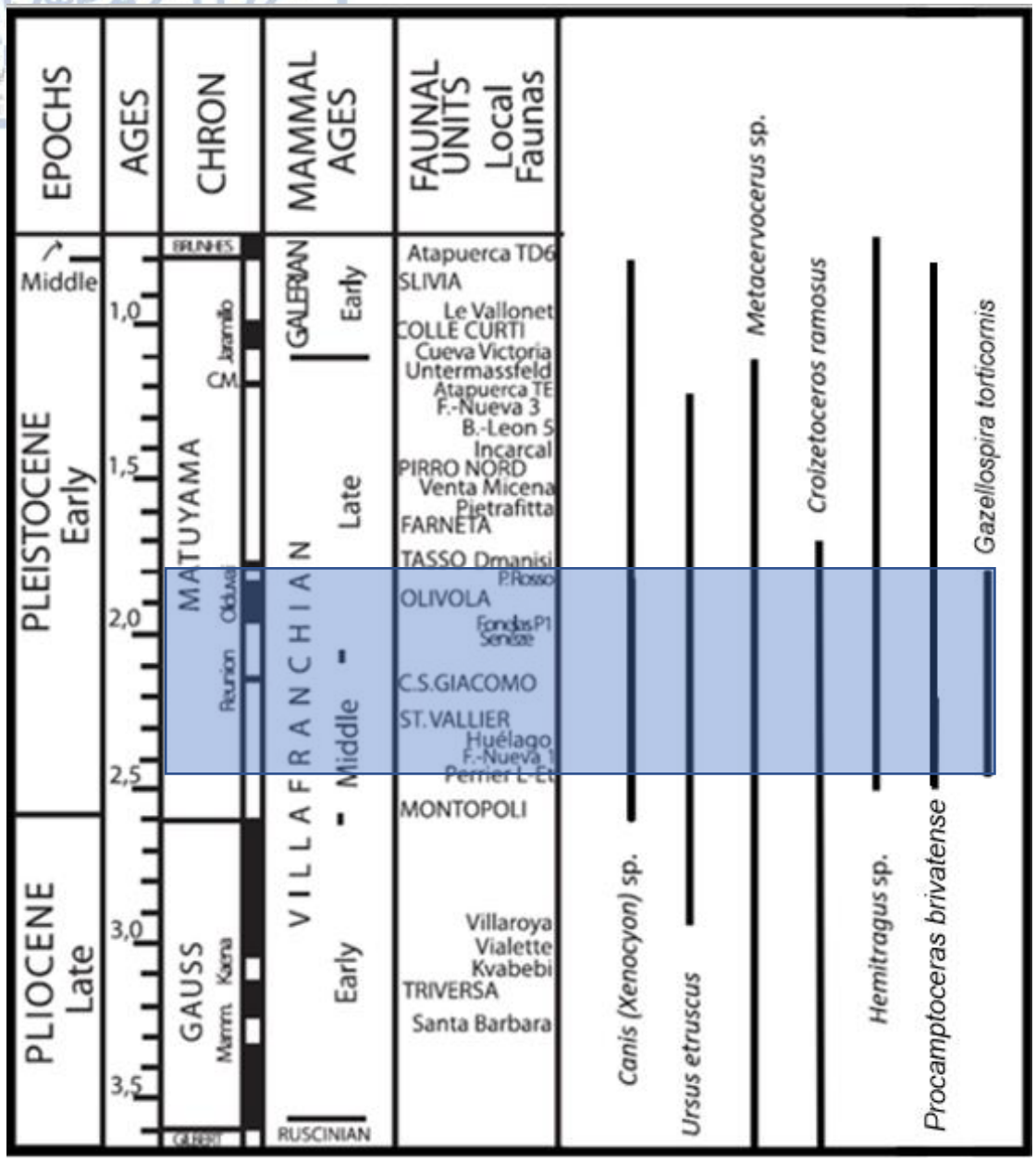


Figure 52: Biochronological table of the time range of different genera and species found in Aghia Kyriaki. Data from: Schaub (1932), Torres (1992), Kostopoulos (1996), Cregut–Bonnoure (2007), Croitor and Stefaniak (2009), Rook and Martinez– Navarro (2010), Croitor (2018), Madurell– Malapeira et al. (2021), Athanassiou, (2022) and Bartolini– Lucenti and Spassov (2022).

From the biochronological information mentioned above, as well as the information depicted in the Fig. 54, we can attribute the fauna of Aghia Kyriaki to a Middle to early late Villafranchian age. More specifically the co–occurence of the taxa *Gazellospira torticornis* and *Hemitragus* sp. limit the biochronological range of the age of the locality to approximately 2.5 to 1.8 Ma. The primitive morphological characteristics of the cranial and dental material of *Ursus etruscus* are also in accordance with the suggested age of the locality.

## 6. PALAEOECOLOGY

According to Meloro (2001, 2007), *Ursus etruscus* is present but not adapted to open or closed environments. According to Kostopoulos and Vasileiadou (2006), the expansion of *Ursus etruscus* seems to have been favored by the cold post–Olduvai conditions and its presence contributed to the open landscape mammal faunas. Also, Mazza and Rustioni (1992) noted that the species has been found mostly in lower middle latitudes, possibly suggesting that it is a typical faunal element of Southern Eurasian areas.

Generally, the presence of deers is indicative of forested areas (Athanassiou, 1996). More specifically, the ecomorphological study of the postcranial elements of *Croizetoceros ramosus* from Spain, conducted by Alcalde Rincon (2013), suggested that the versatile character of the habitat and diet of the species could be in accordance with its locomotive character. More specifically, he suggested that the species was mostly adapted to galloping but was also very adapted to jumping (stotting and jumping gallop), thus, taking into consideration the small size of the taxon, could indicate that *C. ramosus* lived in areas with dense vegetation. *Metacervocerus rhenanus* is considered to have a similar feeding ecology to the one of the modern *Axis* representatives, who are grazers (Croitor, 2006). In particular, the mesowear analysis of *M. rhenanus* teeth from Ceyssaguet suggest a feeding pattern similar to the one of modern deers feeding on juicy green grass and living close to rivers (Croitor and Kaiser, 2002; Croitor, 2006). Finally, Kaiser and Croitor (2006), suggest that *Metacervocerus rhenanus* was an inhabitant of dense woodlands and tall grass areas close to a water body.

Van der Made et al. (2008), based on the ecomorphological traits of the postcranial skeleton of *Hemitragus* sp. representatives, and especially on their highly robust metacarpals and relatively short metacarpals, suggested that these features show the highest adaptation level to a rocky and mountainous environment. Another indocator of a mountainous paleoenvironment is the presence of cf. *Procamptoceras brivatense*, which is a bovid specialized to mountain environments (Brugal and Croitor, 2007).

As far as the Canids are concerned, according to Argant (2004), *Nyctereutes* sp., *Vulpes* sp. (medium sized canids), as well as Mustelidae representatives, are all indicative of the same type of ecological niche. Representatives of these taxa usually dig burrows in loose soil at the edge of watercourses (Argant, 2004), thus we expect the locality of Aghia Kyriaki, to have been close to a watercourse, with loose soil.

Koufos (2014), revised the palaeoenvironmental information of Greek Villafranchian localities based on their Carnivoran guilds, and suggested that the middle Villafranchian of Greece is characterized by open grassland conditions; this is in accordance with the palaeoenvironmental background suggested by Kostopoulos and Koufos (1988b, 2000), based on the faunal synthesis of Ruminantia: open, sub–arid conditions similar to savvanah–like modern woodlands. Moreover, Kostopoulos and Koufos (2000) suggested that no major palaeoenvironmental change was made during the late Villafranchian, which is also characterized by open and open towards mixed environments. In accordance with these, Nomade et al. (2012) suggest that the co–occurrence of Canid species, with a large diversity of Carnivora, numerous Bovids like *Procamptoceras* and Cervidae grazers like *Croizetoceros* in the Villafranchian localities of Europe, are indicative of open habitats with patches of open forests. Therefore, the assumed palaeoenvironmental reconstruction of Aghia Kyriaki fits to the

one suggested from Koufos (2014), Nomade et al. (2012) and Kostopoulos and Koufos (2000).

## 7. CONCLUSIONS

Despite the scarce fossiliferous material from the locality of Aghia Kyriaki, 15 taxa were identified in the present MSc thesis. The faunal list of the fossiliferous locality of Aghia Kyriaki includes the following taxa:

1. Mammalia indet.
2. *Ursus etruscus*
3. Canidae indet., mid–sized
4. *Canis (Xenoycyon)* sp.
5. (?) Mustelidae indet.
6. Ruminantia indet.
7. Cervidae indet.
8. *Metacervocerus* sp.
9. *Croizetoceros ramosus*
10. Bovidae indet.
11. cf. *Gazellospira torticornis*
12. Rupicaprini indet. cf. *Procamptoceras brivatense*
13. *Hemitragus* sp.
14. Chiroptera indet. Blumenbach, 1779 (? Vespertilionidae indet. Gray, 1821)
15. Arvicolidae indet.

Taking into account the biochronological range of each of these taxa in the European area, we suggest a Middle to early late Villafranchian age for the locality of Aghia Kyriaki. More specifically, the co–existence of the taxa cf. *Gazellospira torticornis* and *Hemitragus* sp., limits the age frame of the locality to an estimated age of 2.5– 1.8 Ma.

The presence of a complete cranium and several dental and postcranial elements of *U. etruscus* in the site is notable, since Aghia Kyriaki is so far the Southernmost locality of mainland Greece, with specimens attributed to this certain taxon. Moreover, amongst others we note the earliest presence of *Hemitragus* sp. in Greece, a taxon that had so far only been represented in the Greek area by an evolved form of *Hemitragus orientalis* in Apollonia I (described in Kostopoulos 1996; Cregut Bonnoure, 2020). The presence of the hemimandible AT216, and of lower teeth of the same size, is noteworthy since they show a clear Rupicaprini morphology, and they are morphometrically closer to the species *Procamptoceras brivatense*. The species has only been found in Greece in the localities Vassiloudi and Volakas (Fernandez and Cregut– Bonnoure, 2006) by very few remains. Moreover, the presence of *Canis (Xenocyon)* sp., could be one of the earliest ones in Europe. The lack of dental

elements of Canidae and Mustelidae in the fossiliferous record of Aghia Kyriaki does not allow a safe attribution to a certain taxon. Accordingly, the lack of antler/horncore material of the Aghia Kyriaki ruminants is not helpful either towards a more accurate taxonomical attribution of their representatives.

The taphonomic study of the site, showed that a catastrophic event scenario is excluded. However, all the relevant parameters examined in this MSc thesis agree that the most possible scenario is that the cacasses of the animals were placed in the cave or their bones were transported from a short distance by water and gravity and finally dropped in the cavity from an opening at the roof of the cave, and obtained different weathering stages based on the time the bones were exposed to unprotected surficial conditions, the time of burial as well as the climatic conditions of the region. Thus, the specimens seem to have been gradually accumulated in the locality of Aghia Kyriaki.
As far as Palaeoecology is concerned, we can assume that the palaeoenvironment of Aghia Kyriaki was a mosaic, with open areas, dense woodlands and rocky areas, close to a water body, a palaeoenvironmental interpretation consistent with the one suggested for the middle and late Villafranchian.

Clearly, the locality of Aghia Kyriaki bears a diverse faunal list, with a remarkable palaeoenvironmental mosaic, despite the scarce fossiliferous material that has so far been collected. The complete skull of *U. etruscus*, could be used in further studies, that could compare it in depth with other important specimens attributed to the same species; comparative analysis of the skull, combined with biochronological information of the site of Aghia Kyriaki from the current thesis, could also be used in a future project regarding the evolution of *U. etruscus*. Also, the measurements of the studied specimens could attribute in both Greek and European bibliography, as comparative sources, while at the same time the importance of some of the specimens, as discussed above, make Aghia Kyriaki a very promising newly discovered fossiliferous locality.

Due to the fact that the available fossiliferous material of the locality is scarce, further research and systematic excavations with focus on stratigraphy and possibly the implementation of palaeoenvironmental methods is needed. Thus, we can make a more specific attribution to a certain age, as well as reinforce the aforementioned results of this thesis and shed further light to this remarkable Villafranchian locality.

**BIBLIOGRAPHY**

Abbazzi, L., 2004. Remarks on the validity of the generic name *Praemegaceros* Portis 1920, and an overview on *Praemegaceros* species in Italy. Series. Rendiconti Accademia dei Lincei – Scienze Fisiche Matematiche Naturali 9 (15), 115–132.

Agustí, J., Antón, M., 2002. Mammoths, Sabretooths and Hominids: 65 Million Years of Mammalian Evolution in Europe. Columbia UniverColumbia University Press, New York, 311.

Agusti, J., Anton, M., 2005. Mammoths, Sabertooths, and Hominids: 65 Million Years of Mammalian Evolution in Europe. Columbia University Press, pp. 225, 295,

Agustı, J., Moya -Sola, S., Pons-Moya, J., 1987. La sucesion de Mamıferos en el Pleistoceno inferior de Europa: proposicion de una escala bioestratigrafica. Paleontologıa I Evolucio, Memoria Especial 1: 287–295.

Agustı, J., Vekua, A., Oms. O., Lordkipanidze, D., Bukshianidze, M., Kiladze, G., Rook, L. 2009. The middle Pliocene site of Kvabebi and the faunal background to early human occupation of southern Caucasus. Journal of Quaternary Sciences. 28(27):3275-3280.

Alberdi, M.T., Caloi, L., Palombo, M.R., 1998. Large mammal associations from the early Pleistocene: Italy and Spain. Mededelingen Nederlands Instituut Voor Toegepaste Geowetenschappen TNO 60: 521–532.

Alekperova N. A. 1964. A finding of a new for Azerbaidjan deer *Cervus* (*Rusa*) sp. from Upper Pliocene deposits. Buletin of the Academy of Sciences of Azerbaidjan SSR, geologicalgeographical series, 2: 59–62.

Alkalde Rincon, G. M., 2013. CARACTERIZACIÓN ECOMORFOLÓGICA DEL ESQUELETO POSTCRANEAL EN RUMIANTES (ARTIODACTYLA, MAMMALIA): APLICACIÓN EN LA INFERENCIA DE LAS ADAPTACIONES ECOLÓGICAS DE LOS RUMIANTES DEL PLIO–PLEISTOCENO DE ESPAÑA). Universidad Complutense de Madrid. Facultad de Ciencias Geologicas, Departamento de Paleontologia. Madrid, 2012.

Argant, A. 2004. Les Carnivores du gisement Pleiocene final de Saint- Vallier (Drome, France). Geobios 37, DOI: 10.1016/S0016-6995(04)80013-5

Arribas, A., 2008. Vertebrados del Plioceno superior terminal en el suroeste de Europa: Fonelas P–1 y el Proyecto Fonelas. Instituto Geologico y Minero de Espana, serie Cuadernos del Museo Geominero 10, 1–607.

Athanassiou, A. 2022. The Fossil Record of Continental Fossil Deer (Mammalia: Artiodactyla: Cervidae) in Greece, in: Vlachos, E. Fossil Vertrebrates of Greece Vol. 2. Laurasiatherians, Artidactyles, Perissodactyles, Carnivorans and Island Endemics. Springer, pp.205–247.

Azzaroli, A., 1962. Rinoceronti pliocenici del Valdarno inferiore. Palaeontographia Italica, 57(27), pp.11–20.

Azzaroli, A., 1977. The Villafranchian stage in Italy and the Plio–Pleistocene boundary. Giornale di Geologia, 41(1–2): 61–79.Azzaroli, A., 1983. Quaternary mammals and the end–Villafranchian dispersal event– a turning point in the history of Eurasia. Palaeogeography, Palaeoclimatology, Palaeoecology 44, 117–139.

Azzaroli, A., De Giuli, C., Ficcarelli, G., Torre, D., 1988. Late Pliocene to early mid–Pleistocene mammals in Eurasia: faunal succession and dispersal events. Palaeogeogr Palaeoclimatol Palaeoecol 66: 77–100.

Babin, C.,1991. Principes de Paléontology. Paris: Armand Colin.

Bartolini– Lucenti, S., Rook, L., 2016. A review on the late Villafranchian medium–sized canid *Canis arnensis* based on the evidence from Poggio Rosso (Tuscany, Italy). Quaternary Science Reviews 151:58–71.

Barmann, E., Rossner, G.E. 2011. Dental nomenclature in Ruminantia: Towards a standard terminological framework. Mammalian Biology: Zeitschrift fur Saugetierkunde 76(6):762-768.

Bartolini– Lucenti, S., Spassov, N., 2022. Cave canem! The earliest *Canis* (*Xenocyon*) (Canidae, Mammalia) of Europe: Taxonomic affinities and paleoecology of the fossil wild dogs. Quaternary Science Reviews 276: 107315.

Bartolini–Lucenti, S., Madurell– Malapeira, J., Martínez– Navarro, B., Palmqvist, P., Lordkipanidze, D., Rook, L., 2021. The early hunting dog from Dmanisi with comments on the social behaviour in Canidae and hominins. Sci Rep. 11 (1):1–10. doi:10.1038/s41598–021–92818–4.

Baryshnikov, G.F. 2007. Fauna of Russia and neighbouring countries. Mammals, Ursidae. Nauka, Saint Petersburg.

Baryshnikov, G. 2012. Pleistocene Canidae (Mammalia, Carnivora) from the Paleolithic Kudaro caves in the Caucasus. Journal of Theriology 11(2):77-120. DOI: 10.15298/rusjtheriol.11.2.01

Baryshnikov, G.F., Tsoukala, E. 2010. New analysis of the Pleistocene carnivores from Petralona Cave (Macedonia, Greece) based on the collection of the Thessaloniki Aristotle University. Geobios 43:389–402

Behrensmeyer, A.K. and Kidwell, S.M., 1985. Taphonomy's contributions to paleobiology. Paleobiology, 11: 105–119.

Behrensmeyer, A.K., Kidwell, S.M. and Gastaldo, R.A., 2000. Taphonomy and paleobiology. In (Erwin, D.H. & Wing, S.L., eds.) Deep Time: Paleobiology's Perspective. Lawrence, KS: The Paleontological Society, pp. 103–147.

Bellucci, L., Iurino, D.A., Sardella, R., 2014. CARNIVORES FROM THE MIDDLE VILLAFRANCHIAN SITE OF COSTE SAN GIACOMO (ANAGNI BASIN, CENTRAL ITALY). Conference: XII EAVP Meeting at Torino. DOI: 10.13140/2.1.3801.4722

Berggren, W. and van Couvering, J., 1974. The Late Neogene. Biostratigraphy, geochronology, and paleoclimatology of the last 15 million years in marine and continental sequences. ISBN: 9780080868431

Berta, A. 1987. Origin, diversification zoogeography of South American Canidae. Fieldiana Zoology. 39, 455–471.

Bertini, A. 2010. Pliocene to Pleistocene palynoflora and vegetation in Italy: State of the art. Quaternary International 225, 5–24. doi: 10.1016/j.quaint.2010.04.025.

Boeuf, O., 1983. Le site villafranchien de Chilhac (Haute–Loire, France). Etude paléontologique et biochronologique. Thèse, Université de Paris VII.

Bolomey, A., 1965. Die Fauna zweier villafrankischer Fundstellen in Rumanien, Berichte der geologischen Gesellschaft der DDR, Berlin 10, pp. 77–88.

Boudadi– Maligne, M., 2010. LES CANIS PLEISTOCENES DU SUD DE LA FRANCE: APPROCHE BIOSYSTEMATIQUE, EVOLUTIVE ET BIOCHRONOLOGIQUE. Archéologie et Préhistoire. Université Bordeaux 1, 2010. Français. NNT: 4126.

Bourdier, F., 1961. Le Bassin du Rhone au Quaternaire. In: Geologie et Prehistoire, Tome 1. CNRS, Paris. Texte.

Bout, P., 1960. Le Villafranchien du Velay et du basin Hydrographique Moyen et Supérieure de l'Allier. Ph.D. Thesis, Jeanne d'Arc, Le Puy en Velay, 344 pp.

Bout, P., 1967. Observations sur le Villafranchien d'Auvergne et du Velay (Compte rendu de l'excursion de l'AFEQ du 19 au 22 mai 1966). Bulletin de l'Association Francaise pour l'etude du Quaternaire, 4(1), pp.3–64.

Brunet, M., Heintz, E., 1984. Un exemple de gradualisme phyletlque chez les Cervidés villafranchlens d' Europe. Coll. intrn. C.N.R.S. No 330 "Modalités, rythmes et mécanismes de 1" evolution biologique": 79–81.

Bukhsianidze, M., 2005. The fossil bovidae of dmanisi. In: PhD Dissertation, International Doctorate ''Environmental, Humans and Compartmental Dynamics'', University of Ferrara, 192.

Castello, J.R., 2016. BOVIDS of the World. Antelopes, Gazelles, Cattle, Goats, Sheep, and Relatives. PRINCETON UNIVERSITY PRESS PRINCETON AND OXFORD. ISBN 978–0–691–16717–6. Pp. 1–665.

Cherin, M., Berte, D.F., Rook, L., Sardella, R., 2014. Re–Defining *Canis etruscus* (Canidae, Mammalia): A New Look into the Evolutionary History of Early Pleistocene Dogs Resulting from the Outstanding Fossil Record from Pantalla (Italy). J Mammal Evol 21:95–110. DOI 10.1007/s10914–013–9227–4

Cherin, M., Alba, D.M., Crotti, M., Menconero, S., Moulle, P.E., Sorbelli, L., Madurell-Malapeira, J. 2020. The post-Jaramillo persistence of *Sus strozzii* (Suidae, Mammalia) in Europe: New evidence from the Vallparadís Section (NE Iberian Peninsula) and other coeval sites. Quaternary Science Reviews, 223:106234.

Clark, P., Archer, D., Pollard, D., Blum, J.D., Rial, J.A., Brovkin, V., Mix, A.C., Pisias, N.G., Roy, R., 2006. The Middle Pleistocene transition: characteristics, mechanisms, and implications for long term changes in atmospheric pCO2. Quaternary Science Reviews 25, 3150–3184. doi: 10.1016/j.quascirev.2006.07.008.

Cregut Bonnoure, E. 1979. La faune de mammifieres du Pleistocene moyen de la Caune de l'Arago a Tautavel (Pyrenees Orientales). Travaux du laboratoire de Paleontologie humaine et de Prehistoire, Marseille, 3:381.

Cregut- Bonnoure, E. 1988. (A new discovery of *Hemitragus* Hodgson, 1841 (Mammalia, Bovidae) in the middle Pleistocene site of Balaruc VII (Sete, Herault). Biostratigraphic interest of this genus and of Capra Linne, 1758).

Cregut- Bonnoure, E., 1989. Un niuveau Caprinae, *Hemitragus cedrensis* nov. sp. (Mammalia, Bovidae) des niveaux pleistocenes moyen de la grotte des Cedres (Le plan d'Aups, Var). Interet biogeographique. Geobios, 22(5):653-663.

Cregut- Bonnoure, E., 1999. Les petits Bovidae de Venta Micena (Andalousie) et de Cueva Victoria (Murcia). Los homínidos y su entorno en el Pleistoceno inferior y medio de Eurasia: actas del Congreso Internacional de Paleontología Humana, Orce 1995 / coord. por Josep Gibert i Clols, 1999, ISBN 84-8416-938-3, 191-228.

Cregut- Bonnoure, E., 2006. European Ovibovini, Ovini and Caprini (Caprinae, Mammalia) from the Plio-Pleistocene: New interpretations.

Cregut– Bonnoure, E., 2007. Apport des Caprinae et Antilopinae (Mammalia, Bovidae) à la biostratigraphie du Pliocène terminal et du Pléistocène d'Europe. Quaternaire, 18:1.

Cregut Bonnoure, E., Spassov, N. 2002. *Hemitragus orientalis* nov. sp. (Mammalia, Bovidae, Caprinae), a new species from Oriental Europe. Revue de Paleobiologie 21(2):553-573.

Cregut– Bonnoure, E., 2020. Les Ovibovini, Caprini et Ovini (Mammalia, Artiodactyla, Bovidae, Caprinae) du Plio–Pléistocène d'Europe, Systématique, évolution et biochronologie, Volumes I and II. BAR Publishing, ISBN: 9781407354248

Cregut- Bonnoure, E., Valli, A.M.F. 2004. Les Bovidés du gisement pliocène supérieur (Villafranchien moyen) de Saint-Vallier (Drôme, France). Geobios, 37(3). DOI: 10.1016/S0016-6995(04)80017-2

Cregut-Bonnoure, E., Baryshnikov, G. 2005. New results on the Caprini (Bovidae, Caprinae) from Kudaro I and III (Georgia, Caucasus mountains). Quaternaire pp. 145-157.

Cregut– Bonnoure, E., Tsoukala, E., 2017. The Late Pliocene Bovidae and Cervidae (Mammalia) of Milia (Grevena, Macedonia, Greece). Quaternary International 445: 215–249.

Croitor R., Bonifay M.–F. 2001. Étude préliminaire des cerfs du gisement Pleistocène inférieur de Ceyssaguet (Haut–Loire). Paleo, 13: 129–144.

Croitor R., Stefaniak K. 2009. Early Pliocene deer of Central and Eastern European regions and inferred phylogenetic relationships. Palaeontographica: 287: 1–39.

Croitor, R. 2018. Plio–Pleistocene Deer of Western Palearctic: Taxonomy, Systematics, Phylogeny. Institute of Zoology of the Academy of Sciences of Moldova.

Croitor, R., 2006. Early Pleistocene small sized deer of Europe. Hellenic Journal of Geosciences, vol. 41, 89–117.

Croitor, R., 2006. Early Pleistocene small–sized deer of Europe. In: Croitor, R. Plio–Pleistocene deer of Western Palearctic: taxonomy, systematics, functional morphology, paleoecology, evolution, paleobiogeography.

Croitor, R., Bonifay M.–F., Brugal, J.–P., 2012. Systematic revision of the endemic deer *Haploidoceros* n. gen. *mediterraneus* (BONIFAY, 1967) (Mammalia, Cervidae) from the Middle Pleistocene of Southern France. Paläontologische Zeitschrift 82(3):325–346.

Croitor, R., Kaiser, T., 2002. Functional morphology and diet preferences of fossil deer and paleolandscape reconstruction of early Pleistocene of Ceyssaguet. Verhandlungen der Gesell –schaft fur Okologie, Band 32, 465. Cottbus.

Cvetkovic, J., Dimitrijevic, V. 2014. Cave bears (Carnivora, Ursidae) from the Middle Pleistocene of Serbia: A revision. Quaternary International 339-340:197-208.

De Giuili, C., Heintz, E., 1974. *Croizetoceros ramosus* (Cervidae, Artiodactyla, Mammalia) de Montopoli, nouvel element de la faune villafranchienne d'Italie. Atti Soc. Tosc, Sci. Nat. Mem. serie A, 81: 241–251.

De Giuli, C., Masini, F., 1983. A new element of the late Villafranchian (Tasso unit) faunas of Italy: occurrence of Ovibovini (Bovidae, Artiodactyla, mammalia) in the fauna of Casa Frata (Upper Valdarno, Tuscany). Bollettino Della Societa Paleontologica Italiana 22, 271–280.

De Giuli, C., Masini, F., 1987. The latest Villafranchian faunas of Italy. The Casa Frata local fauna (Upper Valdarno, Tuscany). Palaeontographia Italica 74, 1–9.

Di Stefano G., Petronio C. 2002. Systematics and evolution of the Eurasian Plio–Pleistocene tribe Cervini (Artiodactyla, Mammalia). Geologica Romana, 36: 311–334.

Dong, W., 1996. Les Cervidae (Artiodactyla) rusciniens (Pliocene) du Languedoc et du Roussillon (France). Bull Mus natl Hist nat 18:133–163.

Efremov, I.A., 1940. Taphonomy: a new branch of paleontology. Pan American Geologist, 74: 81–93.

Fahey, B., Myers, P., 2000. Canidae (On–line). Animal diversity web. http://animaldiversity.org/accounts/Canidae/. Accessed 17 May 2018.

Fernandez, P., Cregut Bonnoure, E. 2007. Les Caprinae (Rupicaprini, Ovibovini, Ovini et Caprini) de la sequence pléistocène de Kozarnika (Bulgarie du Nord): morphométrie, biochronologie et implications phylogéniques. Revue de Paléobiologie, Genève, 26 (2): 425-503

Gabunia, L., Vekua, A., Lordkipanidze, D., Swisher III, C., Ferring, R., Justus, A., Nioradze, M., Tvalchrelidze, M., Anto´ n, S., Bosinski, G., Joris, O., de Lumley, M., Majsuradze, G., Mouskhelishvili, A., 2000. Earliest Pleistocene hominid cranial remains from Dmanisi, Republic of Georgia: taxonomy, geological setting, and age. Science 288, 1019–1025.

Garcia, N., Arsuaga, J.L. 2001. *Ursus dolinensis*: A new species of Early Pleistocene ursid from Trinchera Dolina, Atapuerca (Spain). Comptes Rendus de l Académie des Sciences - Series IIA - Earth and Planetary Science 332(11):717-725 DOI: 10.1016/S1251-8050(01)01588-9

Garrido, G. 2008. La Asociation de los Generos *Croizetoceros*, *Metacervoceros* y *Eucladoceros* (Cervidae, Artiodactyla, Mammalia) en el yacimento de Fonelas P–1 (Cuenca de Guadix, Granada) in Arribas, A. Vertebrados del Plioceno superior terminal en el suroeste de Europa: Fonelas P–1 y el Proyecto Fonelas. Cuadernos del Museo Geominero, nº 10. Instituto Geológico y Minero de España, Madrid, 2008, 365–396. ISBN 978–84–7840–764–4.

Garrido, G. and Arribas, A. 2008. *Canis accitanus* nov. sp., a new small dog (Canidae, Carnivora, Mammalia) from the Fonelas P–1 Plio–Pleistocene site (Guadix basin, Granada, Spain). Geobios. 41, 751–761.

Gaudzinski, S., 2004. Subsistence patterns of Early Pleistocene hominids in the Levant—taphonomic evidence from the 'Ubeidiya Formation (Israel). Journal of Archaeological Science, 31:65–75.

Gibbard, P. L., Head, M. J., Walker, M. J. C. and the Subcommission on Quaternary Stratigraphy. 2010. Formal ratification of the Quaternary System/Period and the Pleistocene Series/Epoch with a base at 2.58 Ma. J. Quaternary Sci., Vol. 25 pp. 96–102. ISSN 0267–8179.

Gibbard, P.L. & Head, M.J. 2020. The Quaternary Period. In: The Geologic Time Scale 2020. Volume 2 Ed. Felix M. Gradstein, James G. Ogg, Mark D. Schmitz and Gabi M. Ogg. Elsevier BV. Amsterdam, Oxford, Cambridge. p. 1217–1255.Howell (1959)

Gliozzi E., Abbazzi L., Argenti P., Azzaroli A., Caloi L., Capabasso Barbato L., Di Stefano G., Esu D., Ficcarelli G., Girotti O., Kotsakis T., Masini F., Mazza P., Mezzabotta C., Palombo M.R., Petronio C., Rook L., Sala B., Sardella R., Zanalda E.

& Torre D., 1997 Biochronology of selected Mammals, Molluscs and Ostracods from the Middle Pliocene to the Late Pleistocene in Italy. The state of the art. Riv. It. Paleont. Strat. 103 (3): 369–388

Gliozzi, E., Abbazzi, L., Argenti, A., Azzaroli, A., Caloi, L., Capasso Barbato, L., di Stefano, G., Esu, D., Ficcarelli, G., Girotti, O., Kotsakis, T., Masini, F., Mazza, P., Mezzabotta, C., Palombo, M. R., Petronio, C., Rook, L., Sala, B., Sardella, R., Zanalda, E. And Torre, D. 1997. Biochronology of selected Mammals. Molluscs and Ostracodes from the Middle Pliocene to the Late Pleistocene in Italy. The state of the art. Rivista Italiana di Paleontologia e Stratigrafia. 103(3), 369–388.

Gliozzi, E., Abbazzi, L., Argenti, P., Azzaroli, A., Caloi, L., Capasso Barbato, L., Di Stefano, G., Esu, D., Ficcarelli, G., Girotti, O., Kotsakis, T., Masini, F., Mazza, P., Mezzabotta, C., Palombo, M.R., Petronio, C., Rook, L., Sala, B., Sardella, R., Zanalda, E., Torre, D., 1997. Biochronology of selected mammals, molluscs and ostracods from the middle Pliocene to the late Pleistocene in Italy. The state of the art. Rivista Italiana di Paleontologia e Stratigrafia 103, 369–388.

Guerin, C. and Tsoukala, E., 2013. The Tapiridae, Rhinocerotidae and Suidae (Mammalia) of the early Villafranchian site of Milia (Grevena, Macedonia, Greece), Geodiversitas, 35(2), 447–489

Guérin, C., 2007. Biozonation continentale du Plio–Pléistocène d'Europe et d'Asie occidentale par les mammifères: état de la question et incidence sur les limites Tertiaire/Quaternaire et Plio/Pléistocène. Quaternaire. Revue de l'Association française pour l'étude du Quaternaire, 18(1): 23–33.

Guerin, C., Faure, M., 1997. The wild Boar (Sus scrofa priscus) from the Post Villafranchian lower pleistocene of Untermassfeld. In: Kahlke, R.D. (Ed.), Das Pleistozan von Untermassfeld bei Meiningen (Thuringen), vol. 1. Romisch–Germanisches Zentralmuseum, pp. 375–384.

Gunnell, G.F., Simmons, N.B., 2005. Fossil evidence and the origin of bats. J Mamm Evol 12:209–246.

Gunnell, G.F., Simmons, N.B., 2005. Fossil evidence and the origin of bats. J Mamm Evol 12:209–246.

Hand, S., Novacek, M., Godthelp, H., Archer, M., 1994. First Eocene bat from Australia. J Vert Paleontol 14:375–381.

Heintz, E. 1970. Les Cervides Villafranchiens de France et d' Espagne. Vollume I & II. Memoires du Museum National d' Histoire Naturelle. Vol. I:1– 295, Vol. II:1–206.

Heintz, E. 1970. Les Cervides Villafranchiens de France et d' Espagne. Vollume I & II. Memoires du Museum National d' Histoire Naturelle. Vol. I:1– 295, Vol. II:1–206.

Heintz, E., 1974. Les populations de *Croizetoceros ramosus* (Cervidae, Mammalia) dans le temps et dans l' espace, Bull. Soc. Geol. de France, (7), 16, 4: 411–417.

Heintz, E., Aguirre, E., 1976. Le bois de *Croizetoceros ramosus pueblensis*, Cervide de la faune Villafranchienne de la Puebla de Valverde, Teruel (Espagne). Estudios geol. 32: 569–572

Hemmer, H., 2001. Die Feliden aus dem Epivillafranchium von Untermassfeld. In: Kahlke, R.D. (Ed.), Das Pleistozan von Untermassfeld bei Meiningen (Thuringen), vol. 3. Romisch–Germanisches Zentralmuseum, pp. 699–782.

Holman Flower, L.C., 2014. Canid evolution and palaeoecology in the Pleistocene of western Europe, with particular reference to the wolf *Canis lupus* L. 1758. PhD thesis. Royal Holloway University of London. P. 1–558.

Howell, F.C. The Villafranchian and human origins. Science. 1959 Oct 2;130(3379):831-44. doi: 10.1126/science.130.3379.831. PMID: 14403491.

Jiangzuo, Q., Liu, J., Jin, C. 2019. Morphological homology, evolution and proposed nomenclature fir bear dentition. Acta Palaeontological Polonica. 64: 693–710.

Kahlke, R.D. (Ed.), 1997, Das Pleistozan von Untermassfeld bei Meiningen (Thuringen), vol. 1. Romisch–Germanisches Zentralmuseum, pp. 1–418.

Kahlke, R.D. (Ed.), 2001a, Das Pleistozan von Untermassfeld bei Meiningen (Thuringen), vol. 2. Romisch–Germanisches Zentralmuseum, pp. 419–698.

Kahlke, R.D. (Ed.), 2001b, Das Pleistozan von Untermassfeld bei Meiningen (Thuringen), vol. 3. Romisch–Germanisches Zentralmuseum, pp. 699–1030.

Konidaris, G.E., Koufos, G.D., Kostopoulos, D.S. and Merceron, G., 2014. Taxonomy, biostratigraphy and palaeoecology of *Choerolophodon* (Proboscidea, Mammalia) in the Miocene of SE Europe–SW Asia: implications for phylogeny and biogeography, Journal of Systematic Palaeontology. http://dx.doi.org/10.1080/14772019.2014.985339.

Kostopoulos, D.S, Athanassiou, A., 2005. In the shadow of bovids: suids, cervids and giraffids from the Plio–Pleistocene of Greece. Quaternaire hors–série 2:179–190.

Kostopoulos, D.S., 1996. [The Plio–Pleistocene Artiodactyls of Macedonia (Greece): systematics, palaeoecology, biochronology, biostratigraphy]. PhD thesis, Aristotle University of Thessaloniki (in Greek).

Kostopoulos, D.S., Athanassiou, A., 2005. In the shadow of bovids: suids, cervids and giraffids from the Plio–Pleistocene of Greece. Quaternaire hors–serie 2, 179–190.

Κωστόπουλος, Δ., Κουφός, Γ., 2015. Η εξέλιξη του έμβιου κόσμου: χορδωτά. [ηλεκτρ. βιβλ.] Αθήνα:Σύνδεσμος Ελληνικών Ακαδημαϊκών Βιβλιοθηκών. Διαθέσιμο στο: http://hdl.handle.net/11419/1909

Kostopoulos, D.S., Vasileiadou, K., 2006. THE GREEK LATE NEOGENE QUATERNARY URSIDS IN RELATION TO PALAEOGEOGRAPHY AND

PALAEOENVIRONMENT. Scientific Annals, School of Geology Aristotle University of Thessaloniki (AUTH), 98: 285–292.

Koufos, G.D., 1987. *Canis arnensis* del Campana, 1913 from the Villafranchian (Villanyian) of Macedonia (Greece). Paleontologia I Evolucio, Memoria Especial 21, 3–10.

Koufos, G.D., 1997. The canids *Eucyon* and *Nyctereutes* from the Ruscinian of Macedonia, Greece. Palaeontol Evol 30–3:39–48.

Koufos, G.D., 2001. The Villafranchian mammalian faunas and biochronology of Greece. Bollettino Della Societa Paleontologica Italiana 40, 217–223.

Κουφός, Δ.Γ., 2004. Παλαιοντολογία Σπονδυλωτών. Θεσσαλονίκη: Εκδόσεις Ζήτη.

Koufos, G.D., 2006. Neogene Mammal Biostratigraphy and Chronology of Greece. Hell. J. Geosci. 183–214. https://doi.org/10.7312/columbia/9780231150125.003.0028

Koufos, G.D., 2016. Neogene and Quaternary Continental Biostratigraphy of Greece Based on Mammals. Bull. Geol. Soc. Greece L, 55–64. https://doi.org/10.12681/bgsg.11701

Koufos, G.D., 2018. New material and revision of the Carnivora, Mammalia from the Lower Pleistocene locality Apollonia 1, Greece. Quaternary. 1:6. doi:10.3390/quat1010006.

Koufos, G.D., 2022. The Fossil Record of Canids (Mammalia: Carnivora: Canidae) in Greece, in Vlachos, E. Fossil Vertrebrates of Greece Vol. 2. Laurasiatherians, Artidactyles, Perissodactyles, Carnivorans and Island Endemics. Springer, pp. 577–594.

Koufos, G.D., 2022. The Fossil Record of Mustelids (Mammalia: Carnivora: Mustelidae) in Greece., in: Vlachos, E. Fossil Vertrebrates of Greece Vol. 2. Laurasiatherians, Artidactyles, Perissodactyles, Carnivorans and Island Endemics. Springer, pp.641–659.

Koufos, G.D., 2022. The Fossil Record of Mustelids (Mammalia: Carnivora: Mustelidae) in Greece., in: Vlachos, E. Fossil Vertrebrates of Greece Vol. 2. Laurasiatherians, Artidactyles, Perissodactyles, Carnivorans and Island Endemics. Springer, pp.641–659.

Koufos, G.D., Kostopoulos, D.S., 1997. New carnivore material from the Plio Pleistocene of Macedonia (Greece) with the description of a new canid. Munchner Geowissenschaft Abteilung A 34, 33–63.

Koufos, G.D., Syrides, G.E., Kostopoulos, D.S., Koliadimou, K.K., 1992. Apollonia, a new vertebrate site in the pleistocene of the Mygdonia basin (Macedonia, Greece). Comptes Rendus de l'Academie de Sciences de Paris 315, 1041–1046.

Kurten, B. 2007. Pleistocene Mammals of Europe. (1st ed.). Routledge. https://doi.org/10.4324/9781315126470

Lack, J.B., Roehrs, Z.P., Stanley, Jr. C.E., Ruedi, M., Van Den Bussche, R.A., 2010. Molecular phylogenetics of Myotis indicate familial–level divergence for the genus Cistugo (Chiroptera). J Mammal 91:976–992.

Lacombat, F., Abbazzi, L., Ferretti, M.P., Martinez–Navarro, B., Moulle, P.E., Palombo, M.R., Rook, L., Turner, A., Valli, A.M.F. 2008 New data on the early Villafranchian fauna from Vialette (Haute–Loire, France) based on the collection of the Crozatier Museum (Le Puyen–Velay, Haute–Loire, France). Quaternary International 179, 64–71

Lawrence, D.R. 1979a. Biostratinomy. In (Fairbridge, .W. & Jablonski, D., eds.) Encyclopedia of Paleontology. Stroudsburg, PA: Dowden, Hutchinson & Ross, pp. 99–102.

Lawrence, D.R. 1979b. Diagenesis of fossils–fossildiagenese. In (Fairbridge, R.W. & Jablonski, D., eds.) Encyclopedia of Paleontology. Stroudsburg, PA: Dowden, Hutchinson & Ross, pp. 245–247.

Lawrence, D.R. 1979c. Taphonomy. In (Fairbridge, R.W. & Jablonski, D., eds.) Encyclopedia of Paleontology. Stroudsburg, PA: Dowden, Hutchinson & Ross, pp. 793–799.

Lee Lyman, R. 2010. What Taphonomy Is, What it Isn't, and Why Taphonomists Should Care about the Difference. Prometheus Press/ Palaeontological Network Foundation. Journal of Taphonomy. 8:1, 1–16.

Lindsay E. H. 1990 The setting. Lindsay E. H., Fahlbusch V. & Mein P. (Eds.) European Neogene Mammal Chronology. NATO ASI Series, Series A, Life Sciences: 1–14

Lindsay E. H., Opdyke N. and Johinson N. M. 1980 Pliocene dispersal of the horse Equus and late Cenozoic mammal dispersal events. Nature. 287: 135–138

Lisiecki, L.E. and Raymo, M.E., 2005. A Pliocene-Pleistocene stack of 57 globally distributed benthic $\delta^{18}O$ records. Paleoceanography, 20:1.

Lister, A., 1999. The Pliocene deer of the Red Crag Nodule Bed (UK). Deinsea, 7: 215–221.

Lister, A.M., Sher, A.V., van Essen, H., Wei, G. 2005 The pattern and process of mammoth evolution in Eurasia. Quaternary International 126–128, 49–64

Lister, A.M., van Essen, H.E., 2003. *Mammuthus rumanus* the earliest mammoth in Europe. In: Petculescu, A., Stiuca, E. (Eds.), Advances in Vertebrate Palaeontology ''Hent to Pantha''. Institut of Speleology of the Romanian Academy, Bucharest, pp. 47–52.

Longchem, W., Tsoukala, E., Moll, D. 2010. Milia (Grevena, Macedonia, Greece): A dangerous area for *Mammut borsoni*? Quaternaire 3:192-194.

Lordkipanidze, D., Jashashvili, T., Vekua, A., Ponce de Leon, M.S., Zollikofer, C.P.E., Rightmire, G.P., Pontzer, H., Ferring, R., Oms, O., Tappen, M., Bukhsianidze, M., Agustı´, J., Kahlke, R., Kiladze, G., Martı´nez–Navarro, B., Mouskhelishvili, A., Nioradze, M., Rook, L., 2007. Postcranial evidence from early Homo from Dmanisi, Georgia. Nature 449, 305–310.

Madurell– Malapeira, J., Bartolini– Lucenti, S., Prat– Vericat, M., Sorbelli, L., Blasetti, A., Ferretti, M.P., Goro, A., Cherin, M, 2021. Jaramillo–aged carnivorans from Collecurti (Colfiorito Basin, Italy). Historical Biology. DOI 10.1080/08912963.2021.1989590

Madurell–Malapeira, J., 2014. Villafranchian large mammals from the Iberian Peninsula: paleobiogeography, paleoecology and dispersal events. Journal of Iberian Geology, 40:1,167–178.

Madurell–Malapeira, J., Rook, L., Martínez–Navarro, B., Alba, D.M., Garrido, J.A., Moyà–Solà, S., 2013. The latest European painted dog. J Vert Paleontol. 33:1244–1249. doi:10.1080/02724634.2013.770402.

Malez, M., Forsten, A., Lenardic, J., 1999. Fossil horses (Mammalia, Equidae) from the bone breccias of Croatia, northern Balcan. Palaontologische Zeitschrift 66 (3–4), 369–385.

Marciszak, A., Schouwenberg, C., Lipecki, G., Talamo, S., Shpansky, A.V., Malikov, D., Gornig, W. 2019. Steppe brown bear Ursus arctos “priscus” from the Late Pleistocene of Europe. Quaternary International 534. DOI: 10.1016/j.quaint.2019.02.042

Martin, R.A., 2008. Arvicolidae. In: Janis, C.M., Gunell, G. F., Uhen, M.D. Evolution of Tertiary Mammals of North America, Vol. 2. Cambridge University Press.

Martin, R.E.,1999. Taphonomy: A Process Approach. Cambridge: Cambridge University Press.

Martinez– Navarro, B., 2010. La collezione dei grandi carnivori del Plio–Pleistocene al Museo di Storia Naturale di Firenze. In: Monechi, S., Rook, L., Le collezioni geologiche e paleontologiche. Il Museo di Storia Naturale dell’Università degli Studi di Firenze Volume III. p. 260–261.

Martinez–Navarro, B., Palmqvist, P., 1995. Presence of the African Machairodont *Megantereon whitei* (Broom, 1937) (Felidae, Carnivora, mammalia) in the lower pleistocene site of Venta Micena (Orce, Granada, Spain), with some considerations on the origin, evolution and dispersal of the genus. Journal of Archaeological Science 22, 569–582.

Martinez–Navarro, B., Rook, L., 2003. Gradual evolution in the African hunting dog lineage. Systematic implications. Comptes Rendus Pale´ovol 2, 695–702.

Masini, F. and Torre, D. 1990. Large Mammal Dispersal Events at the Beginning of the late Villafranchian. In: Lindsay, E. H., Fahlbusch, V. and Mein, P. (eds.) European Neogene mammal chronology. Nato ASI series A: Life Sciences. Plenum Press, New York. Pp 131–138.

Mazo, A.V. 1989 Nuevos restos de Proboscidea (Mammalia) en la cuenca de Guadix–Baza. In: Alberdi, M.T., Bonadonna, F. (Eds.), Geologı´a y Paleontologìa de la cuenca de Guadix–Baza Trabajos sobre el Neo´ geno–Cuaternario, vol. 11. Museo Nacional de Ciencias Naturales CSIC, Madrid, pp. 225–236

Mazo, A.V., Made, J.v.d., Arribas, A., Sanchez, A., 2003. Hace 3 Millones de Anos. In: Fundacion de Cultura y Deportes de Castilla La Mancha. Junta de Comunidades de Castilla–La Mancha, Ciudad Real, pp. 1–55. Lister et al., 2005

Mazza, P., Rustioni, M., 1992. Morphometric revision of the Eurasian species *Ursus etruscus* Cuvier. Palaeontogr. Ital. 79, 101e146.

Medin, T., Martinez-Navvaro, B., Rivals, F., Madurell-Malapeira, J., Ros-Montoya, S., Espigares, M.P., Figueirido, B., Rook, L., Palmqvist, P. 2017. Late Villafranchian *Ursus etruscus* and other large carnivorans from the Orce sites (Guadix-Baza basin, Andalusia, southern Spain): Taxonomy, biochronology, paleobiology, and ecogeographical context. Quaternary International 431:20-41.

Mein, P., 1975. Resultats du groupe de travail des vertebres. Working Groups. In: Senes, J. (Ed.), Report on Activity of the R.C.M.N.S. Regional Committee on Mediterranean Neogene Stratigraphy, Bratislava, pp. 78–81.

Meloro, C., 2007. Plio–Pleistocene large carnivores from the Italian peninsula: functional morphology and macroecology (PhD dissertation). Università degli Studi di Napoli ‘Federico II’, Napoli.

Meloro, C., 2011. Locomotor adaptations in Plio–Pleistocene large carnivores from the Italian Peninsula: palaeoecological implications. Current Zoology 57, 269–83.

Meloro, C., Louys, J. 2014. Ecomorphology of Radii in Canidae: Application to Fragmentary Fossils from Plio-Pleistocene Hominin Assemblages. Acta Palaeontologica Polonica, 60(4):795-806 (2014). https://doi.org/10.4202/app.00080.2014

Miller–Butterworth, C.M., Murphy, W.J., O’brien, S.J., Jacobs, D.S., Springer, M.S., Teeling, E.C., 2007. A family matter: conclusive resolution of the taxonomic position of the long–fingered bats, Miniopterus. Mol Biol Evol 24:1553–1561.

Mirzoyan, L., Manaseryan, N., 2008. Archaeozoological investigation of the site of Shirakavan, 3rd–1st Millenia BC, Armenia. Archaeology of the Near East VIII. TMO49, Maison de l’Orient et de la Mediterranee, Lyon.

Nomade, S., Pastre, J.F., Guillou, H., Faure, M., Guerin, C., Delson, E., Debard, E., Voinchet, P., Messager, E., 2012. 40Ar/39Ar constraints on some French landmark Late Pliocene to Early Pleistocene large mammalian paleofaunas: paleoenvironmental

and paleoecological implications. Quaternary Geochronology. 21:2–15. http://dx.doi.org/10.1016/j.quageo.2012.12.006

Oms, O., Dinares– Turell, J., Agustı, J., Pares, J.M., 1999. Refinements of the European mammalian biochronology: Magnetic polarity record of the plio–pleistocene Zujar section, (Guadix–Baza basin, SE Spain). Quaternary Research 51, 94–103.

Orlov, Y.A., 1968. Fundamentals of paleontology, vol. 13, Mammals. Israel Program for Scientific Translations, Jerusalem.

Palmqvist, P., Torregrosa, V., Perez–Claros, J.A., Martinez–Navarro, B., Turner, A., 2007. A re–evaluation of the diversity of *Megantereon* (Mammalia, Carnivora, Machairodontinae) and the problem of species identification in extinct carnivores. Journal of Vertebrate Paleontology 27, 160–175.

Palmqvist, P., Torregrosa, V., Perez–Claros, J.A., Martinez–Navarro, B., Turner, A., 2007. A re–evaluation of the diversity of *Megantereon* (Mammalia, Carnivora, Machairodontinae) and the problem of species identification in extinct carnivores. Journal of Vertebrate Paleontology 27, 160–175.

Pareto, L. 1865 Note sur les subdivisions que l'on pourrait e´tablir dans les terrains tertiaires de l'Apennin septentrional. Bulletin de la Societe Geologique de France 22, 210–277

Parparousi, E.M., Kostopoulos, D.S., Iliopoulos, G., 2021. A NEW FOSSILIFEROUS MAMMAL LOCALITY FROM THE VILLAFRANCHIAN OF GREECE: PRELIMINARY RESULTS. In: Belvedere M., Díez Díaz V., Mecozzi B., Sardella R (eds.). Abstract book of the XVIII annual conference of the European Association of Vertebrate Palaeontologists, online, 5th–9th July 2021. Palaeovertebrata, 130.

Perini, F.A., Russo, C.A.M., Schrago, C.G., 2010. The evolution of South American endemic canids: a history of rapid diversification and morphological parallelism. J Evol Biol 23(2):311–322. https://doi.org/10.1111/j.1420–9101.2009.01901.x

Petronio C., Bellucci L., Martinetto E., Pandolfi L. & Salari L. 2011 Biochronology and palaeoenviromental changes from the Middle Pliocene to the Late Pleistocene in Central Italy. Geodiversitas 33 (3): 485–517

Petrucci, M., Cipullo, A., Martinez– Navarro, B., Rook, L., Sardella, R., 2013. The late Villafranchian (Early Pleistocene) carnivores (Carnivora, Mammalia) from Pirro Nord (Italy). Palaeontographica Beitrage Zur Naturgeschichte der Vorzeit. Abt. A: Palaeozoology– Stratigraphy Vol. 298. 1–6:113–145.

Pfeiffer T. 1999. Die Stellung von Dama (Cervidae, Mammalia) im System plesiometacarpaler Hirsche des Pleistozäns – Phylogenetische Rekonstruktion – Metrische Analyse. Courier Forschungsinstitut Senckenberg, 211: 1–218.

Piskoulis, P., Chatzopoulou, K. 2022. The Fossil Record of Bats (Mammalia: Chiroptera) in Greece. In: Vlachos, E. Fossil Vertrebrates of Greece Vol. 2.

Laurasiatherians, Artidactyles, Perissodactyles, Carnivorans and Island Endemics. Springer, pp.93–111.

Pomel, M. 1853. Catalogue méthodique et descriptif des vertèbres fossiles découverts dans le bassin hydrographique supérieur de la Loire et surtout dans la vallée de son affluent principal, l'Allier. Paris: Chez J.–B. Bailliere, 193 p.

Pons Moya, J., 1987. Los Carnivoros (Mammalia) de Venta Micena (Granada, Espana). Paleont. Y Evol., Mem., Spec., 1:109–128.

Pradella, C., Rook, L., 2007 Mesopithecus (Primates, Cercopithecoidea) from Villafranca d'Asti (early Villafranchian; NW Italy) and palaeoecological context of its extinction. Swiss Journal of Geosciences 100, 145–152

Prat Vericat, M. Rufi, I., Llenas, M., Madurell- Malapeira, J. 2020. Middle Pleistocene Ursus deningeri from Grotte de la Carrière (Réseau Lachambre, Têt Valley, Eastern Pyrenees). Journal of Iberian Geology https://doi.org/10.1007/s41513-020-00124-1

Radulesco C., Samson P.–M., Petculescu, A. Stiuca E. 2003. Pliocene Large Mammals of Romania. Coloquios de Paleontologia, Vol. Ext. 1: 549–558.

Rabeder, G. 1999. Die Evolution des Höhlenbärengebisses. Mitteilungen der Kommission für Quartärforschung der Österreichischen. Akademie der Wissenschaften, 11: 1–102.

Radulesco, C. 2005. Artiodactyles du Pliocène et du Pléistocène inférieur de Roumanie. In: E. Crégut–Bonnoure (Ed.), Les Ongulés holartiques du Pliocène et du Pléistocène, Quaternaire, Hors–série, 2: 191–200.

Radulescu, C., Samson, P.M., 2001 Biochronology and evolution of the early Pliocene to the early pleistocene mammalian faunas of Romania. Bollettino Della Societa Paleontologica Italiana 40, 285–291

Ravel, A., Marivaux, L., Tabuce, R., Adaci, M., Mahboubi, M., Mebrouk, F., Bensalah, M., 2011. The oldest African bat from the early Eocene of El Kohol (Algeria). Naturwissenschaften 98:397–405.

Rivals, F. 2002. Les petits bovides pleistocenes dans le basin mediterraneen et le Caucase, Etude paleontologique, biostratigraphique, archeozoologique et paleoecologique. PhD thesis. Universite de Perpignan, N. attribute par la bibliotheque: 2002PERP0476

Rodrigo, M.A. 2011. Los bóvidos Villafranquienses de La Puebla de Valverde y Villarroya: sistemática, filogenia y paleobiología. Tesis de la Universidad de Zaragoza. ISSN 2254-7606. ISBN 978-84-697-6476-3

Roger, S., Coulon, C., Thouveny, N., Feraud, G., Van Velzen, A., Fauquette, S., Cocheme , J.J., Prevot, M., Verosub, K.L., 2000. $^{40}Ar/^{39}Ar$ dating of a tephra layer in the Pliocene Seneze maar lacustrine sequence (French Massif Central): constraint on

the age of the Reunion–Matuyama transition and implications on paleoenvironmental archives. Earth and Planetary Science Letters 183 (3–4), 431–440.

Rook, L. 1992. “Canis” monticinensis sp. nov., a new Canidae (Carnivora: Mammalia) from the Late Messinian of Italy. Bolletino della Societa Paleontologia Italiana. 31, 151–156.

Rook, L. and Torre, D. 1996a. The Wolf–event in Western Europe and the beginning of the late Villafranchian. Neues Jahrb. Geol. Paläontol. Monarshefte. 8, 495–501.

Rook, L., 1994. The plio–pleistocene Old World Canis (Xenocyon) ex gr. Falconeri. Bollettino Della Societa Paleontologica Italiana 33 (1), 71–82.

Rook, L., 1994. The Plio–Pleistocene Old World *Canis* (*Xenocyon*) ex. gr. *falconeri*. Bollettino della Societa Paleontologica Italiana 33:71–82.

Rook, L., 2009. The wide ranging genus *Eucyon* Tedford & Qiu, 1996 (Mammalia, Carnivora, Canidae, Canini) in the Mio–Pliocene of the Old World. Geodiversitas 31(4):723–741.

Rook, L., 2009. The wide ranging genus *Eucyon* Tedford & Qiu, 1996 (Mammalia, Carnivora, Canidae, Canini) in the Mio–Pliocene of the Old World. Geodiversitas 31(4):723–741.

Rook, L., Delfino, M., Ferretti, M.P. and Abbazzi, L. 2007. Vertebrate Records – Early Pleistocene. In: Elias, S.A. (ed.) Encyclopaedia of Quaternary Sciences. Volume 4. Elsevier, Oxford. Pp 3132–3139.

Rook, L., Martinez–Navarro, B., Howell, F.C., 2004. Occurrence of *Theropithecus* sp. in the late Villafranchian of southern Italy and implication for early Pleistocene “out of Africa’’. Journal of Human Evolution 47, 267–277.

Sabol M. 2003. New findings of Late Pliocene vertebrates from Hajnácka I site (southernSlovakia). Coloquios de Paleontología, Vol. Ext. 1: 595–602.

Sala, B., Masini, F., Ficcarelli, G., Rook, L., Torre, D., 1992. Mammal dispersal events in the middle and late Pleistocene of Italy and western Europe. Courier Forschungs–Institut Senckenberg 153, 58–68.

Samson P., Radulesco, C., Kisgyorgy Z. 1970. Nouvelles données sur la faune de mammifères du Villafranchien inférieur de Capeni–Vighis (dépression de Braşov, Roumanie). Eiszeitalter und Gegenwart, 22: 64–88.

Sanz, M., Daura, J., Brugal, J.–P., 2013. First occurrence of the extinct deer *Haploidoceros* in the Iberian Peninsula in the Upper Pleistocene of the Cova del Rinoceront (Castelldefels, Barcelona). Comptes Rendus Palevol 13(1):27–40.

Sardella, R. and Palombo, M.R. 2007. The Pliocene–Pleistocene boundary: which significance for the so called ‘Wolf Event’? Evidences from Western Europe. Quaternaire. 18(1), 65–71.

Schaub, S. 1932. Dle Ruminantier des ungarischen Praeglacials. Eclogae geologicae Helvetiae, Basel, 25 :319-330.

Shipman, P., 1993. Life History of a Fossil. An introduction to taphonomy and paleoecology. Cambridge: Harvard University Press.

Sigé, B., 1991. Rhinolophoidea et Vespertilionoidea (Chiroptera) du Chambi (Eocèneinférieur de Tunisie). Aspects biostratigraphique, biogéographique et paléoécologique de l'origine des chiroptèresmodernes. N Jb Geol Paläont Abh 182:355–376.

Simmons, N.B., 2005a. Order Chiroptera. In: Wilson DE, Reeder DM (eds) Mammal species of the world: a taxonomic and geographic reference, vol 1. JHU Press, Baltimore, MD, pp 312–529.

Simmons, N.B., 2005b. An Eocene big bang for bats. Science 307:527–528.

Simmons, N.B., Seymour, K.L., Habersetzer, J., Gunnell, G.F., 2008. Primitive Early Eocene bat from Wyoming and the evolution of flight and echolocation. Nature 451:818–821.

Smith, T., Rana, R.S., Missiaen, P., Rose, K.D., Sahni, A., Singh, H., Singh, L., 2007. High bat (Chiroptera) diversity in the Early Eocene of India. Naturwiss 94:1003–1009.

Sotnikova, M. And Rook, L. 2010. Dispersal of the Canini (Mammalia, Canidae; Caninae) across Eurasia during the Late Miocene to Early Pleistocene. Quaternary International. 212(2), 86–97.

Sotnikova, M.V., Baigusheva, V.S. and Titov, V.V. 2002. Carnivores of the Khapry Faunal Assemblage and their stratigraphic implications. Stratigraphy and Geological Correlation. 10(4), 375–390.

Spaan, A., 1992. A revision of the deer from Tegelen (Province of Limburg, The Netherlands). Scripta Geol 98:1–85.

Spassov N. 2005. Brief review of the Pliocene ungulate fauna of Bulgaria. In: E. Crégut–Bonnoure (Ed.), Les Ongulés holartiques du Pliocène et du Pléistocène, Quaternaire, Hors–série, 2: 201– 212.

Spassov, N., 1997. Villafranchian succession of mammalian Megafaunas from Bulgaria and the Biozonation of south–east Europe. Me´moires et Travaux de l'Institut de Montpellier 21, 669–676

Spassov, N., 2000. Biochronology and zoogeographic affinities of the Villafranchian Fauas of south Europe. Historia Naturalis Bulgarica 12, 89–128.

Stefaniak K. 1995. Late Pliocene cervids from Węże 2 in southern Poland. Acta Palaeontlogica Polonica, 40 (3): 327–340.

Stefaniak K. 2015. Neogene and Quaternary Cervidae from Poland. Institute of Systematics and Evolution of Animals Polish Academy of Sciences, 204 p.

Stiner, M.C., Howell, F.C., Martínez–Navarro, B., Tchernov, E., Bar–Yosef, O., 2001. Outside Africa: Middle Pleistocene Lycaon from Hayonim Cave, Israel. Boll Soc Paleontol Ital. 40:293–302.

Suraprasit, K., Jaeger, J.J., Chaimanee, Y., Chavasseau, O., Yamee, C., Tian, P., Panha, S. The Middle Pleistocene vertebrate fauna from Khok Sung (Nakhon Ratchasima, Thailand): biochronological and paleobiogeographical implications. Zookeys. 30(613):1-157. doi: 10.3897/zookeys.613.8309. PMID: 27667928; PMCID: PMC5027644.

Tabuce, R., Antunes, M.T., Sigé, B., 2009. A new primitive bat from the earliest Eocene of Europe. J Vert Paleontol 29:627–630.

Tedford, R. H. and Qui, Z. 1996. A new canid genus from the Pliocene of Yushe, Shanxi Province. Vertebrata PalAsiatica. 34, 27–40.

Tedford, R.H., Wang, X., Taylor, B.E., 2009. Phylogenetic systematics of the North American fossil Caninae (Carnivora: Canidae). Bull Am Mus Nat Hist. 325:1–218. doi:10.1206/574.1.

Teeling, E.C., Springer, M.S., Madsen, O., Bates, P., O'brien, S.J., Murphy, W.J., 2005. A molecular phylogeny for bats illuminates biogeography and the fossil record. Science 307:580–584.

Tejedor, M.F., Czaplewski, N.J., Goin, F.J., Aragón, E., 2005. The oldest record of South American bats. J Vert Paleontol 25:990–993.

Torre, D. 1979. The Ruscinian and the Villafranchian dogs of Europe. Bolletino della Societa Paleontologia Italiana. 18(2), 162–165.

Torre, D., Abbazzi, L., Bertini, A., Fanfani, F., Ficcarelli, G., Masini, F., Mazza, P., Rook, L., 2001. Structural changes in Italian late Pliocene – Pleistocene large mammal assemblages. Boll Soc Paleontol I 40: 303–306.

Torre, D., Ficcarelli, G., Masini, F., Rook, L., Sala, B., 1992. Mammal dispersal events in the early Pleistocene of Western Europe. Cour Forschungsinst Senckenberg 153: 51–58.

Torre, D., Ficcarelli, G., Masini, F., Rook, L., Sala, B., 1992. Mammal dispersal events in the early pleistocene of western Europe. Courier Forschungs–Institut Senckenberg 153, 51–58.

Valli, A.M.F., 2004. Les Cervidae du gisement Pliocène supérieur (Villafranchien moyen) de Saint–Vallier (Drôme, France). Geobios 37: S191–S232.

van Loghem,W., Tsoukala E., Mol, D., 2010. Milia (Grevena, Macedonia, Greece): a dangerous area for Mammut borsoni? Quaternaire, hors série 3, 192–194

Van Valkenburgh, B. 1988a. Trophic diversity in past and present guilds of large predatory mammals. Paleobiology. 14(2), 155–173.

Vasileiadou, K., Böhme, M., Neubauer, T.A., Georgalis, G.L., Syrides, G.E., Papadopoulou, L., Zouros, N., 2017. Early Miocene gastropod and ectothermic vertebrate remains from the Lesvos Petrified Forest (Greece). Pal Z 91:541–564.

Vasileiadou, K., Zouros, N., 2012. Early Miocene micromammals from the Lesvos Petrified Forest (Greece): preliminary results. Palaeobiodiv Palaeoenviron 92:249–264.

Villalba de Alvarsado, M., Collado Giraldo, H., Luis Arsuaga, J., Bello Rodrigo, J.R., Van Heteren, A.H., Gomez- Olivencia, A. 2021. Looking for the earliest evidence of Ursus arctos LINNAEUS, 1758 in theIberian Peninsula: the Middle Pleistocene site of Postes cave. https://doi.org/10.1111/bor.12537. ISSN 0300-9483.

Viret, J., 1954. Le loess à bancs durcis de Saint–Vallier (Drôme) et sa faune de mammifères villafranchiens. Nouv Arch Mus Hist Nat Lyon 4:1–200

Vislobokova, I., 1992. Neogene deer in Eurasia, Paleontologia i Evolucio, 24–25; 149–154.

Vislobokova, I., Erbaeva, M., Sotnikova, M., 1993. The early Villafranchian stage in the development of the mammalian fauna of northern Eurasia. Strat.–Geol. Kami, 1, 5: 87–96.

Vislobokova, I., Sotnikova, M.V., Dodonov, A., 2001. Late Miocene–Pliocene mammalian faunas of Russia and neighbouring countries. Bollettino Della Societa Paleontologica Italiana 40, 307–313.

Vislobokova, I., Sotnikova, M.V., Erbaeva, M.A. 1995. The Villafranchian mammalian faunas of the Asiatic part of former USSR. Il Quaternario 8, 367–376

Von den Driesch, A. 1976. A Guide to the measurement of the animal bones from archaeological sites. Peabody Museum Bulletin 1. Harvard: Peabody Museum of Archaeology and Ethnology.

Voohries, M.R., 1969. Taphonomy and population dynamics of an early Pliocene vertebrate fauna, Knox Country, Nebraska. University of Wyoming Contributions to Geology, special paper 1, 1–69.

Vos J. De, Mol D., Reumer J. W. F. 1995. Early Pleistocene Cervidae (Mammalia, Artyodactyla) from the Oosterschelde (the Netherlands), with a revision of the cervid genus *Eucladoceros* Falconer, 1868. Deinsea, 2: 95–121.

Wang, X. and Tedford, R.H. 2007. In: Jensen, P. (ed.) The Behavioural Biology of Dogs. CAB International. Pp 3–20.

Williams H. S. 1901 Discrimination of time value in geology. Journal of Geology. 9: 570–585

Wilson, M.V.H., 1988. Taphonomic processes: information loss and information gain. Geoscience Canada, 15: 131–148.

Wund, M., 2018. Mustelidae. In: Animal diversity web. http://animaldiversity.org/accounts/Mustelidae/. Accessed 27 Apr 2018.